Fall 1995

A Relativistic Model for Heavy Mesons

Jialin Zeng
Old Dominion University

A RELATIVISTIC MODEL FOR HEAVY MESONS

by

Jialin Zeng
B.S. July 1982, South China Normal University
M.S. December 1989, Old Dominion University

A Dissertation submitted to the Faculty of
Old Dominion University in Partial Fullfillment of the
Requirement for the Degree of

DOCTOR OF PHILOSOPHY

PHYSICS

OLD DOMINION UNIVERSITY
November 1995

Approved by:

J. W. Van Orden (Director)

ABSTRACT

A RELATIVISTIC MODEL FOR HEAVY MESONS

Jialin Zeng
Old Dominion University, 1995
Director: Dr. J. W. Van Orden

Motivated by the present interest in the heavy quark effective theory, we construct a model for heavy mesons based on a relativistic bound state wave equation, the Gross equation. The kernel we use is based on scalar confining and vector Coulomb potentials. Wave functions are treated to leading order and energies to order $1/m_Q$ in the heavy-light systems, and to order $1/m_Q^2$ in heavy-heavy systems. Our results are in good agreement with experimental measurements. This model may be used to study weak decay properties in the framework of the heavy quark effective theory and ultimately to extract V_{cb} from experimental data.

Acknowledgements

I would like to thank Dr. J. Wallace Van Orden for the guidance, encouragement, kindness and patience that he has given me during the development of this project. He not only initiated the idea of this work, but also worked out many problems independently so that the comparison of our calculations could ensure the accuracy of this work. As my advisor, he has helped me step by step throughout the whole project. Without his help, this work would not have been possible.

I am very grateful to Dr. Winston Roberts, for his unselfish support and many extremely helpful discussions. As a great teacher and collaborator, he has not only given me guidance with his great physical insights, but also given me a lot of friendly advice and encouragement. Over the last three years, I have taken much of his time and have learned very much from him. His willingness in helping students will always be my model and inspiration. His sharing of his independent calculations on some problems not only contributed to the development of the model but also helped me to improve my skill in solving problems.

I would also like to thank Dr. Paul E. Ulmer, Dr. James L. Cox, Jr., Dr. Ali A. Nowroozi and Dr. Kar Y. Lee for their critical reading of this dissertation.

I would like to express my gratitude to my parents, my mother-in-law and all my sisters. Without their unselfish sacrifice, I would not have been able to finish this work. I also want to thank my son Robert for the love and joy he gives me.

I am most grateful to my loving husband Rod Meyer for sharing all my happiness and grief, for always believing in me, encouraging me and supporting me, and for making my life meaningful.

Table of Contents

List of Tables

List of Figures

Chapter 1

Introduction and Motivation

This work constructs a potential model for heavy mesons by means of a quasipotential approach. Based on the spectator equation [1], we have constructed the Hamiltonian for the heavy meson systems and calculated the heavy meson spectra. The model is constructed in such a way that the heavy quark effective theory can be applied to calculate weak decay amplitudes and form factors, and to extract V_{cb} from experimental data.

As mesons are made up of elementary particles, we begin with a brief survey of elementary particles and their interactions to provide necessary background for further development in subsequent chapters.

1.1 Elementary Particles

At the beginning of this century, people believed that all matter was made of atoms. After Rutherford's discovery of the nucleus in 1911, and the early development of quantum mechanics, physicists were convinced that atoms were made of nuclei and electrons. After the discovery of neutrons in 1932, physicists were convinced that nuclei were made of protons and neutrons which are collectively called nucleons.

In the 1940's and 1950's, some new particles appeared and the number of particles was increasing. By the end of the 1960's, more than thirty new particles

had been found. Although it was not clear if these new particles were elementary, physicists were able to observe some of their properties and separate all the known particles into three groups: hadrons, leptons and gauge bosons.

Hadrons are the particles that experience strong forces. The hadrons that are fermions are called baryons. The hadrons that are bosons are called mesons. Nucleons and pions are examples of hadrons. They are the lightest baryons and mesons respectively.

It was later realized that the observed hadrons were not elementary particles. In 1964, a composite model of hadrons, which is now called the quark model, was proposed by Zweig and Gell-Mann independently [2, 3, 4]. According to this model, hadrons were composed of constituents which were called quarks by Gell-Mann. Since then, the quark model has been improved by extensive theoretical studies and supported by overwhelming experimental evidence.

At present, it is believed that quarks, leptons and gauge bosons are elementary particles. Quarks and leptons are the elementary fermions. Quarks experience strong, electromagnetic and weak interactions. Leptons experience electromagnetic and weak interactions. Gauge bosons play the roles of transmitting forces between the elementary fermions.

To date, there exist six flavors of quarks. They are up (u), down (d), strange (s), charm (c), bottom (b) and top (t) quarks. Some properties of these quarks are listed in Table 1.

In addition to the properties listed in Table 1, quarks have another degree of freedom called color. Each quark (flavor) may have any of the three colors which may be called red, green and blue. It is the color charge that distinguishes quarks from leptons, whose lack of this color degree of freedom forbids them from participating in any strong interactions.

Each quark has an antiquark as its antiparticle. We use $\bar{q}$ to represent the antiquark of quark q. The antiquark is identical to its corresponding quark except for the reversal of its electric charge, intrinsic parity, color and some other quantum numbers.

In the lepton sector, there are six leptons. Three of the leptons are charged,

Table 1: Some properties of quarks

quarks	*spin*	*electric charge*	*intrinsic parity*	*mass(GeV)*	*heavy/light*
u	$\frac{1}{2}$	$\frac{2}{3}\|e\|$	+	~ 0.3	*light quark*
d	$\frac{1}{2}$	$-\frac{1}{3}\|e\|$	+	~ 0.3	*light quark*
s	$\frac{1}{2}$	$-\frac{1}{3}\|e\|$	+	~ 0.5	*light quark*
c	$\frac{1}{2}$	$\frac{2}{3}\|e\|$	+	~ 1.5	*heavy quark*
b	$\frac{1}{2}$	$-\frac{1}{3}\|e\|$	+	~ 5	*heavy quark*
t	$\frac{1}{2}$	$\frac{2}{3}\|e\|$	+	~ 170	*heavy quark*

namely the electron (e^-), muon (μ^-) and tau (τ^-), each carrying an electric charge of $-|e|$. The other three are electrically neutral, and they are known as the electron neutrino (ν_e), muon neutrino (ν_μ) and tau neutrino (ν_τ). Like quarks, each lepton also has an antilepton.

In quantum field theory, when particles interact with each other, they exchange gauge bosons. There exist different gauge bosons for different interactions. They are the massless gluons of strong interactions, massless photon of electromagnetic interactions and massive weak bosons $W^\pm$, Z^0 of weak interactions. W^+ and W^- carry electric charge $+|e|$ and $-|e|$ respectively. The other gauge bosons do not carry electric charge.

Hadrons consist of quarks and gluons. By assuming that hadrons are bound states of quarks and antiquarks, the naive quark model has achieved great success in explaining many hadron properties. It is now a common assumption that baryons are bound states of three valence quarks ($q_1q_2q_3$), while mesons are bound states of one valence quark and one valence antiquark ($q_1\bar{q}_2$). Heavy mesons are the mesons that contain at least one heavy quark.

1.2 Evidence for Color

To understand why color is introduced, consider the example of the baryon Δ^{++}. The Δ^{++} is a bound state of three u quarks with total angular momentum $J = 3/2$. It is also the lightest particle with configuration uuu and, therefore, is the ground state of uuu. This means that all three quarks are in an s ($l = 0$) state and, therefore, the spatial wave function of the three u quark system is symmetric under the interchange of any two u quarks. Furthermore, since there is no orbital angular momentum, the spins of the quarks are the only contributions to the total angular momentum, and the spin wave function is symmetric since $J = 3/2$. As a result, the Δ^{++} wave function

$$|\Delta^{++}> = |uuu> |space> |spin>$$

is symmetric under the interchange of any two of its constituents. This violates the Pauli principle.

To correct this problem, Greenberg [5] proposed that quarks have an additional degree of freedom which is now called color. Under this proposal, each quark has a hidden color degree of freedom, and the color wave function of Δ^{++} is antisymmetric under the interchange of any two quarks, thus preserving the Pauli principle.

This proposal is supported by experiments measuring the cross sections of $e^+e^- \rightarrow hadrons$ and $e^+e^- \rightarrow \mu^+\mu^-$. Theoretically, the cross sections for these two processes are related by [6]

$$\frac{\sigma(e^+e^- \rightarrow hadrons)}{\sigma(e^+e^- \rightarrow \mu^+\mu^-)} = \sum_{color} \sum_{q} Q_q^2, \qquad (1)$$

where q denotes the quark flavor and Q_q is the charge of the quark q in units of $|e|$: $Q_u = 2/3$, $Q_d = -1/3$, etc. It is found that this expression agrees with data only if there exist three different colors [7, 8].

1.3 QCD and QED

In order to understand how quarks are bound to form hadrons, one needs to understand how quarks interact with one another.

Since quarks carry electric charge, they must experience electromagnetic interactions. However, there exist some hadrons that are composed of quarks with electric charges of the same sign. For example, $\Delta^{++} = uuu$. The electromagnetic interactions the u quarks experience are repulsive. Therefore, the interaction that binds quarks into hadrons must be another kind of interaction that is stronger than the electromagnetic interaction. This interaction is called the strong interaction and is the same interaction that binds nucleons into nuclei.

The correct theory for strong interactions is now believed to be the quantum field theory Quantum Chromodynamics (QCD). To bring out the flavor of this theory, we use Quantum Electrodynamics (QED) as our basis for comparison, since QED is very well understood. Its calculations of atomic and molecular properties agree with experiments extremely well.

The Lagrangian for QED is

$$L_{QED} = -\frac{1}{4}F_{\mu\nu}F^{\mu\nu} + i\bar{\psi}\gamma^{\mu}D_{\mu}\psi - m\bar{\psi}\psi \ , \tag{2}$$

where

$$F_{\mu\nu} = \partial_{\mu}A_{\nu} - \partial_{\nu}A_{\mu}$$

is the QED field strength tensor,

$$D_{\mu} = \partial_{\mu} - ieA_{\mu}$$

is the covariant derivative, e is the electric charge of the electron, γ^{μ} are the Dirac γ-matrices as shown in Appendix A, ψ is the electron field, m is the mass of the electron, and A_{μ} is the photon field.

The Lagrangian for QCD is

$$L_{QCD} = -\frac{1}{4}F^{a}_{\mu\nu}F^{\mu\nu}_{a} + i\sum_{q}\bar{\psi}^{i}_{q}\gamma^{\mu}\left(D_{\mu}\right)_{ij}\psi^{j}_{q} - \sum_{q}m_{q}\bar{\psi}^{i}_{q}\psi_{qi} \ , \tag{3}$$

where

$$F^a_{\mu\nu} = \partial_\mu A^a_\nu - \partial_\nu A^a_\mu + g_s f_{abc} A^b_\mu A^c_\nu$$

is the QCD field strength tensor,

$$(D_\mu)_{ij} = \delta_{ij}\partial_\mu - i g_s \sum_a \frac{\lambda^a_{ij}}{2} A^a_\mu ,$$

λ^a are the generators in the fundamental representation of SU(3), ψ_{qi} are the Dirac spinors associated with each quark field of color i and flavor q, A^a_μ $(a = 1, 2, \cdots 8)$ are the gluon fields, g_s is the QCD coupling constant, and f_{abc} are the structure constants of the SU(3) algebra defined by

$$\left[\frac{\lambda^a}{2}, \frac{\lambda^b}{2}\right] = i f^{abc} \frac{\lambda_c}{2} .$$

The Lagrangians of QCD and QED are very similar in general structure, in that both are local gauge theories with spin 1/2 fermions. Both have the gauge term ($F_{\mu\nu}F^{\mu\nu}$), the interaction term ($\bar{\psi}\gamma^\mu D_\mu \psi$) and the mass term ($m\bar{\psi}\psi$). The differences reside in the fact that L_{QED} is invariant under a local $U(1)$ gauge transformation

$$\psi(x) \longrightarrow \psi'(x) = e^{ie\phi(x)}\psi(x),$$

and under this gauge transformation the photon field transforms as

$$A_\mu(x) \longrightarrow A'_\mu(x) = A_\mu(x) + \partial_\mu \phi(x) .$$

In contrast, L_{QCD} is invariant under a local nonabelian $SU(3)$ gauge transformation

$$\psi(x) \longrightarrow \psi'(x) = e^{ig_s \sum_a \lambda^a \theta_a(x)/2}\psi(x),$$

and the gluon fields transform as

$$A^a_\mu(x) \longrightarrow A'^a_\mu(x) = A^a_\mu(x) + \partial_\mu \theta^a(x) - g_s f^{abc}\theta_b(x) A_{c\mu}(x),$$

where $\phi(x)$ and $\theta^a(x)$ are position-dependent parameters. In QED, there is a single gauge boson, the photon. In QCD, there are eight gauge bosons known as gluons. The significant difference between these two theories is that the gluons in QCD carry color charge and this allows self-coupling of gluons, while in QED, photons do not couple to each other since they do not carry electric charge.

The possibility of this gluon-gluon coupling leads to an important property of QCD — asymptotic freedom. To understand this property, let's start with another concept — the running coupling constant, *i.e.* a coupling constant that varies with the energy scale.

In both QED and QCD, the running coupling constants α and α_s are used to measure the strength of interactions between two (electric- or color-) charged particles. In QED,

$$\alpha(Q^2) = \frac{e^2(Q^2)}{4\pi} , \tag{4}$$

where $Q^2 = -q^2$ and q is the four-momentum transferred during the interactions. In QCD,

$$\alpha_s(Q^2) = \frac{g_s^2(Q^2)}{4\pi} . \tag{5}$$

The quantities of e and g_s have been defined in the Lagrangian.

The running coupling constants in QED and QCD behave very differently. In QED, an electron is surrounded by a cloud of virtual positron-electron (e^+e^-) pairs as a result of the vacuum polarization. This causes the effect of charge screening, just as happens in a dielectric medium. When two electrons interact with each other, the transmitted photons need to probe through the cloud that shields the bare charges. The strength of the interaction therefore depends on the energy and momentum of the transmitted photons.

As Q^2 increases the resolution of the photon probe increases and smaller distances are probed. The smaller the distance probed, the less shielding is experienced. As a result, the electron charge "felt" by another electron increases with Q^2. The result is that the running coupling constant increases with Q^2.

In QCD, a quark is not only surrounded by a cloud of quark-antiquark ($q\bar{q}$)

pairs but also by gluons, which are also color charged. As it turns out, this additional contribution reverses the effect from $q\bar{q}$ pairs and leads to an antiscreening effect. The running coupling constant of QCD decreases with increasing Q^2.

When contributions up to one loop level are considered, the running coupling constant of QCD is [9]

$$\alpha_s(Q^2) = \frac{12\pi}{(33 - 2n_f)\ln\left(\frac{Q^2}{\Lambda^2}\right)}, \tag{6}$$

where n_f is the number of flavors of quarks with mass-squared less than Q^2 and Λ is the QCD scale parameter, which has a value somewhere between 0.1 GeV and 0.5 GeV.

One immediately observes that for $Q^2 \gg \Lambda^2$, $\alpha_s(Q^2)$ is small. This means that when the momentum transfer is large, or when the two quarks are separated by a short distance, the strength of the strong interaction between the two quarks is weak. This is the property of asymptotic freedom.

Isolated quarks have never been observed. This has led to the hypothesis of quark confinement. It is believed that the only particle states that we can observe are colorless ones. Since quarks have color, one cannot observe a free quark. When quarks are bound into hadrons, only the combination that results in colorless bound states can exist. This means that not all combinations of quarks and antiquarks are allowed. For example, qqq and $q\bar{q}$ are readily observed, while $qq\bar{q}$ and qq are thought not to exist.

1.4 Quark Potential Model Approach

At large Q^2, or short distances, QCD is asymptotically free. Since the running coupling constant is small, perturbative techniques like those used to solve QED can be applied to solve QCD in this region. However, as the quark separation r increases, or equivalently as Q^2 decreases, $\alpha_s(Q^2)$ becomes large as indicated by (6), and QCD is confined. In this region, perturbation theory breaks down, and we need other methods to solve QCD.

Various approaches have been developed to extract hadron properties from QCD. Among them, the lattice approach [10] may be the most promising method since, in principle, it calculates hadron properties exactly from the QCD Lagrangian. By formulating QCD on a lattice, in which quarks are located at lattice sites and gluons on the links between the lattice sites, one can perform numerical calculations by using the Feynman path integral technique. By this approach, one finds the indication that the interquark potential is linear at large separations of quarks. Application of lattice QCD to many physical processes is currently limited by available computing power.

The method of QCD sum rules [11] is another approach that has been extensively studied. By making the Wilson operator product expansion for a time-ordered product of quark currents, an n-point function can be expressed in terms of the Wilson coefficients and the vacuum expectation values of quark and gluon condensate operators. The Wilson coefficients contain the information about small-distance separation of quarks and can be calculated by perturbative techniques. The vacuum matrix elements contain the information for large-distance separation of quarks and can be treated phenomenologically. As a result, on one hand, one can obtain an expression for the n-point function in terms of QCD parameters such as $\alpha_s(Q^2)$ and the quark masses. On the other hand, the n-point function can also be expressed in terms of hadron properties. Equating these two expressions for the n-point function using a matching procedure, one can express the hadron properties in terms of the QCD parameters.

In spite of the remarkable progress being made by the approaches of lattice QCD and QCD sum rules, many technical problems remain unsolved at present. The hadron properties that can be extracted by these two approaches are still very limited.

An alternative approach that has been quite successful in providing physical insight into hadron physics is the quark potential model approach. The idea of this approach is very simple. To study hadron properties, one can study the bound states of quarks. A traditional and direct way to study particle bound states is to first obtain the equations of motion for the particles and solve them. In principle,

the equations of motion for quarks in hadrons can be derived from QCD. Unfortunately, the exact solution of these equations of motion is unavailable. However, since the general features of strong interactions can still be extracted from QCD, one can make models to mimic such interactions. In these models, one formulates approximate equations of motion for quarks in hadrons based on currently understood QCD properties. Using these models, many hadron properties can be calculated. Although the approximations made by this approach are often crude and lack direct theoretical support from QCD, this approach has provided a simple picture for understanding hadron physics and has been surprisingly successful in explaining large amounts of data.

The earliest quark potential models are also the simplest nonrelativistic quark models. In these models the equations of motion for quarks in hadrons are approximated by a Schrödinger equation with spin-independent interquark potentials [12, 13, 14, 15]. The spin-independent potentials are constructed according to the property of asymptotic freedom and quark confinement of QCD. In the asymptotically free region where quarks are separated by a short distance r or where Q^2 is large, QCD can be studied using perturbative techniques. When only the first order terms are considered, the interquark potential for the short-range region comes from the one-gluon exchange potential V_{OGE}. Suppressing the color indices, the Dirac structure of the potential can be taken to have the form

$$V_{OGE} = \gamma^{(1)} \cdot \gamma^{(2)} V_v(Q^2) \,, \tag{7}$$

where $\gamma^{(i)}$ denotes the γ-matrices for particle i and

$$V_v(Q^2) = -\frac{4}{3}\alpha_s(Q^2)\frac{4\pi}{Q^2} \,. \tag{8}$$

In the non-relativistic expansion of (7), one replaces the γ-matrices by unity, and (7) reduces to a spin-independent potential as its lowest order approximation, which is the potential shown in (8). Written in coordinate space, we cast $V_v(r)$ into the form

$$V_v(r) = -\frac{4}{3}\frac{\alpha_s(r)}{r} \,. \tag{9}$$

Note that $\alpha_s(r)$ is *not* the Fourier transform of $\alpha_s(Q^2)$. In fact, (9) serves to define $\alpha_s(r)$.

In the confining region, where quarks are separated by a large distance or where Q^2 is small, the study of lattice QCD indicates that the interquark potential increases linearly with the distance between the quarks [16, 17, 18, 19]. Many models, therefore, have assumed the confining potential to be a linear potential in coordinate space

$$V_{conf}(r) = br + c\,, \tag{10}$$

where b is the string tension from lattice QCD and c represents an r-independent shift of the potential.

When incorporating both these features of QCD—asymptotic freedom and confinement—into a quark potential model, the interquark potential can be naively constructed as the Coulomb-plus-linear potential

$$V(r) = -\frac{4}{3}\frac{\alpha_s(r)}{r} + br + c\,, \tag{11}$$

which is spin-independent.

One of the earliest models of mesons to include spin-dependent effects is the model for charmonium by De Rújula, Georgi and Glashow [20]. This model uses the Coulomb-plus-linear potential as the spin-independent potential and includes the spin-dependent effects from the one-gluon exchange interaction. The resulting spin-dependent potential is similar to the Breit-Fermi interaction [21, 22, 23] in positronium. The charmonium spectrum calculated from this model agrees well with the experimental data for most of the states. However, some splittings of states disagree with data sharply, which indicates that spin-dependent effects arising from the confining potential should also be considered [24].

Although nonrelativistic models have described heavy quarkonium ($c\bar{c}$, $b\bar{b}$) systems with reasonable success, they are not adequate for studying systems with one or more light quarks. The reason for this is that while $< \mathbf{p} > /m_Q \ll 1$ for heavy quarks, this is not necessarily true for light quarks. As a result, the relativistic corrections to the Schrödinger equation may be large for the light quarks.

To improve the nonrelativistic models, Godfrey and Isgur [25] proposed a relativized model for mesons. In this model, relativistic kinematics are included by modifying the kinetic term in the Schrödinger equation, so that the mechanical energy of the quarks is given by the relativistic expression $\sum_{i=1}^{2}(m_i^2 + \mathbf{p}_i^2)^{1/2}$ instead of the nonrelativistic expression $\sum_{i=1}^{2}(m_i + \mathbf{p}_i^2/2m_i)$. In addition, the spin-dependent effects are modified by including the spin-orbit interaction associated with the long-range confining potential. Meson spectra calculated with this model are remarkably close to experimental masses in all flavor sectors. However, this model is not covariant.

According to special relativity, laws of physics must be Lorentz covariant. That is, the mathematical equations describing the physics must have the same form in all inertial frames. One way to construct a covariant model for meson systems is to start from the Bethe-Salpeter equation [26], since this equation is a covariant two-body equation. In this method, the quark-antiquark potential is summarized by the Bethe-Salpeter kernel, which in general has the Lorentz structure (See, for example, [27].)

$$V = V_S\, 1 \otimes 1 + V_V\, \gamma^\mu \otimes \gamma_\mu + V_P\, \gamma^5 \otimes \gamma^5 + V_A\, \gamma^\mu\gamma^5 \otimes \gamma_\mu\gamma^5 + \frac{1}{2} V_T\, \sigma^{\mu\nu} \otimes \sigma_{\mu\nu},$$

where V_S, V_V, V_P, V_A and V_T are scalar, vector, pseudoscalar, axial-vector, and tensor potentials. In meson systems, the one-gluon exchange interaction gives rise to a vector term. The Lorentz structure of the confining potential is still unclear since this potential cannot be derived from QCD. However, it has been argued by Gromes [27] that the main contribution of confinement to the kernel in the charmonium system should be vector and/or scalar. This is because the leading contribution from other terms gives spin-spin interactions or zero, which contradicts the experimental data. On the other hand, it has been found [28] that there are no normalizable bound state solutions to the Dirac equation with vector confinement because of the Klein paradox [29]. Although the confining potential may have a much more complicated Lorentz structure, it is often assumed to be a scalar potential. The Bethe-Salpeter kernel for meson systems can therefore be

approximated as the sum of the vector and scalar terms:

$$V = \gamma^{(1)} \cdot \gamma^{(2)} V_v + V_s \ , \tag{12}$$

where V_s is the linear confining potential V_{conf} in the coordinate space.

1.5 Weak Interactions and V_{cb}

1.5.1 Weak Interactions

Hadrons experience not only the strong and electromagnetic interactions, but also the weak interactions. The hadrons that decay exclusively through weak interactions have much longer lifetimes than those which decay through strong or electromagnetic interactions. The cross sections of weak processes are also correspondingly much smaller. It is now believed that the correct theory for weak interactions is the Standard Model of electroweak interactions [30, 31, 32]. According to this theory, the electromagnetic and weak interactions are two aspects of a single interaction, the electroweak interaction. During a weak process, one or more of three different gauge bosons may be exchanged. They are the massive bosons W^+, W^- and Z^0 with $M_{W^\pm} \approx 80$ GeV and $M_{Z^0} \approx 90$ GeV.

The $W^\pm$ bosons mediate the charge-changing weak interactions. This is because W^+ and W^- carry electric charge and, therefore, can alter the electric charge of a particle with which they interact. One example of such a process is the β-decay of the neutron, $n \rightarrow p + e^- + \bar{\nu}_e$. This process is represented by Figure 1. The neutron emits a gauge boson W^- and changes to a proton. The W^- then decays into an $e^-\bar{\nu}_e$ pair. In this process, the electric charge of the decaying neutron is changed by the emission of W^-.

In contrast, the Z^0 boson mediates the charge-preserving weak interactions since Z^0 carries no electric charge and the particles that participate in the interactions preserve their electric charge.

On a more fundamental level, the weak interactions that are experienced by hadrons involve quarks and leptons. In the example of neutron β-decay described

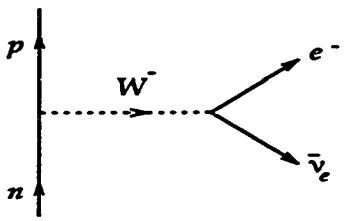

Figure 1: Feynman diagram representing the β-decay of neutron.

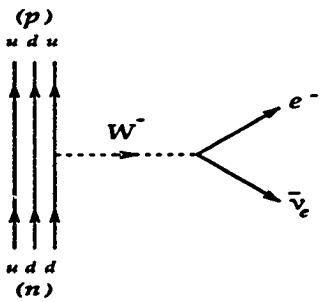

Figure 2: Feynman diagram representing the decay of a d quark into a u quark in β-decay of neutron.

earlier by Figure 1, the decay process can be understood as that in which one of the d quarks in the neutron has decayed into a u quark by emitting a W^-, as shown in Figure 2. This change of quark flavor results in the transformation of the neutron into a proton.

Only left-handed leptons and quarks participate in charge-changing weak interactions. In the standard model, the charge-changing interactions of leptons and quarks are described by the Lagrangian [33, 34]

$$L^{cc} = -\frac{g}{\sqrt{2}}\left[\bar{\nu}_L \gamma^\lambda \ell_L + \bar{U}'_L \gamma^\lambda D'_L\right] W^+_\lambda + h.c.. \tag{13}$$

Here $h.c.$ represents the hermitian conjugate of the first term, g is the weak gauge coupling constant, W is the charged gauge boson field,

$$\nu = \begin{pmatrix} \nu_e \\ \nu_\mu \\ \nu_\tau \end{pmatrix}, \quad \ell = \begin{pmatrix} e \\ \mu \\ \tau \end{pmatrix}, \quad U' = \begin{pmatrix} u' \\ c' \\ t' \end{pmatrix}, \text{ and } D' = \begin{pmatrix} d' \\ s' \\ b' \end{pmatrix}, \tag{14}$$

are the weak eigenstates, and the subscript L denotes the left-handed component of the particles. In the leptonic sector of L^{cc}, the weak eigenstates ν and ℓ are just the physical lepton fields. However, in the quark sector of L^{cc}, the weak eigenstates U' and D' are not the physical quark fields. The physical quark fields (the mass eigenstates) are

$$U = \begin{pmatrix} u \\ c \\ t \end{pmatrix} \quad \text{and} \quad D = \begin{pmatrix} d \\ s \\ b \end{pmatrix}, \tag{15}$$

which are linear combinations of the weak eigenstates. L^{cc} can be written in terms of the mass eigenstates as

$$L^{cc} = -\frac{g}{\sqrt{2}} \left[\bar{\nu}_L \gamma^\lambda \ell_L + \bar{U}_L \gamma^\lambda V_{CKM} D_L \right] W_\lambda^+ + h.c., \tag{16}$$

where

$$V_{CKM} = \begin{pmatrix} V_{ud} & V_{us} & V_{ub} \\ V_{cd} & V_{cs} & V_{cb} \\ V_{td} & V_{ts} & V_{tb} \end{pmatrix} \tag{17}$$

is the Cabibbo-Kobayashi-Maskawa (CKM) matrix [35, 36].

The leptons are naturally grouped into three doublets:

$$\begin{pmatrix} \nu_e \\ e^- \end{pmatrix}_L, \quad \begin{pmatrix} \nu_\mu \\ \mu^- \end{pmatrix}_L, \quad \begin{pmatrix} \nu_\tau \\ \tau^- \end{pmatrix}_L. \tag{18}$$

Only leptons from within the same doublet interact via the charge-changing interactions. Therefore, the only lepton transitions we have are $e^- \leftrightarrow \nu_e$, $\mu^- \leftrightarrow \nu_\mu$, $\tau^- \leftrightarrow \nu_\tau$ and their corresponding antilepton transitions.

The six quarks also form three doublets with the positively charged quarks as upper members and the negatively charged quarks as lower members:

$$\begin{pmatrix} u \\ d \end{pmatrix}_L, \quad \begin{pmatrix} c \\ s \end{pmatrix}_L, \quad \begin{pmatrix} t \\ b \end{pmatrix}_L. \tag{19}$$

Like the leptons, the quark weak eigenstates have transitions only between members of the same doublets. However, since the weak eigenstates are not the same

as the mass eigenstates, the charge-changing transitions of a quark are not exclusively from or to the other member of its doublet. For example, the u quark participates not only in the $u \leftrightarrow d$ transitions but also the $u \leftrightarrow s$ and $u \leftrightarrow b$ transitions. As a result, the u quark participates in transitions involving d quarks, s quarks and b quarks via the mixing

$$d'' = V_{ud}\, d + V_{us}\, s + V_{ub}\, b\,. \tag{20}$$

The nine matrix elements V_{ij} determine the strength of the quark mixing. They have to be determined by experiments and can be parametrized in terms of three mixing angles and one phase factor [37].

The electroweak sector of the standard model provides quantitative physical descriptions of all the electroweak phenomena and can explain many experimental data. Its predictions on the existence as well as the masses of $W^{\pm}$ and Z^0 have now been confirmed [38, 39, 40, 41]. Although it is still in the stage of undergoing further experimental tests and some of its predictions such as the existence of the Higgs boson still need to be confirmed, the standard model is now believed to be the correct theory of electromagnetic and weak interactions.

The standard model has many parameters. Among them are the fine structure constant α, the weak mixing angle θ_W, the masses of the quarks, leptons and Higgs boson, as well as the three quark mixing angles and the one phase factor that determine the strength of the quark flavor-changing processes. Without precise determination of these parameters, many phenomena cannot be fully understood. One example is CP-violation [42]. While the phase in the CKM matrix can give rise to the CP-violating decay in the neutral kaon system, it may not be the only source. Precise determination of the CKM matrix elements can help resolve this issue.

At present, the existing experimental values of many of the CKM elements are more or less model-dependent. Removing as much model-dependence as possible is important in improving the accuracy of the values. With the development of the heavy quark effective theory (HQET) [43, 44, 45, 46], it has become clear that the heavy quark symmetry in the heavy quark limit can help to remove much of

the model dependence from one of the CKM elements, V_{cb}.

1.5.2 Heavy Quark Symmetry and HQET

A system containing one heavy quark (e.g. c, b, t quarks whose masses are much larger than Λ_{QCD}) and other light constituents can be described as the heavy quark surrounded by a cloud of light quarks and gluons. This cloud which includes all the light degrees of freedom in the system is appropriately called the "brown muck" by Isgur and Wise for its complexity [45].

When the heavy quark (Q) in such a system is sufficiently heavy, its mass (m_Q) becomes irrelevant to the dynamics of the brown muck. This is because, as $m_Q \to \infty$, the velocity of the heavy quark is essentially the same as the velocity of the hadron. This means that in the rest frame of the hadron, the heavy quark is static. Therefore, the equations that describe the dynamics of the brown muck are just the equations that describe the light constituents moving in the color field of the static source at the location of the heavy quark. These equations are independent of m_Q. It follows that in the limit $m_Q \to \infty$, the dynamics of the brown muck is independent of the flavor of the heavy quark. In other words, the system is symmetric under the change of the heavy quark flavors, even if the masses of the heavy quarks are not equal. This is called the heavy quark flavor symmetry of the light degrees of freedom.

This symmetry has been seen often in QED. Isotopes of hydrogen, for example, are systems containing one heavy nucleus and one light electron. These isotopes have almost identical electronic structures even though the heavy nuclei in different isotopes have very different masses. In QCD, if applied to hadrons containing b and c quarks, this symmetry implies that the B mesons and D mesons (those mesons that contain one b quark and those contain one c quark respectively) with the same light quark should have similar spectra.

In the limit $m_Q \to \infty$, another symmetry of the light degrees of freedom arises: the heavy quark spin symmetry. This spin symmetry is the independence of the light degrees of freedom from the spin of the heavy quark. The spin of the heavy quark interacts with the brown muck through magnetic interactions between the

magnetic moment of the heavy quark and that of the brown muck. This is of the order of $1/m_Q$ and vanishes in the limit $m_Q \to \infty$. This results in the spin of the heavy quark becoming irrelevant to the dynamics of the brown muck in this limit. This symmetry has also been seen in QED. One example again is the hydrogen atom. The electronic spectrum of the hydrogen atom hardly depends on the nuclear spin. The hyperfine splitting caused by the flipping of the nuclear spin is only about 10^{-6} of the typical energy spacing in the spectrum.

The realization of the heavy quark flavor-spin symmetry has led to the development of the heavy quark effective theory (HQET) [43, 44, 45, 46]. This theory provides a simplified description of the physical systems in which a heavy quark interacts with light degrees of freedom by exchanging momenta much smaller than the heavy quark mass. It is an effective theory in the limit $m_Q \to \infty$ but also provides a systematic way to include the corrections to this limit as well as QCD radiative corrections.

In HQET, the momentum of the heavy quark in a hadron can be written as

$$P_Q^\mu = m_Q v^\mu + k^\mu , \tag{21}$$

where v is the four-velocity of the heavy quark. The quantity k is a residual momentum which is of the order of Λ_{QCD}, and is much smaller than m_Q. It measures the degree to which the heavy quark is off its mass shell. When the heavy quark interacts with the brown muck, k varies. It is, therefore, a measure of the momentum transfer between the heavy quark and the brown muck. Using this momentum relation, the full heavy quark propagator

$$S_Q = \frac{i\,(\not{P}_Q + m_Q)}{P_Q^2 - m_Q^2 + i\epsilon},$$

where $\not{P}_Q = \gamma \cdot P_Q$, becomes

$$S_Q = \frac{i}{v \cdot k + i\epsilon} + \mathcal{O}\left(\frac{1}{m_Q}\right) \tag{22}$$

in the effective theory.

Quantities that scale with the heavy quark mass become infinite in the formal limit that $m_Q \to \infty$. To construct an effective theory for systems containing heavy

quarks, it is, therefore, desirable to define physical quantities that are independent of the heavy quark mass. The states of the heavy quark are, therefore, specified by four-velocities instead of four-momenta. In the limit $m_Q \to \infty$, the effective heavy quark field $h_v^{(Q)}(x)$ is defined in terms of the QCD heavy quark field $Q(x)$ as

$$h_v^{(Q)}(x) = \frac{1+\not{v}}{2} e^{im_Q v\cdot x} Q(x), \tag{23}$$

where $1+\not{v}$ is present to project out the positive energy solution. The QCD Lagrangian for the heavy quark, $L_Q = \bar{Q}\,(i\not{D} - m_Q)\,Q$, therefore becomes

$$L_Q^{(eff)} = i\,\bar{h}_v^{(Q)}(x)\, v\cdot D\, h_v^{(Q)}(x). \tag{24}$$

For a system containing more than one heavy quark, the Lagrangian of the system should contain a term of $L_Q^{(eff)}$ from each heavy quark. This Lagrangian explicitly exhibits the heavy quark flavor and spin symmetry since neither m_Q nor γ-matrices are present.

HQET also provides a way to systematically include the corrections to the $m_Q \to \infty$ limit. For m_Q finite and large, the full heavy quark field $Q(x)$ and the generalization of $L_Q^{(eff)}$ in (24) is

$$Q(x) = e^{-im_Q v\cdot x}\left[1 + \frac{1}{iv\cdot D + 2m_Q - i\epsilon}\, i\not{D}_\perp\right] h_v^{(Q)}(x), \tag{25}$$

$$\begin{aligned} L_Q^{(HQET)} &= i\,\bar{h}_v^{(Q)}(x)\, v\cdot D\, h_v^{(Q)}(x) \\ &\quad + \bar{h}_v^{(Q)}(x)\, i\not{D}_\perp \frac{1}{iv\cdot D + 2m_Q - i\epsilon}\, i\not{D}_\perp\, h_v^{(Q)}(x). \end{aligned} \tag{26}$$

where $D_\perp^\mu = D^\mu - v^\mu\, v\cdot D$. One can expand $Q(x)$ and $L_Q^{(HQET)}$ in powers of $1/m_Q$ and thus include the $1/m_Q$ or higher order corrections to the limit $m_Q \to \infty$.

To apply HQET to hadronic states, in keeping with what we have done before, a new meson state $|\tilde{M}(v)>$ is defined to remove the heavy mass scale. $|\tilde{M}(v)>$ is related to the usual meson state $|M(p)>$ by

$$|\tilde{M}(v)> = m_M^{-1/2}\,|M(p)>, \tag{27}$$

where m_M denotes the mass of the meson. $|\tilde{M}(v)>$ and $|M(p)>$ therefore have different normalizations. In full QCD, meson states $|M(p)>$ are normalized so

that

$$< M(p')|M(p) >= 2p^0\,(2\pi)^3\,\delta^3(\mathbf{p}-\mathbf{p}')\,.$$

In HQET, the corresponding expression is

$$< \tilde{M}(v')|\tilde{M}(v) >= 2v^0\,(2\pi)^3\,\delta^3(\mathbf{p}-\mathbf{p}')\,.$$

1.5.3 Determination of V_{cb} by Semileptonic B Decays

One of the most important applications of HQET is to obtain one of the CKM matrix elements, V_{cb}, with little model-dependence.

The determination of V_{cb} requires observations of $b \to c$ transitions. Since quarks cannot be detected directly by experiments, such processes are observed through hadronic transitions $B \to D$. One way of determining V_{cb} is to measure the decay rates of exclusive semileptonic B decays $B \to D\ell\bar{\nu}$ or $B \to D^*\ell\bar{\nu}$ and extract V_{cb} from their theoretical expressions.

The effective Hamiltonian for the transition $b \to c\ell\bar{\nu}$ is

$$H_{eff} = \frac{G_F}{\sqrt{2}}\,V_{cb}\,\bar{c}\gamma_\mu(1-\gamma_5)b\;\bar{\ell}\gamma_\mu(1-\gamma_5)\nu\;. \tag{28}$$

Theoretically, the decay rates of the exclusive semileptonic B decays are therefore determined by V_{cb} and the current matrix elements [46, 47]

$$< D(v')|\bar{c}\gamma_\mu b|B(v) >= \sqrt{m_B m_D}\;\left[\xi_+(w)(v+v')_\mu + \xi_-(w)(v-v')_\mu\right]\;, \tag{29}$$

$$< D^*(v',\epsilon)|\bar{c}\gamma_\mu b|B(v) >= i\sqrt{m_B m_{D^*}}\;\xi_V(w)\;\varepsilon_{\mu\nu\alpha\beta}\;\epsilon^{*\nu}v'^{\alpha}v^{\beta}\;, \tag{30}$$

$$\begin{aligned} < D^*(v',\epsilon)|\bar{c}\gamma_\mu\gamma_5 b|B(v) >= \sqrt{m_B m_{D^*}}\;\Big[&\xi_{A_1}(w)(w+1)\epsilon^*_\mu - \xi_{A_2}(w)(\epsilon^*\cdot v)v_\mu \\ &-\xi_{A_3}(w)(\epsilon^*\cdot v)v'_\mu\Big]\;, \end{aligned} \tag{31}$$

where $w = v\cdot v'$, ϵ is the vector meson polarization and the $\xi_i(w)$ are six hadronic form factors. The form factors contain all the information about the B, D and D^* hadronic structures. At present, they are studied primarily by using models or the other approaches mentioned in Section 1.4. When using models, this leads

to model-dependent expressions of decay rates, which are written in terms of V_{cb} and the form factors as [46, 48, 49]

$$\frac{d\Gamma(B \to D\ell\bar{\nu})}{dq^2} = \frac{G_F^2|V_{cb}|^2}{24\pi^3} |\mathbf{P}_D|^3 \, |f_+(q^2)|^2 \, , \tag{32}$$

$$\frac{d\Gamma(B \to D^*\ell\bar{\nu})}{dq^2} = \frac{G_F^2|V_{cb}|^2}{96\pi^3} |\mathbf{P}_{D^*}| \, \frac{q^2}{m_B^2} \left(|H_+|^2 + |H_-|^2 + |H_0|^2\right) \, , \tag{33}$$

where $\mathbf{P}_D$ and $\mathbf{P}_{D^*}$ are the momenta of the D and D^* respectively in the rest frame of the B meson. The form factors $f_+(q^2)$, $H_\pm$ and H_0 are related to the $\xi_i(w)$ by

$$f_+(q^2) = \frac{1}{2\sqrt{m_B\, m_D}} \left[(m_B + m_D)\, \xi_+(w) - (m_B - m_D)\, \xi_-(w)\right] \, , \tag{34}$$

$$H_\pm = \sqrt{m_B\, m_{D^*}}\, (w+1)\, \xi_{A_1}(w) \mp \frac{m_B\, |\mathbf{P}_{D^*}|}{\sqrt{m_B\, m_{D^*}}}\, \xi_V(w) \, , \tag{35}$$

$$H_0 = \frac{m_B}{2\sqrt{m_B\, m_{D^*}\, q^2}} (m_B^2 - m_{D^*}^2 - q^2)\, (w+1)\, \xi_{A_1}(w) - 2|\mathbf{P}_{D^*}|^2 \left(\frac{m_B}{m_{D^*}} \xi_{A_3}(w) + \xi_{A_2}(w)\right) \, , \tag{36}$$

and q^2 is related to w by

$$w = \frac{(m_B^2 + m_D^2 - q^2)}{2 m_B m_D} \, , \tag{37}$$

where $m_{\bar{D}} = m_D$ for $B \to D\ell\bar{\nu}$ and $m_{\bar{D}} = m_{D^*}$ for $B \to D^*\ell\bar{\nu}$.

One can therefore extract V_{cb} by measuring the decay rates and comparing to the theoretical expressions. Clearly, the value of V_{cb} determined by this method is model-dependent because of the model-dependence in the form factors.

In HQET, a current operator $V^\mu = \bar{Q}'\, \Gamma^\mu Q$ has the form

$$V^\mu = \bar{h}_{v'}^{(Q')} \left[1 + \frac{1}{iv'\cdot\bar{D} + 2m_{Q'} - i\epsilon} i\, \bar{\not{D}}_\perp\right] \Gamma^\mu \left[1 + \frac{1}{iv\cdot\bar{D} + 2m_Q - i\epsilon} i\, \bar{\not{D}}_\perp\right] h_v^{(Q)} \, , \tag{38}$$

which can be expanded in powers of $1/m_Q$, $1/m_{Q'}$ as

$$V^\mu = \bar{h}_{v'}^{(Q')}\, \Gamma^\mu\, h_v^{(Q)}$$

$$-\bar{h}_{v'}^{(Q')}\left[\frac{1}{2m_Q}\Gamma^\mu i\vec{\not{D}}+\frac{1}{2m_{Q'}}i\bar{\not{D}}\Gamma^\mu\right]h_v^{(Q)}$$
$$+\mathcal{O}(1/m_Q^2)+\mathcal{O}(1/m_{Q'}^2)\,. \tag{39}$$

The equations (25—27) and (38—39) lead to many simplifications when hadronic matrix elements of heavy quark operators are considered. One very important example of this is the form factors for the weak decays of beauty mesons to those containing charm. At leading order in the above expansions, it is found that

$$\xi_+(w)=\xi_V(w)=\xi_{A_1}(w)=\xi_{A_3}(w)=\xi(w)\,, \tag{40}$$
$$\xi_-(w)=\xi_{A_2}(w)=0\,, \tag{41}$$

with

$$\xi(w)\Big|_{w=1}=1\,. \tag{42}$$

The fact that a single universal form factor $\xi(w)$ remains in equations (29)—(36) shows that HQET has removed much of the model-dependence from the theoretical expressions of the decay rates. Furthermore, at the point of zero recoil where $w=1$, (32) and (33) imply [46, 47]

$$\lim_{w\to1}\frac{1}{(w^2-1)^{3/2}}\frac{d\Gamma(B\to D\ell\bar{\nu})}{dw}=\frac{G_F^2|V_{cb}|^2}{48\,\pi^3}(m_B+m_D)^2\,m_D^3\,\Big|\xi(w=1)\Big|^2, \tag{43}$$
$$\lim_{w\to1}\frac{1}{\sqrt{w^2-1}}\frac{d\Gamma(B\to D^*\ell\bar{\nu})}{dw}=\frac{G_F^2|V_{cb}|^2}{4\,\pi^3}(m_B-m_{D^*})^2\,m_{D^*}^3\,\Big|\xi(w=1)\Big|^2. \tag{44}$$

Since the Isgur-Wise function is normalized at $w=1$ as shown in (42), the theoretical expressions for the decay rates are model-independent at this point of zero recoil. Although direct measurement at this point is experimentally difficult, one can take measurements close to zero recoil and then extrapolate to the zero recoil decay rate. Such extrapolation is model-dependent. But the model-dependence is not large. As a result, V_{cb} extracted in this way is relatively model-independent. However, we need to keep in mind that this simplicity results from the limit $m_b,\,m_c\to\infty$. Precise determination of V_{cb} requires corrections to this limit. In the framework of HQET, such higher order corrections can be systematically included [46, 47]. It is found that, as a consequence of Luke's theorem [50], the

$1/m_Q$ corrections to the decay rates vanish at zero recoil. Thus the leading power corrections to the heavy quark limit are of order $1/m_Q^2$.

1.6 The Present Work

The objective of this work is to construct a model for heavy mesons which can be used eventually to calculate the weak decay amplitudes and extract V_{cb} from experimental data by means of HQET. Such a model should be covariant to allow the extraction of the form factors from the weak decay amplitudes (43) and (44). It should also be constructed so that the Isgur-Wise function $\xi(w)$ can be calculated in a well defined way.

In order to obtain $\xi(w)$, one needs to find the bound state wave function of the heavy mesons. This requires understanding the interactions of quarks and gluons within the heavy mesons. As introduced in Section 1.4, various approaches have been developed to study QCD, and we are interested in the quark potential approach which provides a direct and simple picture of the physics. A model that has been quite successful in predicting the mesonic spectra is the relativized constituent quark model of Godfrey and Isgur [25]. Indeed, it was this model and its applications to weak decays [51] that originally suggested the existence of heavy-quark symmetries, which in turn led to HQET. This model provides relativistic kinematic corrections to the standard nonrelativistic quark model using a linear confining potential and a color Coulomb interaction. Meson spectra calculated with this model are remarkably close to experimental masses in all flavor sectors. However, this model is not covariant.

In the present work, a covariant extension to the Godfrey-Isgur model is constructed using the spectator or Gross equation [1]. This equation has been used with some success in models of the nucleon-nucleon interaction [52, 53], as well as in quark models of mesons composed of equal mass quarks and antiquarks [54, 55, 56]. It is a quasipotential equation, and can be related to the Bethe-Salpeter equation by placing one of the intermediate-state particles on the positive-energy mass-shell. This has the advantages that the prescribed constraint

on the relative energy is manifestly covariant and that in the limit that the mass of one constituent goes to infinity (the static limit), the wave equation reduces to the Dirac equation for the light particle [57].

To construct the model, we use the Gross equation as a basis for derivation of a wave equation for the system. The Bethe-Salpeter kernel is assumed to be the one-gluon exchange interaction plus the scalar linear confining potential as in (12). To compare our model with the predictions of HQET, we extract the meson Hamiltonians using the $1/m_Q$ expansion and calculate the meson spectra and wave functions perturbatively.

In Chapter 2, we introduce the Bethe-Salpeter formalism and the spectator equation which lays down the foundation of the model. In Chapter 3, we present our model by deriving the heavy meson Hamiltonian and obtain the wave functions. In Chapter 4, we present our results for heavy meson spectra.

Chapter 2

Formalism

2.1 The Bethe-Salpeter Equation

Consider two particles scattering through the exchange of bosons. The incoming and outgoing four-momenta of the two particles are represented by p_1', p_2' and p_1, p_2 respectively. The exact description of the interaction of the two particles during the scattering process is described by an infinite number of Feynman diagrams representing all possible ways of exchanging bosons between the two particles. Figure. 3 shows some examples of these diagrams. In these diagrams, the solid lines represent the two interacting particles. The dotted lines represent the bosons exchanged during the interactions. The lines and vertices are associated with Feynman rules which allow calculation of the contribution of each diagram

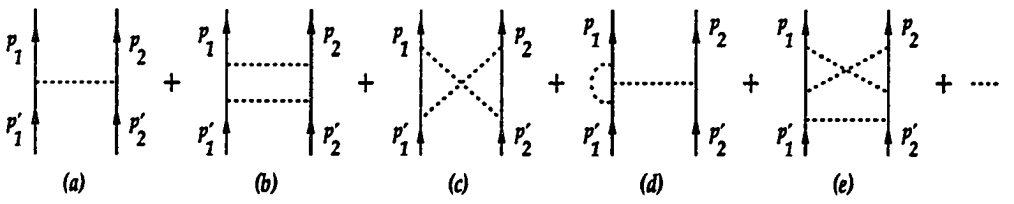

Figure 3: Some examples of Feynman diagrams for the scattering of two particles by exchanging bosons.

to the scattering amplitude.

The infinite sum of Feynman diagrams can be divided into two classes [26]. A Feynman diagram is called a two-particle irreducible diagram if it cannot be split into two simpler diagrams by drawing a line which cuts each of the two particle lines only once and does not cut any boson line. All other diagrams are called reducible diagrams. In Figure 3, (a), (c) and (d) are irreducible Feynman diagrams; (b) and (e) are reducible since (b) can be split into two diagrams of (a), and (e) can be split into one (a) with one (c). It should be noted that all reducible diagrams can be represented by iteration of irreducible diagrams. This can be used to sum all contributions by writing the two-particle scattering amplitude $\mathcal{M}$ as an integral equation called the Bethe-Salpeter equation [26]:

$$\mathcal{M}(p,p';P) = V^{BS}(p,p';P) + i\int \frac{d^4k}{(2\pi)^4} V^{BS}(p,k;P)G^{BS}(k;P)\mathcal{M}(k,p';P)\,. \quad (45)$$

Written in terms of matrices, this equation has the form

$$\mathcal{M} = V^{BS} + V^{BS}G^{BS}\mathcal{M}\,. \quad (46)$$

Iteration of this equation gives the infinite series

$$\mathcal{M} = V^{BS} + V^{BS}G^{BS}V^{BS} + V^{BS}G^{BS}V^{BS}G^{BS}V^{BS} + \cdots\cdots\,. \quad (47)$$

In (45), $p = \frac{1}{2}(p_1 - p_2)$, $p' = \frac{1}{2}(p_1' - p_2')$ and $k = \frac{1}{2}(k_1 - k_2)$. P is the total four-momentum of the two-particle system which is conserved during the scattering process and, therefore, has $P = p_1' + p_2' = p_1 + p_2$. V^{BS} is the Bethe-Salpeter kernel which is represented by the sum of all two-body irreducible Feynman diagrams. G^{BS} is the Bethe-Salpeter two-body propagator. When the two interacting particles are fermions, $G^{BS}(k;P) = S_F^{(1)}(k_1,m_1)S_F^{(2)}(k_2,m_2)$, where $S_F^{(i)}(k_i,m_i)$ is the free Dirac propagator for particle i as given in Appendix A and m_i is the mass of particle i. The Bethe-Salpeter equation is represented by the Feynman diagrams of Figure 4 . From this figure, one can see that the particles with four-momenta p_i and p_i' are the external particles; the particles with four-momentum k_i are the intermediate-state particles. In the Bethe-Salpeter equation, the intermediate-state particles are off-shell which means that the on-shell condition $k_i^2 = m_i^2$ is not satisfied.

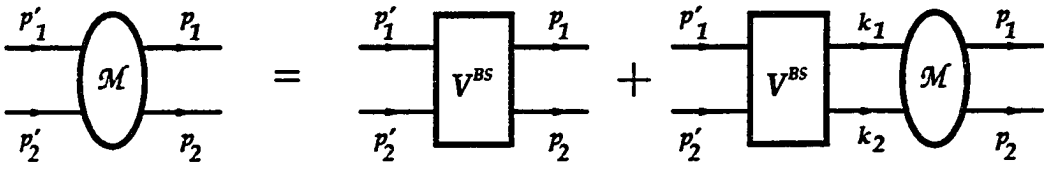

Figure 4: Feynman diagrams representing the Bethe-Salpeter equation for the scattering amplitude.

A bound state with mass W produces a pole in the scattering amplitude at $P^2 = W^2$. One can therefore study the bound state by studying the pole. Separating the pole from the rest of the $\mathcal{M}$ matrix gives

$$\mathcal{M}(p,p';P) = \frac{\Gamma(p;P)\Gamma^{\dagger}(p';P)}{P^2 - W^2 + i\eta} + \mathcal{R}(p,p';P)\ , \tag{48}$$

where $\mathcal{R}(p,p';P)$ is the regular part of the scattering matrix and all the information about the pole, and therefore about the bound state, is contained in the first term. Substituting (48) into the Bethe-Salpeter equation (45), one obtains

$$\begin{aligned}
&\frac{\Gamma(p;P)\Gamma^{\dagger}(p';P)}{P^2 - W^2 + i\eta} + \mathcal{R}(p,p';P) \\
&= V^{BS}(p,p';P) + i\int \frac{d^4k}{(2\pi)^4} V^{BS}(p,k;P) G^{BS}(k;P) \\
&\qquad \cdot \left(\frac{\Gamma(k;P)\Gamma^{\dagger}(p';P)}{P^2 - W^2 + i\eta} + \mathcal{R}(p,p';P) \right),
\end{aligned} \tag{49}$$

where Γ is the bound-state vertex function. Multiplying both sides of the equation by $P^2 - W^2 + i\eta$, we can see that at the pole of the $\mathcal{M}$ matrix, where $P^2 = W^2$, Γ satisfies the homogeneous equation

$$\Gamma(p;P) = i\int \frac{d^4k}{(2\pi)^4} V^{BS}(p,k;P)\ G^{BS}(k;P)\ \Gamma(k;P)\ . \tag{50}$$

This is called the Bethe-Salpeter equation for the bound-state vertex function. It can be written in terms of matrices as

$$\Gamma = V^{BS} G^{BS} \Gamma\ , \tag{51}$$

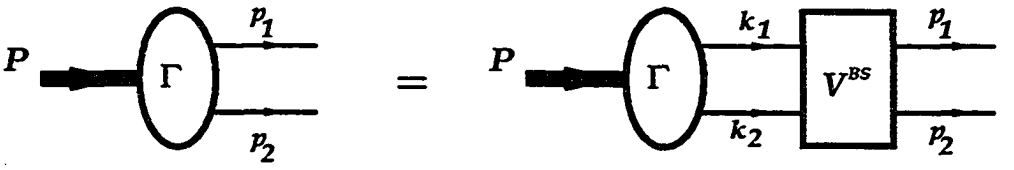

Figure 5: Feynman diagrams representing the Bethe-Salpeter equation for the bound state vertex function.

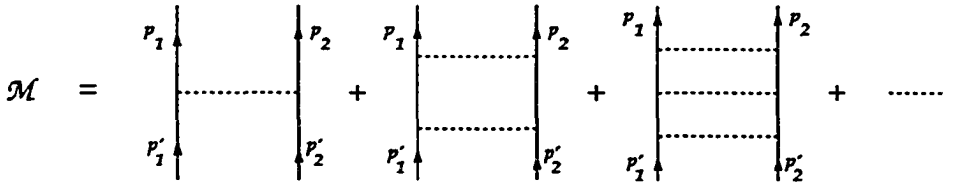

Figure 6: The Bethe-Salpeter scattering amplitude in the ladder approximation.

and is represented by the Feynman diagram of Figure 5.

The Bethe-Salpeter bound state wave function is defined to be

$$\psi(p,P) = G^{BS}(p;P)\Gamma(p;P) \ . \tag{52}$$

The Bethe-Salpeter equation (50) is an exact equation for the two-body relativistic bound-state problem. However, solving the equation involves the calculation of an infinite number of irreducible Feynman diagrams for the kernel which is, in general, impractical. In practice, it is therefore necessary to approximate the kernel so that the equation is solvable. The most common and simpliest approximation is to keep only the lowest order irreducible Feynman diagram in the perturbation expansion of the kernel which is the one-boson exchange diagram shown in Figure 3 (a). This approximation is often referred to as the ladder approximation because by making such an approximation, the infinite series of $\mathcal{M}$, (47), is represented by a series of Feynman diagrams that look like ladders as shown in Figure 6.

The solution of the Bethe-Salpeter equation in the ladder approximation loses

one important property that the full Bethe-Salpeter equation has. This lost property is called the one-body limit and it can be understood by studying a system consisting of one heavy and one light Dirac particle. In the limit that the mass of the heavy particle goes to infinity, such a system reduces to one light Dirac particle moving in a fixed potential. Thus in this limit, the equation for the heavy-light system should also be reduced to a one-body Dirac equation for the light particle. This is the correct one-body limit. For the study of a heavy-light system, as well as the application of the heavy quark symmetry, the one-body limit is an important property for the equation of the system. It is therefore necessary to recover this limit which is lost while making the ladder approximation. This is often accomplished by the procedure of quasipotential reduction.

2.2 Quasipotential Reduction

The Bethe-Salpeter equation (46) can be rewritten as two equations in terms of a new two-body propagator (G) and a new kernel (V) :

$$\mathcal{M} = V + VG\mathcal{M} \,, \tag{53}$$

$$V = V^{BS} + V^{BS}\left(G^{BS} - G\right)V \,. \tag{54}$$

Too see this, first note that (53) can be iterated and rearranged into an equivalent equation

$$\mathcal{M} = V + \mathcal{M}GV \,. \tag{55}$$

We then rewrite the Bethe-Salpeter equation (46) and equation (55) so that (46) becomes

$$\mathcal{M} = \left(1 - V^{BS}G^{BS}\right)^{-1} V^{BS} \,, \tag{56}$$

and (55) becomes

$$\mathcal{M} = V\left(1 - GV\right)^{-1} \,. \tag{57}$$

Assuming (53) has the same solution as the Bethe-Salpeter equation (46), the scattering amplitude $\mathcal{M}$ in (56) and (57) should therefore be the same,

$$\left(1 - V^{BS}G^{BS}\right)^{-1} V^{BS} = V\left(1 - GV\right)^{-1} \,. \tag{58}$$

Multiplying this equation by $\left(1 - V^{BS}G^{BS}\right)$ from the left and $\left(1 - GV\right)$ from the right gives (54) .

Therefore, assuming that (53) has the same solution as the Bethe-Salpeter equation (46) has led to the restriction on G and V by (54). In other words, (53) is completely equivalent to the Bethe-Salpeter equation (46) provided G and V satisfy (54).

Rewritting the Bethe-Salpeter equation as two equations (53) and (54) has allowed useful reductions to be made. Such reductions are often made to the two-body propagator G so that $G^{BS} - G$ is small enough to omit the second term in (54) and $V = V^{BS}$ is obtained. By doing so, the Bethe-Salpeter equations for the scattering amplitude and the vertex function are reduced to

$$\mathcal{M} = V^{BS} + V^{BS}G\mathcal{M} \; . \tag{59}$$

$$\Gamma = V^{BS}G\,\Gamma \; . \tag{60}$$

Written as integral equations, (59) and (60) are

$$\mathcal{M}(p,p';P) = V^{BS}(p,p';P) + i\int \frac{d^4k}{(2\pi)^4} V^{BS}(p,k;P)G(k;P)\mathcal{M}(k,p';P)\,, \tag{61}$$

$$\Gamma(p;P) = i\int \frac{d^4k}{(2\pi)^4} V^{BS}(p,k;P)\,G(k;P)\,\Gamma(k;P)\,. \tag{62}$$

This procedure of reducing the Bethe-Salpeter equation is called quasipotential reduction [58, 59, 60]. The resulting equations are called quasipotential equations.

As can be seen in (59) and (60), making different choices of G results in different quasipotential equations. Since some of the properties of the full Bethe-Salpeter equation would be undoubtly omitted while making the approximation on G, different quasipotential equations are usually used according to the systems that are being studied, so that the important physics of the systems would not be omitted while making the approximations. Various quasipotential equations have been developed. Among them, the Blankenbecler-Sugar equation [61] is a well known equation for studying relativistic scattering and production processes. However,

this equation is specifically constructed for equal mass systems. A straight forward extension to unequal mass systems loses the one-body limit as the mass of one of the particles approaches infinity.

Since it is desirable to use an equation with the correct one-body limit for studying heavy-light systems, many equations are constructed to preserve this limit. Among them, we have used the Gross or the spectator equation [1] to construct our model. In addition, we have investigated the Wallace-Mandelzweig equation [62] and the Cooper-Jennings equation [63]. (The results are presented in Appendix F.) In particular, the Cooper-Jennings equation is explicitly constructed to agree with the Blankenbecler-Sugar equation in the equal mass limit but also has the correct one-body limit. By comparing our model to these equations, we find that the Hamiltonians resulting from the Gross equation are more reasonable and have simpler physical interpretations.

There exist varieties of quasipotential equations. Which one has the best result compared to the Bethe-Salpeter equation? As stated by Brown and Jackson [64]: "There are too many degrees of freedom in the problem to expect that this question will have an unambiguous answer. The coupling constant and mass of the exchanged-boson or -bosons, the number of irreducible diagrams included, and the range of kinematic variables to be considered will all have a role to play in the determination of the best approximate equation."

2.3 The Gross Equation

From the derivation of (53—60), one can see that it is crucial to choose G so that the omission of the second term in (54) is a good approximation. Consider a series expansion of the quasipotential kernel in the boson-fermion coupling constant. The kernel, (54) can be expanded as

$$V = V^{BS(2)} + V^{BS(4)} + V^{BS(2)}\left(G^{BS} - G\right)V^{(2)} + \cdots\cdots . \qquad (63)$$

Gross has chosen the two-body propagator G based on the criteria [57]:

(1) The resulting equation has the correct one-body limit;

(2) The series expansion of the kernel converges rapidly as the number of terms approaches infinity. Since practical calculations in nuclear physics rarely go beyond 4 terms in the series, this criterion is that the fourth order kernel be as small as possible, and in particular, vanishes in the one-body limit;

(3) The kernel is independent of energy;

(4) The kernel is well defined with no spurious singularities.

The Gross equation can be obtained from the Bethe-Salpeter equation by placing one of the particles on its positive-energy mass shell.

When the two interacting particles are both Dirac particles, and the particle being put on shell is particle 2, the Gross two-body propagator is

$$G(k;P) = S_F^{(1)}(k_1,m_1)\left[(-2\pi i)\delta\left(k_2^0 - E(\mathbf{k_2},m_2)\right)\frac{\gamma^{(2)}\cdot k_2 + m_2}{2E(\mathbf{k_2},m_2)}\right]. \qquad (64)$$

where $E(\mathbf{k},m) = \sqrt{\mathbf{k}^2+m^2}$ is the on shell energy for a particle with momentum $\mathbf{k}$ and mass m.

Putting $G(k;P)$ in (62) and carrying out the integral over dk^0, the spectator vertex function for particle 2 being on shell is

$$\Gamma(\check{p};P) = \int \frac{d^3k}{(2\pi)^3}\frac{m_2}{E(\mathbf{k_2},m_2)}V(\check{p},\check{k};P)S_F^{(1)}(\check{k}_1,m_1)\Lambda^{+(2)}(\check{k}_2,m_2)\Gamma(\check{k};P), \qquad (65)$$

where $\check{k}_1$, $\check{k}_2$, $\check{k}$ and $\check{p}$ represent k_1, k_2, k and p for particle 2 being on shell,

$$\check{k}_2 = \left(E(\mathbf{k_2},m_2),\ \mathbf{k_2}\right), \qquad (66)$$

$$\check{k}_1 = \left(P^0 - E(\mathbf{k_2},m_2),\ \mathbf{k_1}\right), \qquad (67)$$

$$\check{k} = \left(\frac{P^0}{2} - E(\mathbf{k_2},m_2),\ \mathbf{k}\right), \qquad (68)$$

$$\check{p} = \left(\frac{P^0}{2} - E(\mathbf{p_2},m_2),\ \mathbf{p}\right), \qquad (69)$$

$$\Lambda^{+(2)}(k_2,m_2) = \sum_{m'_{s_2}} u^{(2)}(\mathbf{k_2},m'_{s_2})\bar{u}^{(2)}(\mathbf{k_2},m'_{s_2})\ . \qquad (70)$$

In (70) , $u^{(2)}(\mathbf{k_2},m'_{s_2})$ is the Dirac spinor for particle 2, as defined in Appendix A, and m'_{s_2} is the spin projection of the particle along the z axis.

Equation (65) is covariant since the constraint of having one particle on shell is itself covariant. So the covariance of the full Bethe-Salpeter equation is preserved. This equation can therefore be used to study relativistic effects.

Chapter 3

The Meson Hamiltonians

In this chapter, we present our model by deriving and solving the Hamiltonians for the heavy meson systems. We will use different techniques for the heavy-light mesons ($Q\bar{q}$, $q\bar{Q}$) and for the heavy-heavy mesons ($Q\bar{Q}$). The Hamiltonians are expanded in powers of $1/m_Q$ so that heavy quark symmetry can be studied and the model can be used to extract V_{cb} according to HQET, in the future.

We derive the Hamiltonian for the meson systems from the spectator vertex equation (65) . For our model the heavy quark (particle 2) is placed on shell while the light quark (particle 1) remains off shell.

As introduced in Section 2.3, the spectator vertex function for particle 2 being on shell can be written as

$$\Gamma(\check{p};P) = \int \frac{d^3k}{(2\pi)^3} \sum_{m'_{s_2}} \frac{m_2}{E(\mathbf{k_2},m_2)} V(\check{p},\check{k};P) u^{(2)}(\mathbf{k_2},m'_{s_2}) \\ S_F^{(1)}(\check{k}_1,m_1)\bar{u}^{(2)}(\mathbf{k_2},m'_{s_2})\Gamma(\check{k};P) \ , \qquad (71)$$

where we have substituted the explicit form of $\Lambda^{+(2)}(\check{k}_2,m_2)$ into the spectator vertex equation (65) .

The kernel $V(\check{p},\check{k},P)$ in our model is the sum of the scalar confining potential and the one gluon exchange potential as in (12),

$$V(\check{p},\check{k};P) = V_s(Q^2) + \gamma^{(1)}\cdot\gamma^{(2)}V_v(Q^2) \ , \qquad (72)$$

where

$$Q^2 = (\mathbf{k}-\mathbf{p})^2 - \Big(E(\mathbf{k_2},m_2) - E(\mathbf{p_2},m_2)\Big)^2 \,. \tag{73}$$

This choice of interaction assumes that the Lorentz gauge is used in the color Coulomb interaction.

3.1 $Q\bar{q}$ and $q\bar{Q}$ Mesons

3.1.1 Deriving the Hamiltonian

To study $Q\bar{q}$ and $q\bar{Q}$ mesons, we define the spectator wave function for the bound states as

$$\psi_{m_{s_2}}(\check{p},P) = S_F^{(1)}(\check{p}_1,m_1)\,\bar{u}^{(2)}(\mathbf{p_2},m_{s_2})\,\Gamma(\check{p};P)\,. \tag{74}$$

The spectator equation (71) can then be written in terms of the wave function as

$$S_F^{(1)^{-1}}(\check{p}_1,m_1)\,\psi_{m_{s_2}}(\check{p},P) = \int \frac{d^3k}{(2\pi)^3}\frac{m_2}{E(\mathbf{k_2},m_2)}\sum_{m'_{s_2}} V_{m_{s_2}m'_{s_2}}(\check{p},\check{k};P)\psi_{m'_{s_2}}(\check{k},P)\,, \tag{75}$$

where

$$V_{m_{s_2}m'_{s_2}}(\check{p},\check{k};P) = \bar{u}^{(2)}(\mathbf{p_2},m_{s_2})\,V(\check{p},\check{k};P)\,u^{(2)}(\mathbf{k_2},m'_{s_2})\,. \tag{76}$$

This wave equation is covariant and can be easily boosted from frame to frame. We will work in the bound-state rest frame since it is generally easier to solve the wave equation in this frame where the angular expansions of the wave function and potential are defined. Also, since we wish to examine the approach to the limit $m_2 \to \infty$, it is useful to rewrite this equation in a noncovariant form by defining

$$\Psi_{m_{s_2}}(\check{p},P) = \sqrt{\frac{m_2}{E(\mathbf{p_2},m_2)}}\,\psi_{m_{s_2}}(\check{p},P) \tag{77}$$

and

$$U_{m_{s_2}m'_{s_2}}(\check{p},\check{k};P) = \sqrt{\frac{m_2}{E(\mathbf{p_2},m_2)}}V_{m_{s_2}m'_{s_2}}(\check{p},\check{k};P)\sqrt{\frac{m_2}{E(\mathbf{k_2},m_2)}} \tag{78}$$

to give

$$S_F^{(1)^{-1}}(\check{p}_1, m_1)\Psi_{m_{s_2}}(\check{p}, P) = \int \frac{d^3k}{(2\pi)^3} \sum_{m'_{s_2}} U_{m_{s_2} m'_{s_2}}(\check{p}, \check{k}; P)\Psi_{m'_{s_2}}(\check{k}, P) \qquad (79)$$

Using the explicit form of the Dirac spinors in (79) and the Dirac γ-matrices to reduce particle 2 to the Pauli spin space, and defining a wave function which is an operator in the Dirac space of particle 1 and the Pauli space of particle 2, $\Psi = \sum_{m'_{s_2}} \chi_{m'_{s_2}} \Psi_{m'_{s_2}}$, (79) becomes

$$(\gamma^{(1)} \cdot \check{p}_1 - m_1)\, \Psi(\check{p}, P) = \int \frac{d^3k}{(2\pi)^3} U(\check{p}, \check{k}; P)\, \Psi(\check{k}, P)\,, \qquad (80)$$

where

$$\begin{aligned} U(\check{p}, \check{k}; P) = & \left[\frac{\left(E(\mathbf{p_2}, m_2) + m_2\right)\, \left(E(\mathbf{k_2}, m_2) + m_2\right)}{4\, E(\mathbf{p_2}, m_2)\, E(\mathbf{k_2}, m_2)} \right]^{\frac{1}{2}} \\ & \times \left\{ \left[1 - \frac{\boldsymbol{\sigma}^{(2)} \cdot \mathbf{p_2}\, \boldsymbol{\sigma}^{(2)} \cdot \mathbf{k_2}}{\left(E(\mathbf{p_2}, m_2) + m_2\right)\, \left(E(\mathbf{k_2}, m_2) + m_2\right)} \right] V_s(Q^2) \right. \\ & + \gamma^{(1)^0} \left[1 + \frac{\boldsymbol{\sigma}^{(2)} \cdot \mathbf{p_2}\, \boldsymbol{\sigma}^{(2)} \cdot \mathbf{k_2}}{\left(E(\mathbf{p_2}, m_2) + m_2\right)\, \left(E(\mathbf{k_2}, m_2) + m_2\right)} \right] V_v(Q^2) \\ & \left. - \boldsymbol{\gamma}^{(1)} \cdot \left[\frac{\boldsymbol{\sigma}^{(2)} \cdot \mathbf{p_2}\, \boldsymbol{\sigma}^{(2)}}{E(\mathbf{p_2}, m_2) + m_2} + \frac{\boldsymbol{\sigma}^{(2)}\, \boldsymbol{\sigma}^{(2)} \cdot \mathbf{k_2}}{E(\mathbf{k_2}, m_2) + m_2} \right] V_v(Q^2) \right\}. \end{aligned} \qquad (81)$$

Expanding (80) to order $1/m_2$, we find

$$\begin{aligned} & \left[\gamma^{(1)^0} \left(P^0 - m_2 - \frac{\mathbf{p_2}^2}{2m_2} \right) - \boldsymbol{\gamma}^{(1)} \cdot \mathbf{p_1} - m_1 \right] \Psi(\check{p}, P) = \\ & \int \frac{d^3k}{(2\pi)^3} \left[V_s(\mathbf{q}^2) + \gamma^{(1)^0} V_v(\mathbf{q}^2) \right. \\ & \left. - \frac{1}{2m_2} \boldsymbol{\gamma}^{(1)} \cdot \left(\boldsymbol{\sigma}^{(2)} \cdot \mathbf{p_2}\, \boldsymbol{\sigma}^{(2)} + \boldsymbol{\sigma}^{(2)}\, \boldsymbol{\sigma}^{(2)} \cdot \mathbf{k_2} \right) V_v(\mathbf{q}^2) \right] \Psi(\check{k}, P), \end{aligned} \qquad (82)$$

where $\mathbf{q} = \mathbf{k_1} - \mathbf{p_1} = \mathbf{p_2} - \mathbf{k_2}$, and we have expanded $V(Q^2)$ by Taylor expansion

$$\begin{aligned} V(Q^2) &= V(\mathbf{q}^2) + \left(Q^2 - \mathbf{q}^2 \right) V'(\mathbf{q}^2) + \cdots\cdots \\ &= V(\mathbf{q}^2) - \frac{1}{4m_2^2} \left(\mathbf{p_2}^2 - \mathbf{k_2}^2 \right)^2 V'(\mathbf{q}^2) + \mathcal{O}(1/m_2^3)\,. \end{aligned} \qquad (83)$$

Since we are working in the bound state rest frame in which $P = (W, \mathbf{0})$, $\mathbf{p}_1 = -\mathbf{p}_2 = \mathbf{p}$, $\mathbf{k}_1 = -\mathbf{k}_2 = \mathbf{k}$, $\check{p}^0 = W/2 - E(\mathbf{p}, m_2)$ and $\check{k}^0 = W/2 - E(\mathbf{k}, m_2)$, where W is the bound-state mass, the wave equation (82) can be written as

$$\left[\gamma^{(1)^0}\left(W - m_2 - \frac{\mathbf{p}^2}{2m_2}\right) - \boldsymbol{\gamma}^{(1)}\cdot\mathbf{p} - m_1\right]\Psi(\mathbf{p}) = \int \frac{d^3k}{(2\pi)^3} U(\mathbf{p},\mathbf{k})\,\Psi(\mathbf{k}). \quad (84)$$

Here

$$U(\mathbf{p},\mathbf{k}) = V_s(\mathbf{q}^2) + \gamma^{(1)^0}V_v(\mathbf{q}^2) + \frac{1}{2m_2}\boldsymbol{\gamma}^{(1)}\cdot\left(2\mathbf{k} - \mathbf{q} + i\mathbf{q}\times\boldsymbol{\sigma}^{(2)}\right)V_v(\mathbf{q}^2), \quad (85)$$

and we have used the relations

$$\boldsymbol{\sigma}^{(i)}\cdot\mathbf{p}_i\,\boldsymbol{\sigma}^{(i)} + \boldsymbol{\sigma}^{(i)}\,\boldsymbol{\sigma}^{(i)}\cdot\mathbf{k}_i = \mathbf{p}_i + \mathbf{k}_i + i\left(\mathbf{k}_i - \mathbf{p}_i\right)\times\boldsymbol{\sigma}^{(i)}, \quad (86)$$

and

$$\Psi(\check{p}, P) = \Psi(\check{p}^0, \mathbf{p}, P^0, \mathbf{P}) = \Psi\left(\frac{W}{2} - E(\mathbf{p}, m_2), \mathbf{p}, W, \mathbf{0}\right) = \Psi(\mathbf{p}). \quad (87)$$

Equation (84) can be Fourier transformed to coordinate space, multiplied from the left by $\gamma^{(1)^0}$ and then rearranged to give the wave equation

$$H\Psi(\mathbf{r}) = W\Psi(\mathbf{r}), \quad (88)$$

where the hermitian Hamiltonian is $H = H_0 + H_1$ with

$$H_0 = \boldsymbol{\alpha}^{(1)}\cdot\frac{1}{i}\boldsymbol{\nabla} + \beta^{(1)}m_1 + \beta^{(1)}V_s(r) + V_v(r) + m_2, \quad (89)$$

$$H_1 = \frac{1}{2m_2}\left[-\nabla^2 - i\left\{V_v(r), \boldsymbol{\alpha}^{(1)}\cdot\boldsymbol{\nabla}\right\} + \boldsymbol{\alpha}^{(1)}\cdot\boldsymbol{\sigma}^{(2)}\times\hat{\mathbf{r}}V_v'(r)\right], \quad (90)$$

and $\hat{\mathbf{r}}$ is the unit vector in the radial direction. Note that H_0 is the Hamiltonian in the heavy quark limit $m_2 \to \infty$, and H_1 is the first order correction to this limit.

In H_0 and H_1, $V_s(r)$ and $V_v(r)$ are the scalar and vector potentials as introduced in Chapter 1,

$$V_s(r) = br + c, \quad (91)$$

$$V_v(r) = -\frac{4}{3}\frac{\alpha_s(r)}{r}, \quad (92)$$

In most nonrelativistic models, $\alpha_s(r)$ has been approximated as an r-independent constant. The Godfrey-Isgur model parameterizes $\alpha_s(Q^2)$ as [25]

$$\alpha_s(Q^2) = \sum_k \alpha_k e^{-Q^2/4\gamma_k^2} , \tag{93}$$

so that the Fourier transformation of $V_v(Q^2)$, (92) is obtained with $\alpha_s(r)$ given by

$$\alpha_s(r) = \sum_k \alpha_k \frac{2}{\sqrt{\pi}} \int_0^{\gamma_k r} e^{-x^2} dx \ = \sum_k \alpha_k \ \mathrm{erf}(\gamma_k r) . \tag{94}$$

In our model, we adopt the same approach as that of Godfrey and Isgur in treating $\alpha_s(r)$.

3.1.2 Solving the Wave Equation

The eigenstates and eigenenergies of the hamiltonian H determined by (88) can be calculated directly. However, the objective of the calculations presented here is to produce wave functions which can be used in the calculation of form factors and decay constants as an expansion in powers of the inverse of the heavy quark mass m_2. In order to maintain consistency in this expansion, we calculate the masses and wave functions perturbatively. To do so, we first solve the unperturbed equation

$$H \ \Psi^{(0)}(\mathbf{r}) = W^{(0)} \ \Psi^{(0)}(\mathbf{r}), \tag{95}$$

to get the zeroth order bound state mass and wave function, $W^{(0)}$ and $\Psi^{(0)}$. We then treat H_1 as a perturbation and calculate the first order correction

$$W^{(1)} = \int d^3r \ \Psi^{(0)\dagger}(\mathbf{r}) \ H_1 \ \Psi^{(0)}(\mathbf{r}). \tag{96}$$

The bound state mass to first order is then

$$W = W^{(0)} + W^{(1)}. \tag{97}$$

Solving the Unperturbed Equation

The operators

$$\left\{K^{(1)}, \mathbf{j}^{(1)^2}, j_z^{(1)}, S^{(2)^2}, S_z^{(2)}\right\}, \tag{98}$$

$$\left\{K^{(1)}, \mathbf{j}^{(1)^2}, S^{(2)^2}, J^2, J_z\right\} \tag{99}$$

are two sets of mutually commuting operators which also commute with H_0. We can therefore find two sets of simultaneous eigenvectors of these operators. They are labeled by the corresponding set of quantum numbers as $\left|n\kappa_1 j_1 m_{j_1} s_2 m_{s_2}\right\rangle$ and $\left|n\kappa_1 j_1 s_2 J M_J\right\rangle$. Here $K^{(1)} = \beta^{(1)}\left(\mathbf{S}^{(1)}\cdot\mathbf{j}^{(1)} - \frac{1}{2}\right)$, $\mathbf{j}^{(1)} = \mathbf{L} + \mathbf{S}^{(1)}$, $\mathbf{S}^{(1)} = \frac{1}{2}\gamma_5^{(1)}\cdot\boldsymbol{\alpha}^{(1)}$, $\mathbf{S}^{(2)} = \frac{1}{2}\boldsymbol{\sigma}^{(2)}$ and $\mathbf{J} = \mathbf{j}^{(1)} + \mathbf{S}^{(2)}$.

$\left|n\kappa_1 j_1 m_{j_1} s_2 m_{s_2}\right\rangle$ and $\left|n\kappa_1 j_1 s_2 J M_J\right\rangle$ are related by using Clebsch-Gordan coefficients:

$$\left|n\kappa_1 j_1 s_2 J M_J\right\rangle = \sum_{m_{j_1} m_{s_2}} \left\langle j_1 m_{j_1} s_2 m_{s_2} \middle| j_1 s_2 J M_J\right\rangle \left|n\kappa_1 j_1 m_{j_1} s_2 m_{s_2}\right\rangle. \tag{100}$$

In coordinate space, $\left|n\kappa_1 j_1 m_{j_1} s_2 m_{s_2}\right\rangle$ and $\left|n\kappa_1 j_1 s_2 J M_J\right\rangle$ are represented by $\psi_{n\kappa_1 j_1 m_{j_1}}(\mathbf{r})\chi_{m_{s_2}}$ and $\Psi_{n\kappa_1 j_1 s_2 J M_J}(\mathbf{r})$ respectively; (100) therefore becomes

$$\Psi_{n\kappa_1 j_1 s_2 J M_J}(\mathbf{r}) = \sum_{m_{j_1} m_{s_2}} \left\langle j_1 m_{j_1} s_2 m_{s_2} \middle| j_1 s_2 J M_J\right\rangle \psi_{n\kappa_1 j_1 m_{j_1}}(\mathbf{r})\chi_{m_{s_2}}. \tag{101}$$

$\psi_{n\kappa_1 j_1 m_{j_1}}(\mathbf{r})$ is the wave function for particle 1, which can be constructed as [29]

$$\psi_{n\kappa_1 j_1 m_{j_1}}(\mathbf{r}) = \begin{pmatrix} \frac{G_{n\ell j_1}(r)}{r}\mathcal{Y}_{\ell j_1}^{m_{j_1}}(\Omega) \\ \frac{iF_{n\ell j_1}(r)}{r}\mathcal{Y}_{\bar{\ell} j_1}^{m_{j_1}}(\Omega) \end{pmatrix}, \tag{102}$$

with

$$\mathcal{Y}_{\ell j_1}^{m_{j_1}}(\Omega) = \sum_{m_\ell, m_{s_1}} \left\langle \ell m_\ell s_1 m_{s_1} \middle| \ell s_1 j_1 m_{j_1}\right\rangle Y_{\ell m_\ell}(\Omega)\chi_{m_{s_1}}, \tag{103}$$

The eigenvalue $\kappa_1 = \pm(j_1 + \frac{1}{2})$ can be any nonzero integer. The values of ℓ and $\bar{\ell}$ associated with various values of κ_1 are displayed in Table 2. We can see from Table 2 that κ_1 and ℓ have a one-to-one correspondence, therefore $\psi_{n\kappa_1 j_1 m_{j_1}}(\mathbf{r})\chi_{m_{s_2}}$ and $\Psi_{n\kappa_1 j_1 s_2 J M_J}(\mathbf{r})$ can be equivalently specified as $\psi_{n\ell j_1 m_{j_1}}(\mathbf{r})\chi_{m_{s_2}}$ and $\Psi_{n\ell j_1 s_2 J M_J}(\mathbf{r})$.

Since both $\psi_{n\ell j_1 m_{j_1}}(\mathbf{r})\chi_{m_{s_2}}$ and $\Psi_{n\ell j_1 s_2 J M_J}(\mathbf{r})$ are eigenfunctions of H_0 corresponding to the same eigenvalues $W^{(0)}$, they both satisfy the same wave equation (95). For finding $W^{(0)}$, it is easier to solve the equation for $\psi_{n\ell j_1 m_{j_1}}(\mathbf{r})\chi_{m_{s_2}}$

$$H_0\psi_{n\ell j_1 m_{j_1}}(\mathbf{r})\chi_{m_{s_2}} = W^{(0)}\psi_{n\ell j_1 m_{j_1}}(\mathbf{r})\chi_{m_{s_2}}. \tag{104}$$

Table 2: Values of ℓ and $\bar{\ell}$ for various values of κ

	ℓ	$\bar{\ell}$
$\kappa < 0$	$j_1 - \frac{1}{2}$	$j_1 + \frac{1}{2}$
$\kappa > 0$	$j_1 + \frac{1}{2}$	$j_1 - \frac{1}{2}$

This equation can be reduced by using the explicit forms of H_0 (89), $\psi_{n\ell j_1 m_{j_1}}(\mathbf{r})$ (102) and the Dirac matrices $\boldsymbol{\alpha}$, β (see Appendix A) along with the identity

$$\boldsymbol{\sigma}^{(1)} \cdot \hat{\mathbf{r}} \mathcal{Y}^{m_{j_1}}_{\ell j_1}(\Omega) = -\mathcal{Y}^{m_{j_1}}_{\bar{\ell} j_1}(\Omega) \tag{105}$$

to extract the coupled radial wave equations [29]

$$\frac{dG_{n\ell j_1}(r)}{dr} + \frac{\kappa_1}{r} G_{n\ell j_1}(r) = \left[m_1 + V_s(r) - V_v(r) + E^{(0)}_{n\ell j_1} \right] F_{n\ell j_1}(r), \tag{106}$$

$$\frac{dF_{n\ell j_1}(r)}{dr} - \frac{\kappa_1}{r} F_{n\ell j_1}(r) = \left[m_1 + V_s(r) + V_v(r) - E^{(0)}_{n\ell j_1} \right] G_{n\ell j_1}(r), \tag{107}$$

where

$$E^{(0)}_{n\ell j_1} = W^{(0)}_{n\ell j_1} - m_2. \tag{108}$$

By numerically solving these coupled equations, as described in Appendix B, we obtain the zeroth order invariant mass $W^{(0)}$ as well as the wave functions $G_{n\ell j_1}(r)$ and $F_{n\ell j_1}(r)$, from which $\psi_{n\ell j_1 m_{j_1}}(\mathbf{r})\chi_{m_{s_2}}$ and $\Psi_{n\ell j_1 s_2 J M_J}(\mathbf{r})$ can be obtained by (102) and (101).

Calculating the First Order Correction

For H_1 in (90), both the first and second terms commute with the two sets of operators given in (98) and (99). However, the third term does not commute with

most of those operators, but instead commutes with

$$\left\{J^2, J_z, \mathcal{P}\right\}, \tag{109}$$

where $\mathcal{P}$ is the parity operator and the eigenvalues of $\mathcal{P}$ for $Q\bar{q}$, $\bar{Q}q$ bound states are $P = (-1)^{\ell+1}$. The eigenstates of the total Hamiltonian $H = H_0 + H_1$ can then be labeled by the set of quantum numbers $\left\{n, J, M_J, P\right\}$. However, since the first order perturbation only shifts and splits the states without mixing them, when considering only to the first order of perturbation, the eigenstates of the full Hamiltonian are usually denoted by the quantum numbers $\left\{n, \kappa_1, j_1, J, P\right\}$, where κ_1 and j_1 are nearly good quantum numbers, or equivalently denoted by $\left\{n, \ell, j_1, J, P\right\}$. M_J is not used to specify the states because the matrix element in (96) is found independent of M_J. Also, since $s = \frac{1}{2}$ is true for all flavors of quark, there is no need to use s_1 and s_2 to specify the states. These indices will, therefore, be suppressed in denoting the wave functions.

To calculate the first order perturbation by (96), we use $\Psi_{n\ell j_1 JM_J}(\mathbf{r})$ as $\Psi^{(0)}$ since J, M_J are good quantum numbers of H_1 . The matrix elements are calculated in Appendix C. Here we show the results:

$$\begin{aligned} W^{(1)}_{n\ell j_1 JP} = \frac{1}{2m_2}\int dr\ \Big\{ & G^2_{n\ell j_1}(r)\left[\left(E^{(0)}_{n\ell j_1} - m_1 - V_s(r)\right)^2 - V_v^2(r)\right] \\ & + F^2_{n\ell j_1}(r)\left[\left(E^{(0)}_{n\ell j_1} + m_1 + V_s(r)\right)^2 - V_v^2(r)\right] \\ & + 2\,V_v'(r)\,F_{n\ell j_1}(r)\,G_{n\ell j_1}(r) \times \mathcal{J}(\ell, J)\Big\} \end{aligned} \tag{110}$$

where

$$\begin{aligned} \mathcal{J}(\ell, J) \;=\; & \delta_{\ell,J+1}\,\delta_{j_1,J+\frac{1}{2}}\left(-\frac{2J+2}{2J+1}\right) + \delta_{\ell,J-1}\,\delta_{j_1,J-\frac{1}{2}}\left(-\frac{2J}{2J+1}\right) \\ + \;& \delta_{\ell,J}\,\delta_{j_1,J+\frac{1}{2}}\left(\frac{2J+2}{2J+1}\right) + \delta_{\ell,J}\,\delta_{j_1,J-\frac{1}{2}}\left(\frac{2J}{2J+1}\right) . \end{aligned} \tag{111}$$

The normalization of $\Psi_{n\ell j_1 JM_J}(\mathbf{r})$ is given by

$$\int d\mathbf{r}\ \Psi^{\dagger}_{n\ell j_1 JM_J}(\mathbf{r})\ \Psi_{n\ell j_1 JM_J}(\mathbf{r}) = \int dr\left[G^2_{n\ell j_1}(r) + F^2_{n\ell j_1}(r)\right] = 1\ . \tag{112}$$

3.2 $Q\bar{Q}$ Mesons

3.2.1 Deriving the Hamiltonian

The situation for mesons made of a heavy quark and the corresponding antiquark is somewhat more complicated. The problem is that the prescription of placing particle 2 on mass shell in the Bethe-Salpeter vertex equation (50) to obtain the spectator vertex equation (65) is clearly asymmetric. This results in a spectator vertex function which is no longer an eigenfunction of the charge conjugation operator. The solution of this problem is to construct a set of coupled equations for the vertex functions which have either particle 1 or particle 2 on mass shell. These equations have been solved in [54, 55, 56] for $q\bar{q}$-systems containing only light quarks.

However, since we are interested in expanding about the infinite mass limit, this additional complication is not necessary and a Hamiltonian with leading $1/m_Q$ corrections can be constructed from (71) (such a procedure was first introduced in [65]). The starting point is the spinor decomposition of the Dirac propagator of particle 1

$$S_F^{(1)}(\check{k}_1, m_1) = \frac{m_1}{E(\mathbf{k}_1, m_1)} \sum_{m'_{s_1}} \left[\frac{u^{(1)}(\mathbf{k}_1, m'_{s_1}) \bar{u}^{(1)}(\mathbf{k}_1, m'_{s_1})}{W - E(\mathbf{k}_1, m_1) - E(\mathbf{k}_2, m_2) + i\eta} + \frac{v^{(1)}(-\mathbf{k}_1, m'_{s_1}) \bar{v}^{(1)}(-\mathbf{k}_1, m'_{s_1})}{W + E(\mathbf{k}_1, m_1) - E(\mathbf{k}_2, m_2) - i\eta} \right]. \tag{113}$$

Using (113) in (71), we can write

$$\Gamma(\check{p}; P) = \sum_{m'_{s_1} m'_{s_2}} \int \frac{d^3k}{(2\pi)^3} \sqrt{\frac{m_1 m_2}{E(\mathbf{k}_1, m_1) E(\mathbf{k}_2, m_2)}}\, V(\check{p}, \check{k}; P) \left[u^{(1)}(\mathbf{k}_1, m'_{s_1}) u^{(2)}(\mathbf{k}_2, m'_{s_2}) \Psi^{(+)}_{m'_{s_1} m'_{s_2}}(\check{k}, P) + v^{(1)}(-\mathbf{k}_1, m'_{s_1}) u^{(2)}(\mathbf{k}_2, m'_{s_2}) \Psi^{(-)}_{m'_{s_1} m'_{s_2}}(\check{k}, P) \right], \tag{114}$$

where

$$\Psi^{(+)}_{m'_{s_1} m'_{s_2}}(\check{k}, P) = \sqrt{\frac{m_1 m_2}{E(\mathbf{k}_1, m_1) E(\mathbf{k}_2, m_2)}}\, \frac{\bar{u}^{(1)}(\mathbf{k}_1, m'_{s_1}) \bar{u}^{(2)}(\mathbf{k}_2, m'_{s_2}) \Gamma(\check{k}; P)}{W - E(\mathbf{k}_1, m_1) - E(\mathbf{k}_2, m_2)},$$

and

$$\Psi^{(-)}_{m'_{s_1} m'_{s_2}}(\check{k}, P) = \sqrt{\frac{m_1 m_2}{E(\mathbf{k_1}, m_1) E(\mathbf{k_2}, m_2)}} \frac{\bar{v}^{(1)}(-\mathbf{k_1}, m'_{s_1}) \bar{u}^{(2)}(\mathbf{k_2}, m'_{s_2}) \Gamma(\check{k}; P)}{W + E(\mathbf{k_1}, m_1) - E(\mathbf{k_2}, m_2)}.$$

Working in the bound state rest frame, and multiplying (114) to the left respectively by

$$\sqrt{\frac{m_1 m_2}{E(\mathbf{p_1}, m_1) E(\mathbf{p_2}, m_2)}} \bar{u}^{(1)}(\mathbf{p_1}, m_{s_1}) \bar{u}^{(2)}(\mathbf{p_2}, m_{s_2})$$

and

$$\sqrt{\frac{m_1 m_2}{E(\mathbf{p_1}, m_1) E(\mathbf{p_2}, m_2)}} \bar{v}^{(1)}(-\mathbf{p_1}, m_{s_1}) \bar{u}^{(2)}(\mathbf{p_2}, m_{s_2}),$$

(114) can be rewritten as a pair of coupled integral equations

$$\begin{aligned} &\Big[W - E(\mathbf{p_1}, m_1) - E(\mathbf{p_2}, m_2) \Big] \Psi^{(+)}_{m_{s_1} m_{s_2}}(\check{p}, P) \\ &= \sum_{m'_{s_1} m'_{s_2}} \int \frac{d^3k}{(2\pi)^3} \Big[U^{++}_{m_{s_1} m_{s_2} m'_{s_1} m'_{s_2}}(\check{p}, \check{k}; P) \, \Psi^{(+)}_{m'_{s_1} m'_{s_2}}(\check{k}, P) \\ &\qquad + U^{+-}_{m_{s_1} m_{s_2} m'_{s_1} m'_{s_2}}(\check{p}, \check{k}; P) \, \Psi^{(-)}_{m'_{s_1} m'_{s_2}}(\check{k}, P) \Big], \end{aligned} \tag{115}$$

and

$$\begin{aligned} &\Big[W + E(\mathbf{p_1}, m_1) - E(\mathbf{p_2}, m_2) \Big] \Psi^{(-)}_{m_{s_1} m_{s_2}}(\check{p}, P) \\ &= \sum_{m'_{s_1} m'_{s_2}} \int \frac{d^3k}{(2\pi)^3} \Big[U^{-+}_{m_{s_1} m_{s_2} m'_{s_1} m'_{s_2}}(\check{p}, \check{k}; P) \, \Psi^{(+)}_{m'_{s_1} m'_{s_2}}(\check{k}, P) \\ &\qquad + U^{--}_{m_{s_1} m_{s_2} m'_{s_1} m'_{s_2}}(\check{p}, \check{k}; P) \, \Psi^{(-)}_{m'_{s_1} m'_{s_2}}(\check{k}, P) \Big], \end{aligned} \tag{116}$$

where the channel potentials are defined to be:

$$\begin{aligned} &U^{++}_{m_{s_1} m_{s_2} m'_{s_1} m'_{s_2}}(\check{p}, \check{k}; P) \\ &\quad = \sqrt{m_1 / E(\mathbf{p_1}, m_1)} \sqrt{m_2 / E(\mathbf{p_2}, m_2)} \sqrt{m_1 / E(\mathbf{k_1}, m_1)} \sqrt{m_2 / E(\mathbf{k_2}, m_2)} \\ &\qquad \times \bar{u}^{(1)}(\mathbf{p_1}, m_{s_1}) \bar{u}^{(2)}(\mathbf{p_2}, m_{s_2}) V(\check{p}, \check{k}; P) u^{(1)}(\mathbf{k_1}, m'_{s_1}) u^{(2)}(\mathbf{k_2}, m'_{s_2}), \end{aligned} \tag{117}$$

$$U^{+-}_{m_{s_1} m_{s_2} m'_{s_1} m'_{s_2}}(\check{p}, \check{k}; P)$$
$$= \sqrt{m_1/E(\mathbf{p}_1, m_1)}\sqrt{m_2/E(\mathbf{p}_2, m_2)}\sqrt{m_1/E(\mathbf{k}_1, m_1)}\sqrt{m_2/E(\mathbf{k}_2, m_2)}$$
$$\times \bar{u}^{(1)}(\mathbf{p}_1, m_{s_1})\bar{u}^{(2)}(\mathbf{p}_2, m_{s_2})V(\check{p}, \check{k}; P)v^{(1)}(-\mathbf{k}_1, m'_{s_1})u^{(2)}(\mathbf{k}_2, m'_{s_2}), \quad (118)$$

$$U^{-+}_{m_{s_1} m_{s_2} m'_{s_1} m'_{s_2}}(\check{p}, \check{k}; P)$$
$$= \sqrt{m_1/E(\mathbf{p}_1, m_1)}\sqrt{m_2/E(\mathbf{p}_2, m_2)}\sqrt{m_1/E(\mathbf{k}_1, m_1)}\sqrt{m_2/E(\mathbf{k}_2, m_2)}$$
$$\times \bar{v}^{(1)}(-\mathbf{p}_1, m_{s_1})\bar{u}^{(2)}(\mathbf{p}_2, m_{s_2})V(\check{p}, \check{k}; P)u^{(1)}(\mathbf{k}_1, m'_{s_1})u^{(2)}(\mathbf{k}_2, m'_{s_2}), \quad (119)$$

$$U^{--}_{m_{s_1} m_{s_2} m'_{s_1} m'_{s_2}}(\check{p}, \check{k}; P)$$
$$= \sqrt{m_1/E(\mathbf{p}_1, m_1)}\sqrt{m_2/E(\mathbf{p}_2, m_2)}\sqrt{m_1/E(\mathbf{k}_1, m_1)}\sqrt{m_2/E(\mathbf{k}_2, m_2)}$$
$$\times \bar{v}^{(1)}(-\mathbf{p}_1, m_{s_1})\bar{u}^{(2)}(\mathbf{p}_2, m_{s_2})V(\check{p}, \check{k}; P)v^{(1)}(-\mathbf{k}_1, m'_{s_1})u^{(2)}(\mathbf{k}_2, m'_{s_2}). \quad (120)$$

Using (72) for the kernel $V(\check{p}, \check{k}; P)$ and the explicit form of the Dirac spinors defined in Appendix A, the coupled equations (115) and (116) can then be reduced to the Pauli spin space and expanded in powers of $1/m_i$. To order $1/(m_i m_j)$, only $U^{++}\Psi^{(+)}$ contributes. Defining a wave function which is an operator in the spin spaces of both particles as

$$\Psi = \sum_{m'_{s_1} m'_{s_2}} \chi_{m'_{s_1}} \chi_{m'_{s_2}} \Psi^{(+)}_{m'_{s_1} m'_{s_2}}, \quad (121)$$

and using the relations between $\mathbf{p}$, $\mathbf{k}$ and $\mathbf{p_i}$, $\mathbf{k_i}$ in the meson rest frame, as shown in Appendix D, the coupled equations become

$$\left(W - m_1 - m_2 - \frac{\mathbf{p}^2}{2m_1} - \frac{\mathbf{p}^2}{2m_2}\right)\Psi(\mathbf{p}) = \int \frac{d^3k}{(2\pi)^3}\,\mathcal{U}(\mathbf{p}, \mathbf{k})\,\Psi(\mathbf{k}), \quad (122)$$

with

$$\mathcal{U}(\mathbf{p}, \mathbf{k}) = V_s(\mathbf{q}^2) + V_v(\mathbf{q}^2) - \frac{1}{4m_2^2}\left[V'_s(\mathbf{q}^2) + V'_v(\mathbf{q}^2)\right]\left(\mathbf{p}^2 - \mathbf{k}^2\right)^2$$
$$-V_s(\mathbf{q}^2)\left[\left(\frac{1}{2m_1^2} + \frac{1}{2m_2^2}\right)\mathbf{k}^2 + \left(\frac{1}{8m_1^2} + \frac{1}{8m_2^2}\right)\mathbf{q}^2\right.$$

$$
\begin{aligned}
&- \left(\frac{1}{2m_1^2} + \frac{1}{2m_2^2}\right) \mathbf{k}\cdot\mathbf{q} - i\left(\frac{\boldsymbol{\sigma}^{(1)}}{4m_1^2} + \frac{\boldsymbol{\sigma}^{(2)}}{4m_2^2}\right)\cdot\left(\mathbf{q}\times\mathbf{k}\right)\Bigg] \\
&-V_V(\mathbf{q}^2)\Bigg[\left(\frac{1}{8m_1^2} + \frac{1}{8m_2^2} - \frac{1}{4m_1m_2}\right)\mathbf{q}^2 - \frac{\mathbf{k}^2}{m_1m_2} + \frac{\mathbf{k}\cdot\mathbf{q}}{m_1m_2} \\
&+i\left(\frac{\boldsymbol{\sigma}^{(1)}}{4m_1^2} + \frac{\boldsymbol{\sigma}^{(2)}}{4m_2^2}\right)\cdot\left(\mathbf{q}\times\mathbf{k}\right) + i\left(\frac{\boldsymbol{\sigma}^{(1)} + \boldsymbol{\sigma}^{(2)}}{2m_1m_2}\right)\cdot\left(\mathbf{q}\times\mathbf{k}\right) \\
&+\frac{\mathbf{q}^2}{4m_1m_2}\left(\boldsymbol{\sigma}^{(1)}\cdot\boldsymbol{\sigma}^{(2)}\right) - \frac{(\boldsymbol{\sigma}^{(1)}\cdot\mathbf{q})(\boldsymbol{\sigma}^{(2)}\cdot\mathbf{q})}{4m_1m_2}\Bigg]. \qquad (123)
\end{aligned}
$$

Equation (122) can then be Fourier transformed to coordinate space to extract the Hamiltonian

$$H = H_0 + H_1\ , \qquad (124)$$

with

$$H_1 = H_c + H_{so} + H_{hyp} + H_{SR} + H_{VR}\ . \qquad (125)$$

Here

$$H_0 = -\frac{\nabla^2}{2m_1} - \frac{\nabla^2}{2m_2} + V_s(r) + V_v(r) + m_1 + m_2\ , \qquad (126)$$

$$
\begin{aligned}
H_c \;=\; &\left(\frac{1}{8m_1^2} + \frac{1}{8m_2^2}\right)\left[\nabla^2 V_s(r)\right] \\
&+\left(\frac{1}{8m_1^2} + \frac{1}{8m_2^2} - \frac{1}{4m_1m_2}\right)\left[\nabla^2 V_v(r)\right] \\
&-\left(\frac{V_v(r)}{m_1m_2} - \frac{V_s(r)}{2m_1^2} - \frac{V_s(r)}{2m_2^2}\right)\nabla^2 \\
&-\left(\frac{V_v'(r)}{m_1m_2} - \frac{V_s'(r)}{2m_1^2} - \frac{V_s'(r)}{2m_2^2}\right)\frac{\partial}{\partial r}\ , \qquad (127)
\end{aligned}
$$

$$
\begin{aligned}
H_{so} \;=\; &-\frac{1}{2r}\left[V_s'(r) + V_v'(r)\right]\left(\frac{\mathbf{S}^{(1)}}{m_1^2} + \frac{\mathbf{S}^{(2)}}{m_2^2}\right)\cdot\mathbf{L} \\
&+\frac{1}{r}V_v'(r)\left(\frac{\mathbf{S}^{(1)}}{m_1^2} + \frac{\mathbf{S}^{(2)}}{m_2^2} + \frac{\mathbf{S}^{(1)} + \mathbf{S}^{(2)}}{m_1m_2}\right)\cdot\mathbf{L}, \qquad (128)
\end{aligned}
$$

$$
\begin{aligned}
H_{hyp} \;=\; &\frac{1}{4m_1m_2}\Big\{\left[\nabla^2 V_v(r)\right]\left(\boldsymbol{\sigma}^{(1)}\cdot\boldsymbol{\sigma}^{(2)}\right) \\
&-\left[\boldsymbol{\sigma}^{(1)}\cdot\nabla\left(\boldsymbol{\sigma}^{(2)}\cdot\nabla V_v(r)\right)\right]\Big\}\ , \qquad (129)
\end{aligned}
$$

$$H_{\mathrm{S(V)R}} = -\frac{1}{4m_2^2}\left[\nabla^2,\left[\nabla^2, F_{\mathrm{S(V)R}}(\mathbf{x})\right]\right] , \tag{130}$$

where $\mathbf{S^{(i)}} = \frac{1}{2}\boldsymbol{\sigma}^{(i)}$ is the spin of quark i and $F_{\mathrm{S(V)R}}(\mathbf{x})$ is the Fourier transform of $dV_{s(v)}(\mathbf{q}^2)/d\mathbf{q}^2$. The details of obtaining $H_{\mathrm{S(V)R}}$ are given in Appendix E.

For $V_s(r)$ and $V_v(r)$ being the scalar and vector potentials in (91) and (92), and considering $m_1 = m_2 = m_Q$,

$$H_0 = -\frac{\nabla^2}{m_Q} + V_s(r) + V_v(r) + 2m_Q , \tag{131}$$

$$H_c = \frac{1}{m_Q^2}\left\{\frac{1}{4}\left[\nabla^2 V_s(r)\right] - \left[V_v(r) - V_s(r)\right]\nabla^2 + \left[V_s'(r) - V_v'(r)\right]\frac{\partial}{\partial r}\right\} , \tag{132}$$

$$H_{\mathrm{so}} = \frac{1}{2m_Q^2 r}\left[3V_v'(r) - V_s'(r)\right]\mathbf{S}\cdot\mathbf{L} , \tag{133}$$

$$\begin{aligned} H_{\mathrm{hyp}} \;=\; & \frac{1}{m_Q^2}\left\{\frac{1}{2}\left[\frac{1}{r}V_v'(r) - V_v''(r)\right]\left(\mathbf{S}\cdot\hat{\mathbf{r}}\mathbf{S}\cdot\hat{\mathbf{r}} - \frac{1}{3}\mathbf{S}^2\right)\right. \\ & \left. + \left[\nabla^2 V_v(r)\right]\left(\frac{1}{3}\mathbf{S}^2 - \frac{1}{2}\right)\right\} , \end{aligned} \tag{134}$$

$$H_{\mathrm{SR}} = \frac{b}{m_Q^2}\left(\frac{\mathbf{L}^2}{2r} - 3\frac{\partial}{\partial r} - r\frac{\partial^2}{\partial r^2} - \frac{1}{r}\right) - \frac{c}{m_Q^2}\left(\frac{1}{r}\frac{\partial}{\partial r} + \frac{1}{2}\frac{\partial^2}{\partial r^2} - \frac{\mathbf{L}^2}{2r^2}\right) , \tag{135}$$

$$\begin{aligned} H_{\mathrm{VR}} = & \frac{V_v(r)}{2m_Q^2 r^2}\mathbf{L}^2 \\ & -\frac{1}{3m_Q^2\sqrt{\pi}}\sum_i \alpha_i\gamma_i\, e^{-\gamma_i^2 r^2}\left(10\gamma_i^2 - 4\gamma_i^4 r^2 + 8\gamma_i^2 r\frac{\partial}{\partial r} - \frac{8}{r}\frac{\partial}{\partial r} - 4\frac{\partial^2}{\partial r^2}\right) , \end{aligned} \tag{136}$$

where $\mathbf{S} = \mathbf{S^{(1)}} + \mathbf{S^{(2)}}$ is the spin of the meson.

H_0 is the nonrelativistic Hamiltonian for equal mass quarks in scalar and vector potentials. H_c contains central and orbital contributions. H_{so} is the spin-orbit interaction. H_{hyp} is the hyperfine interaction consisting of a tensor-force term and a spin-spin interaction. H_{SR} and H_{VR} are scalar and vector retardation terms associated with the third term on the right-hand side of (123).

The spin-independent correction includes H_c, H_{SR} and H_{VR}. In these contributions, H_{SR}, H_{VR} and the term $\left[V_s'(r) - V_v'(r)\right]\frac{\partial}{\partial r}$ in H_c are gauge dependent.

$H_{\rm SR}$ and $H_{\rm VR}$ are from the second term in the expansion of $V(Q^2)$ in (83). Had we chosen the Coulomb gauge, these terms would not have existed. Most other quark models do not include the retardation interactions. (Ref. [66] gives another expression for the retardation effect.) We will show that with the scalar and vector potentials in (91) and (92), retardation contributions are comparable with the spin-dependent interactions.

Note that our spin-dependent interactions $H_{\rm so}$ and $H_{\rm hyp}$ have the same forms as those in many other quark models (for example, [25, 27, 67]), but the spin-independent interactions do not. We have also derived the Hamiltonians by using the Cooper-Jennings equation [63] and the Wallace-Mandelzweig equation [62]. (The details are shown in Appendix F.) We find that the Hamiltonians derived from the Cooper-Jennings equation are identical to (131 - 134). This indicates that (124) and (125) agree with the Blankenbecler-Sugar equation, since the Cooper-Jennings equation has been specifically constructed to agree with the Blankenbecler-Sugar equation in the equal mass limit. The only difference arises from the fact that the Blankenbecler-Sugar equation describes instantaneous interactions while the Gross equation includes retardations. The Hamiltonian derived from the Wallace-Mandelzweig equation includes the same terms as those from the Cooper-Jennings equation as well as a term with $1/m_Q$ order of spin-spin interactions.

3.2.2 Solving the Wave Equation

The operators $\{H_0, \mathbf{L}^2, \mathbf{S}^2, \mathbf{J}^2, \mathbf{J}_z\}$, where $\mathbf{J} = \mathbf{L} + \mathbf{S}$, are a set of mutually commuting hermitian operators. The eigenstates of H_0 can then be labeled by the corresponding set of quantum numbers $\{n, L, S, J, M_J\}$. The wave equation associated with H_0 can then be written as

$$H_0 \Psi^{(0)}_{nLSJM_J}(\mathbf{r}) = W^{(0)}_{nL} \Psi^{(0)}_{nLSJM_J}(\mathbf{r}), \tag{137}$$

where

$$\Psi^{(0)}_{nLSJM_J}(\mathbf{r}) = \mathcal{R}_{nL}(r)\ \mathcal{Y}^{M_J}_{LSJ}(\Omega), \tag{138}$$

and

$$\mathcal{Y}^{M_J}_{LSJ}(\Omega) = \sum_{M_L,M_S} \left\langle LM_L SM_S \middle| LSJM_J \right\rangle Y_{LM_L}(\Omega) \left| SM_S \right\rangle \tag{139}$$

is the spin spherical harmonic.

The hyperfine interaction (134) mixes states with $\Delta L = \pm 2$ for $S = 1$. As a result, L is no longer a good quantum number for solutions of the complete Hamiltonian. However, these states have the same parity and charge quantum numbers since $P = (-1)^{L+1}$ and $C = (-1)^{L+S}$ for $\Psi^{(0)}$. Also, since we calculate only the first order perturbation corrections which only include the splittings and shifts of the states without mixing them, we can still use L as the nearly good quantum number to specify the states. The first-order correction to the mass can then be written as

$$\begin{aligned} W^{(1)PC}_{nLSJ} &= \int d^3r \Psi^{(0)\dagger}_{nLSJM_J}(\mathbf{r}) H_1 \, \Psi^{(0)}_{nLSJM_J}(\mathbf{r}) \\ &= E_c + E_{\rm hyp} + E_{\rm so} + E_{\rm SR} + E_{\rm VR}. \end{aligned} \tag{140}$$

where

$$E_\alpha = \int d^3r \Psi^{(0)\dagger}_{nLSJM_J}(\mathbf{r}) H_\alpha \, \Psi^{(0)}_{nLSJM_J}(\mathbf{r}) \,, \tag{141}$$

with $\alpha =$ c, hyp, so, SR, VR.

By using (138) with the orthogonality of $Y_{LM_L}(\Omega)$ and the Clebsch-Gordan coefficients, we find

$$\int d^3r \, f(r) \, \Psi^{(0)\dagger}_{nLSJM_J} \, \Psi^{(0)}_{nLSJM_J}(\mathbf{r}) = \int_0^\infty r^2 f(r) \left| \mathcal{R}_{nL}(r) \right|^2 dr \,, \tag{142}$$

$$\int d^3r \, f(r) \, \Psi^{(0)\dagger}_{nLSJM_J} \frac{\partial^i}{\partial r^i} \Psi^{(0)}_{nLSJM_J}(\mathbf{r}) = \int_0^\infty r^2 f(r) \, \mathcal{R}^*_{nL}(r) \frac{\partial^i}{\partial r^i} \mathcal{R}_{nL}(r) \, dr \,. \tag{143}$$

Using these relations, we can calculate each term in (140). The bound state mass to first order is

$$W_{nJPC} = W^{(0)}_{nL} + W^{(1)}_{nJPC} \,. \tag{144}$$

The annihilation effect should also contribute to the $Q\bar{Q}$ spectra. However, in mesons, the annihilation contribution first appears at order α_s^2/m_Q^2 [20, 25], while in our model the leading spin-dependent effects are of order α_s/m_Q^2. Since α_s is

small in the heavy quark system, $\alpha_s(m_c) \sim 0.35$ and $\alpha_s(m_b) \sim 0.22$, we expect the annihilation effects on $Q\bar{Q}$ spectra to be small.

Chapter 4

Meson Spectra and Parameters

The bound state masses determined by (97) and (144) depend on the quark masses m_u, m_s, m_c and m_b as applicable for each meson; the parameters of the scalar potential (91) b and c; and the parameters of the vector potential (92) α_i and γ_i for $i = 1, 2, 3$. The model contains a total of twelve parameters. In obtaining the results shown here, the vector potential parameters

$$\begin{aligned} \alpha_2 &= 0.15, \qquad \alpha_3 = 0.2, \\ \gamma_1 &= 0.5, \qquad \gamma_2 = 1.581, \qquad \gamma_3 = 15.81, \end{aligned} \tag{145}$$

are fixed at the same values as given in Ref. [25]. The remaining vector potential parameter α_1 is reexpressed as

$$\alpha_1 = \alpha_{crit} - \alpha_2 - \alpha_3. \tag{146}$$

where α_{crit} is the value of the running coupling constant at $Q^2 = 0$ as parameterized in [25].

α_{crit} and the remaining model parameters are adjusted to fit the masses of a selection of mesons. The resulting values are listed in Table 3.

The fitted meson spectra for the $Q\bar{q}$ sector are listed in Table 4 and the fitted meson spectra for the $Q\bar{Q}$ sector are listed in Table 5. Experimental values are quoted [48] to the nearest 10 MeV due to ambiguities in assigning the calculated values to specific charge states. Additional states which were not used in the

Table 3: Parameters of the model.

parameter	value	comments
α_{crit}	0.674	limiting value of α_s
b	0.180 GeV^2	string tension
c	0.02 GeV	see eq. (91)
m_u	0.258 GeV	
m_s	0.400 GeV	
m_c	1.53 GeV	
m_b	4.87 GeV	

fitting procedure were calculated and a detailed discussion of the results for $Q\bar{q}$ and $Q\bar{Q}$ mesons is presented in the following two subsections.

4.1 $Q\bar{q}$ Sector

For the $Q\bar{q}$ sector, the zeroth-order eigenenergy $E^{(0)}_{n\ell j_1} = W^{(0)}_{n\kappa_1 j_1} - m_2$ is independent of the heavy quark mass, as would be expected in the heavy quark limit. The zeroth-order spectrum, therefore, depends only upon the light quark mass. The first-order correction to the mass $W^{(1)}_{nJP}$ is proportional to $1/m_2$ and splits each of the unperturbed states. These features are illustrated in Figure 7 (and Table 6) which shows the $W^{(0)}_{n\kappa_1 j_1} - m_2$ for a u quark as solid lines and $W_{nJP} - m_2 = W^{(0)}_{n\kappa_1 j_1} + W^{(1)}_{nJP} - m_2$ with a c quark as the heavy quark (dotdashed lines) and with a b quark as the heavy quark (dashed lines). Figure 8 (and Table 7) is a similar spectrum where the light quark is now an s quark.

Note that to zeroth order the ordering of the $j_1 = \ell \pm 1/2$ states is reversed for the $\ell = 2$ state in comparison to the $\ell = 1$ state. This phenomenon, called

Table 4: Fitted meson spectra for $Q\bar{q}$ mesons.

Meson	J^P	Mass (GeV) theory	experiment
D	0^-	1.85	1.87
D^*	1^-	2.02	2.01
D_1	1^+	2.41	2.42
D_2^*	2^+	2.46	2.46
B	0^-	5.28	5.28
B^*	1^-	5.33	5.33
D_s	0^-	1.94	1.97
D_s^*	1^-	2.13	2.11
B_s	0^-	5.37	5.38
B_s^*	1^-	5.43	5.43

Table 5: Fitted meson spectra for $Q\bar{Q}$ mesons.

Meson	J^{PC}	Mass (GeV) theory	experiment
η_c	0^{-+}	3.00	2.98
$J/\psi(1S)$	1^{--}	3.10	3.10
χ_{c0}	0^{++}	3.44	3.42
χ_{c1}	1^{++}	3.50	3.51
χ_{c2}	2^{++}	3.54	3.56
$J/\psi(2S)$	1^{--}	3.73	3.69
$\Upsilon(1S)$	1^{--}	9.46	9.46
$\chi_{b0}(1P)$	0^{++}	9.85	9.86
$\chi_{b1}(1P)$	1^{++}	9.87	9.89
$\chi_{b2}(1P)$	2^{++}	9.89	9.92
$\Upsilon(2S)$	1^{--}	10.02	10.02
$\chi_{b0}(2P)$	0^{++}	10.24	10.24
$\chi_{b1}(2P)$	1^{++}	10.26	10.26
$\chi_{b2}(2P)$	2^{++}	10.28	10.27
$\Upsilon(3S)$	1^{--}	10.39	10.36

multiplet inversion, has been predicted [68] for $Q\bar{q}$ mesons with $m_2 \gg m_1$. It results from the dominance of the Thomas-precession over the spin-dependent forces in this limit.

The dependence of $W^{(1)}$ on $1/m_2$ is clear in that the shifts and splittings of the various states are larger for the case where the heavy quark is the c quark than where the heavy quark is the b quark. For the states presented here the root mean squared momentum of the zeroth-order wave function is approximately 0.9 GeV. Clearly, both u and s quarks are very relativistic. In addition, it is possible to obtain some sense of the convergence of the p/m expansion for the corrections to the infinite-heavy-quark-mass limit since $\frac{p_{rms}}{m_c} \sim \frac{1}{2}$ while $\frac{p_{rms}}{m_b} \sim \frac{1}{5}$. Therefore, the higher-order corrections that are neglected here should be considerably larger for the c quark than the b quark. Indeed, this problem will become worse with increasing energy level n since p_{rms} should increase with increasing n. This is seen in the shift of the 0^- states relative to the unperturbed states which increases with n.

Figures 9 to 13 (and Tables 8 to 12), show predictions for the masses of $Q\bar{q}$ mesons, W, to first order in the perturbation (solid lines). In the spectra for mesons with $\bar{u}$ and $\bar{s}$ quarks, the available data are plotted for comparison as dotted lines. Ref. [48] has also listed states $D_J(2.440)$ and $D_{sJ}(2.573)$ with uncertain quantum numbers. We believe they correspond to the state $1^+(2.41)$ in Figure 9 and the state $2^+(2.58)$ in Figure 10, respectively. For the $b\bar{c}$ mesons, calculated masses from [25] are plotted due to the absence of data. For the $b\bar{c}$ mesons $\frac{p_{rms}}{m_c} \sim 1$. This shows that although the mass of the c quark is relatively large it is quite relativistic in this case.

In these figures, the results are in good agreement with the data, which vindicates our choices of potentials and parameters. However, the calculated hyperfine splittings are all larger than in the data. The agreement is much better in the b-flavored mesons than in the c-flavored mesons. There are three possible reasons for this discrepancy. First, as has been mentioned earlier, this model is expected to work better for b-flavored mesons than for c-flavored mesons due to the more rapid convergence of the nonrelativistic expansion applied to the heavy quark.

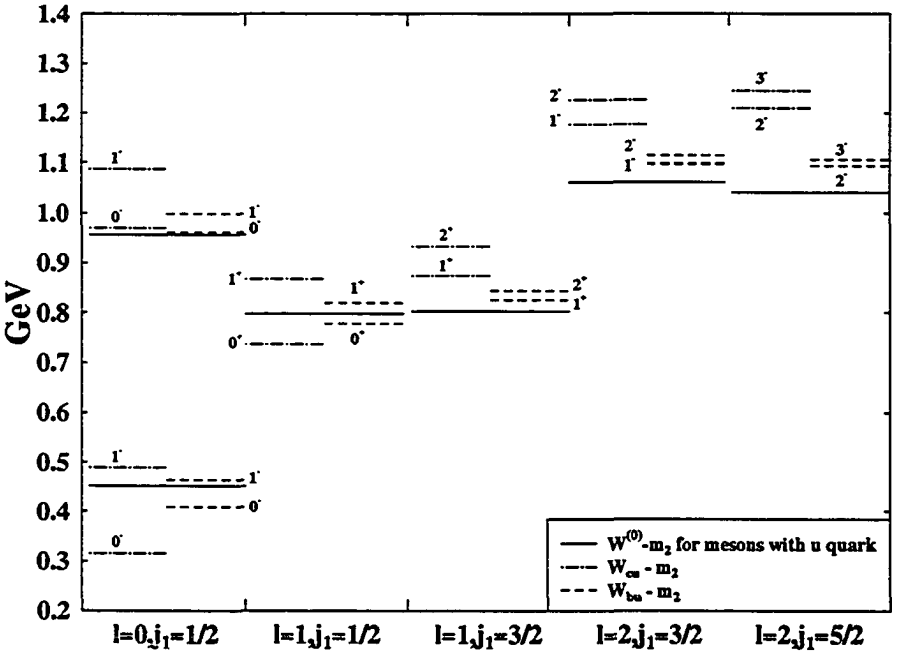

Figure 7: This figure shows $W - m_2$ for $b\bar{u}$ and $c\bar{u}$ to zeroth order and to first order. ℓ and j_1 are the quantum numbers for orbital angular momentum and total angular momentum of the $\bar{u}$ quark. The states have been labeled as J^P, where J and P are the total angular momentum and the parity of the meson, respectively.

Table 6: Data for Figure 7. This table lists the calculated eigenenergy $W - m_2$ for $c\bar{u}$ and $b\bar{u}$ to zeroth order (column 5) and first order corrections (column 6 and 7). n denotes the principle quantum number of the meson states. ℓ and j_1 are the quantum numbers for orbital angular momentum and total angular momentum of the $\bar{u}$ quark. J and P are the total angular momentum and the parity of the meson, respectively.

				(GeV)		
n	ℓ	j_1	J^P	$W^{(0)}_{cu} - m_c = W^{(0)}_{bu} - m_b$	$W_{cu} - m_c$	$W_{bu} - m_b$
1	0	1/2	0^-	0.45202	0.31562	0.40911
1	0	1/2	1^-	0.45202	0.48956	0.46383
2	0	1/2	0^-	0.95738	0.97025	0.96143
2	0	1/2	1^-	0.95738	1.08882	0.99873
1	1	1/2	0^+	0.79806	0.73716	0.77890
1	1	1/2	1^+	0.79806	0.86860	0.82025
1	1	3/2	1^+	0.80262	0.87499	0.82538
1	1	3/2	2^+	0.80262	0.93305	0.84365
1	2	3/2	1^-	1.06167	1.17756	1.09813
1	2	3/2	2^-	1.06167	1.22728	1.11377
1	2	5/2	2^-	1.04117	1.20935	1.09407
1	2	5/2	3^-	1.04117	1.24512	1.10533

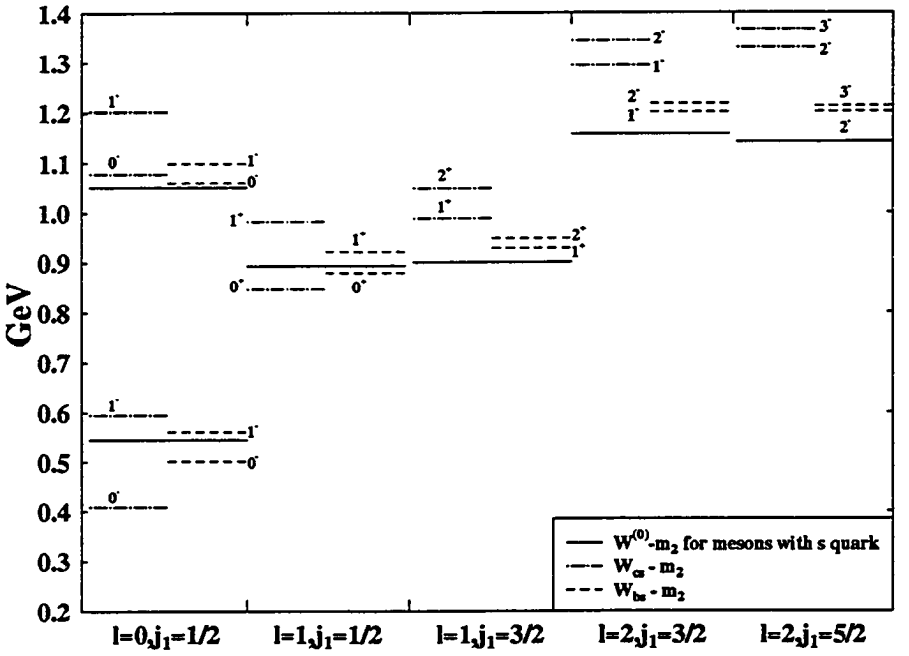

Figure 8: This figure shows $W - m_2$ for $b\bar{s}$ and $c\bar{s}$ to zeroth order and to first order. Also see caption of Figure 7.

Table 7: Data for Figure 8. This table lists the calculated eigenenergy $W - m_2$ for $c\bar{s}$ and $b\bar{s}$ to zeroth order and first order correction. Also see the caption of Table 6.

				(GeV)		
n	ℓ	j_1	J^P	$W_{cs}^{(0)} - m_c = W_{bs}^{(0)} - m_b$	$W_{cs} - m_c$	$W_{bs} - m_b$
1	0	1/2	0^-	0.54451	0.40869	0.50179
1	0	1/2	1^-	0.54451	0.59492	0.56037
2	0	1/2	0^-	1.05236	1.07877	1.06067
2	0	1/2	1^-	1.05236	1.20270	1.09965
1	1	1/2	0^+	0.89366	0.84793	0.87927
1	1	1/2	1^+	0.89366	0.98246	0.92159
1	1	3/2	1^+	0.90130	0.98925	0.92897
1	1	3/2	2^+	0.90130	1.04965	0.94797
1	2	3/2	1^-	1.15804	1.29350	1.20065
1	2	3/2	2^-	1.15804	1.34464	1.21674
1	2	5/2	2^-	1.14181	1.32972	1.20092
1	2	5/2	3^-	1.14181	1.36673	1.21256

Secondly, these calculations do not include any effects associated with possible strong decay of the heavy mesons. The coupling to these strong decay channels will result in shifts in the meson masses as well as decay widths for heavy mesons above decay thresholds. These shifts will be greatest near the decay thresholds.

The third possible reason for the large hyperfine splittings may have its origin in the parameterization of $\alpha_s(r)$, particularly at small r. While many functional forms may be used for this parameterization, each form may be expected to lead to quite different $1/m_Q$ contributions, especially in the hyperfine term. This question is currently under investigation.

The third term on the right hand side of (90) has non-zero matrix elements between states with j_1 differing by 1 and with ℓ differing by either 0 or 2. These mixings do not affect the spectrum to order $\frac{1}{m_Q}$ but should result in shifts in some states at higher order in all of these systems. This should be particularly apparent for the 1^+ states which are nearly degenerate to order $\frac{1}{m_Q}$ for all $Q\bar{q}$ mesons calculated here.

One very interesting aspect of this calculation is the mapping of our model on to the heavy quark effective theory, with a view to evaluating some of the parameters and dynamical quantities (such as universal form factors) of the effective theory. While we do not endeavor to perform such a calculation for all such quantities here, some comments are merited.

Although we have included all of the $1/m_Q$ terms that arise from the spectator equation, it is not clear that these correspond to all of the $1/m_Q$ terms of HQET. In particular, in the spectator equation, the heavy quark is treated as being exactly on its mass shell. In contrast, in HQET, the heavy quark is allowed to be slightly off its mass shell (via the equation $p_\mu = m_Q v_\mu + k_\mu$), and this leads to terms that may be absent from the formulation presented here. The full ramifications of this are also under investigation.

Until this question is resolved, we dare not examine quantities that are intimately bound up in the $1/m_Q$ structure of the effective theory or the model. We can, however, examine quantities that depend only on the leading-order structure of the model, as we believe that this is a reasonably accurate representation of

the effective theory. In particular, in the effective theory, one expects that the heavy quark should act as a static color source. This very important feature is reproduced in the model, as the leading dynamical behavior is described in terms of a Dirac equation for the light quark.

Two quantities of interest in HQET are $\bar{\Lambda}$ and λ_1, which are defined by

$$\begin{aligned} M_M &= m_Q + \bar{\Lambda} + \frac{\Delta M_M^2}{2m_Q}, \\ \left\langle M(v) \left| \bar{h}_Q (iD)^2 h_Q \right| M(v) \right\rangle &= 2M_M \lambda_1. \end{aligned}$$

$\bar{\Lambda}$ is crucial for the effective theory, as it appears as the coefficient in the $1/m_Q$ expansion: the expansion is written in terms of $\bar{\Lambda}/m_Q$, where $\bar{\Lambda}$ is, in essence, the contribution to the mass of the meson from the mass and kinetic energy of the brown muck. The left hand side of the second expression above is proportional to the kinetic energy of the heavy quark. The meson states in the bra and ket above are the leading order representation, and so correspond to our zeroth-order calculation. From our model, we obtain $\bar{\Lambda} = 0.45$ GeV for the ground state pseudoscalar/vector doublet, and $\lambda_1 = 0.67$ GeV^2. These values are in reasonable agreement with the values in the literature [46].

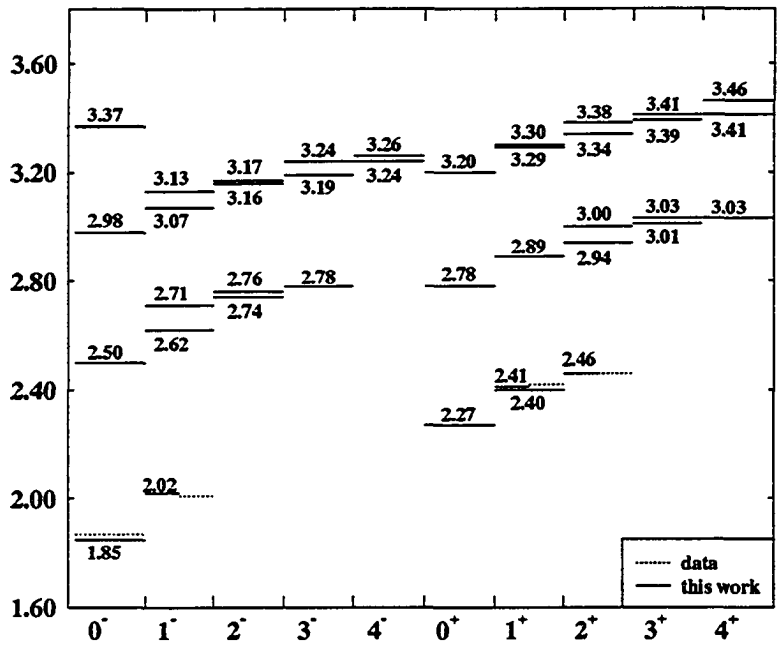

Figure 9: The $c\bar{u}$ spectrum. In this figure, solid lines represent the results of our calculation for the meson masses, W, to first order in the perturbation; dotted lines represent the data. The states have been labeled as J^P, where J and P are the total angular momentum and the parity of the meson, respectively.

Table 8: Data for Figure 9. ΔE_1, ΔE_2 and ΔE_3 (columns 6 to 8) are defined by (208 - 210) in Appendix C. p_{rms} and r_{rms} are the root mean squared p and r, respectively. ℓ and j_1 are the quantum numbers for orbital angular momentum and total angular momentum of the $\bar{u}$ quark. J and P are the total angular momentum and the parity of the meson, respectively.

					(GeV)				(1/GeV)
n	ℓ	j_1	J^P	W_{cu}	ΔE_1	ΔE_2	ΔE_3	p_{rms}	r_{rms}
1	0	1/2	0^-	1.85	0.2190	-0.2250	-0.1305	0.8190	2.1590
2	0	1/2	0^-	2.50	0.3747	-0.2729	-0.0890	1.0712	3.4610
3	0	1/2	0^-	2.98	0.5055	-0.2838	-0.0732	1.2442	4.5851
4	0	1/2	0^-	3.37	0.6322	-0.2898	-0.0647	1.3914	5.5381
1	0	1/2	1^-	2.02	0.2190	-0.2250	0.0435	0.8190	2.1590
2	0	1/2	1^-	2.62	0.3747	-0.2729	0.0297	1.0712	3.4610
1	2	3/2	1^-	2.71	0.3243	-0.1774	-0.0311	0.9966	3.4587
3	0	1/2	1^-	3.07	0.5055	-0.2838	0.0244	1.2442	4.5851
2	2	3/2	1^-	3.13	0.4632	-0.2024	-0.0261	1.1910	4.6267
1	2	5/2	2^-	2.74	0.3157	-0.1267	-0.0209	0.9833	3.7330
1	2	3/2	2^-	2.76	0.3243	-0.1774	0.0186	0.9966	3.4587
2	2	5/2	2^-	3.16	0.4539	-0.1603	-0.0175	1.1790	4.7810
2	2	3/2	2^-	3.17	0.4632	-0.2024	0.0157	1.1910	4.6267
1	2	5/2	3^-	2.78	0.3157	-0.1267	0.0149	0.9833	3.7330
2	2	5/2	3^-	3.19	0.4539	-0.1603	0.0125	1.1790	4.7810
1	4	7/2	3^-	3.24	0.4311	-0.1311	-0.0134	1.1490	4.7048
1	4	7/2	4^-	3.26	0.4311	-0.1311	0.0104	1.1490	4.7048
1	4	9/2	4^-	3.24	0.4350	-0.1065	-0.0109	1.1542	4.8992
1	1	1/2	0^+	2.27	0.2933	-0.2557	-0.0986	0.9478	2.6664
2	1	1/2	0^+	2.78	0.4341	-0.2746	-0.0781	1.1530	3.9983
3	1	1/2	0^+	3.20	0.5642	-0.2834	-0.0675	1.3145	5.0550
1	1	1/2	1^+	2.40	0.2933	-0.2557	0.0329	0.9478	2.6664
1	1	3/2	1^+	2.41	0.2585	-0.1499	-0.0363	0.8898	3.0248
2	1	1/2	1^+	2.89	0.4341	-0.2746	0.0260	1.1530	3.9983
2	1	3/2	1^+	2.89	0.4033	-0.1918	-0.0282	1.1114	4.1834
3	1	1/2	1^+	3.29	0.5642	-0.2834	0.0225	1.3145	5.0550
3	1	3/2	1^+	3.30	0.5365	-0.2121	-0.0246	1.2817	5.1805
1	1	3/2	2^+	2.46	0.2585	-0.1499	0.0218	0.8898	3.0248
2	1	3/2	2^+	2.94	0.4033	-0.1918	0.0169	1.1114	4.1834
1	3	5/2	2^+	3.00	0.3758	-0.1479	-0.0188	1.0727	4.1214
3	1	3/2	2^+	3.34	0.5365	-0.2121	0.0148	1.2817	5.1805
2	3	5/2	2^+	3.38	0.5120	-0.1714	-0.0164	1.2522	5.1685
1	3	7/2	3^+	3.01	0.3751	-0.1143	-0.0145	1.0718	4.3484
1	3	5/2	3^+	3.03	0.3758	-0.1479	0.0134	1.0727	4.1214
2	3	7/2	3^+	3.39	0.5098	-0.1424	-0.0128	1.2495	5.3078
2	3	5/2	3^+	3.41	0.5120	-0.1714	0.0117	1.2522	5.1685
1	3	7/2	4^+	3.03	0.3751	-0.1143	0.0112	1.0718	4.3484
2	3	7/2	4^+	3.41	0.5098	-0.1424	0.0100	1.2495	5.3078
1	5	9/2	4^+	3.46	0.4891	-0.1205	-0.0103	1.2238	5.2290

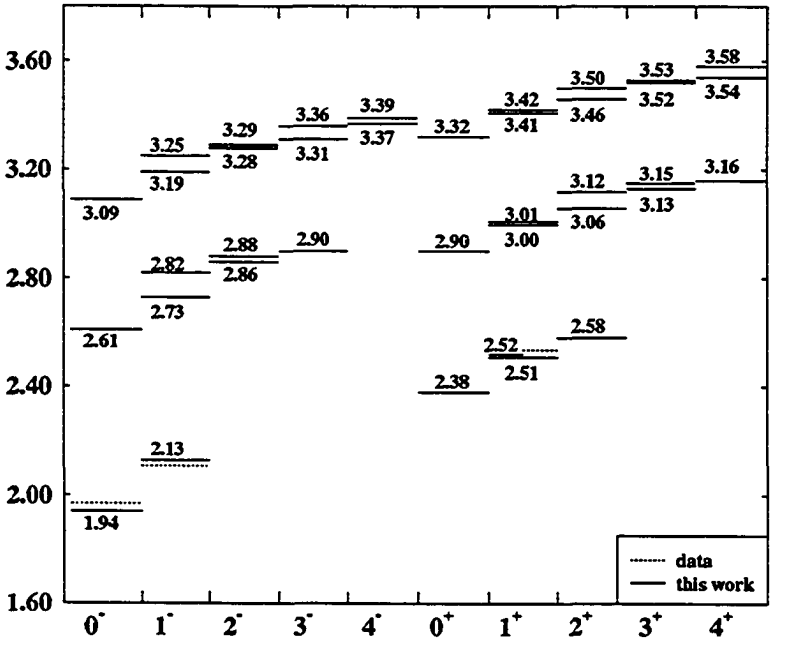

Figure 10: $c\bar{s}$ spectrum. See caption of Figure 9.

Table 9: Data for Figure 10. See caption of Table 8.

					(GeV)				(1/GeV)
n	ℓ	j_1	J^P	W_{cs}	ΔE_1	ΔE_2	ΔE_3	p_{rms}	r_{rms}
1	0	1/2	0^-	1.94	0.2470	-0.2432	-0.1397	0.8698	2.0134
2	0	1/2	0^-	2.61	0.4046	-0.2853	-0.0930	1.1131	3.3236
3	0	1/2	0^-	3.09	0.5372	-0.2936	-0.0757	1.2826	4.4419
1	0	1/2	1^-	2.13	0.2470	-0.2432	0.0466	0.8698	2.0134
2	0	1/2	1^-	2.73	0.4046	-0.2853	0.0310	1.1131	3.3236
1	2	3/2	1^-	2.82	0.3520	-0.1846	-0.0320	1.0383	3.3304
3	0	1/2	1^-	3.19	0.5372	-0.2936	0.0252	1.2826	4.4419
2	2	3/2	1^-	3.25	0.4934	-0.2089	-0.0267	1.2293	4.4878
1	2	5/2	2^-	2.86	0.3422	-0.1327	-0.0216	1.0237	3.5753
1	2	3/2	2^-	2.88	0.3520	-0.1846	0.0192	1.0383	3.3304
2	2	5/2	2^-	3.28	0.4834	-0.1661	-0.0179	1.2167	4.6289
2	2	3/2	2^-	3.29	0.4934	-0.2089	0.0160	1.2293	4.4878
1	2	5/2	3^-	2.90	0.3422	-0.1327	0.0154	1.0237	3.5753
2	2	5/2	3^-	3.31	0.4834	-0.1661	0.0128	1.2167	4.6289
1	4	7/2	3^-	3.36	0.4618	-0.1362	-0.0138	1.1892	4.5559
1	4	9/2	4^-	3.37	0.4643	-0.1105	-0.0113	1.1924	4.7347
1	4	7/2	4^-	3.39	0.4618	-0.1362	0.0107	1.1892	4.5559
1	1	1/2	0^+	2.38	0.3206	-0.2654	-0.1009	0.9908	2.5579
2	1	1/2	0^+	2.90	0.4639	-0.2829	-0.0795	1.1919	3.8675
3	1	1/2	0^+	3.32	0.5962	-0.2907	-0.0684	1.3512	4.9154
1	1	1/2	1^+	2.51	0.3206	-0.2654	0.0336	0.9908	2.5579
1	1	3/2	1^+	2.52	0.2839	-0.1582	-0.0378	0.9325	2.8728
2	1	1/2	1^+	3.00	0.4639	-0.2829	0.0265	1.1919	3.8675
2	1	3/2	1^+	3.01	0.4322	-0.1994	-0.0292	1.1505	4.0368
3	1	1/2	1^+	3.41	0.5962	-0.2907	0.0228	1.3512	4.9154
3	1	3/2	1^+	3.42	0.5679	-0.2190	-0.0252	1.3188	5.0322
1	1	3/2	2^+	2.58	0.2839	-0.1582	0.0227	0.9325	2.8728
2	1	3/2	2^+	3.06	0.4322	-0.1994	0.0175	1.1505	4.0368
1	3	5/2	2^+	3.12	0.4046	-0.1537	-0.0193	1.1132	3.9810
3	1	3/2	2^+	3.46	0.5679	-0.2190	0.0151	1.3188	5.0322
2	3	5/2	2^+	3.50	0.5433	-0.1768	-0.0168	1.2899	5.0238
1	3	7/2	3^+	3.13	0.4030	-0.1191	-0.0149	1.1109	4.1867
1	3	5/2	3^+	3.15	0.4046	-0.1537	0.0138	1.1132	3.9810
2	3	7/2	3^+	3.52	0.5405	-0.1472	-0.0131	1.2866	5.1516
2	3	5/2	3^+	3.53	0.5433	-0.1768	0.0120	1.2899	5.0238
1	3	7/2	4^+	3.16	0.4030	-0.1191	0.0116	1.1109	4.1867
2	3	7/2	4^+	3.54	0.5405	-0.1472	0.0102	1.2866	5.1516
1	5	9/2	4^+	3.58	0.5206	-0.1247	-0.0106	1.2627	5.0757

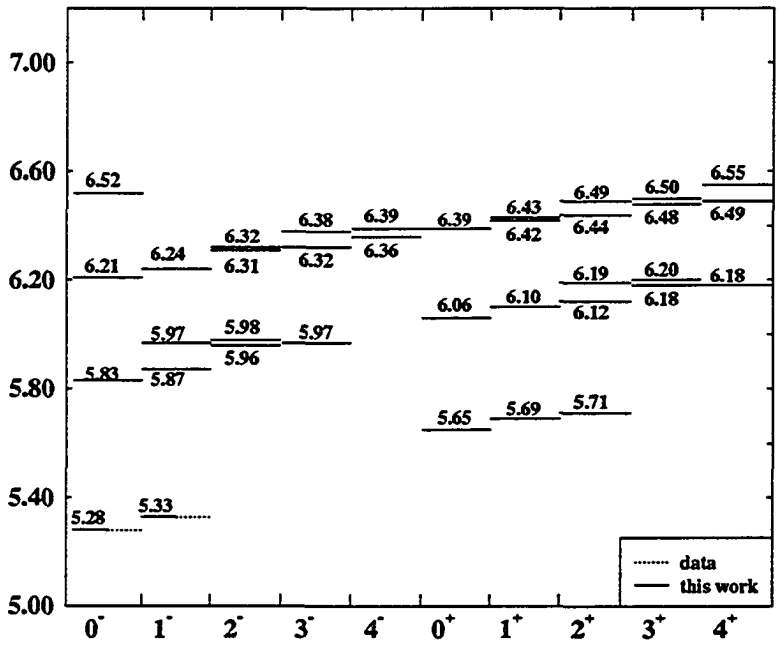

Figure 11: $b\bar{u}$ spectrum. See caption of Figure 9.

Table 10: Data for Figure 11. See caption of Table 8.

					(GeV)				(1/GeV)
n	ℓ	j_1	J^P	W_{bu}	ΔE_1	ΔE_2	ΔE_3	p_{rms}	r_{rms}
1	0	1/2	0^-	5.28	0.0689	-0.0708	-0.0410	0.8190	2.1590
2	0	1/2	0^-	5.83	0.1179	-0.0859	-0.0280	1.0712	3.4610
3	0	1/2	0^-	6.21	0.1590	-0.0893	-0.0230	1.2442	4.5851
4	0	1/2	0^-	6.52	0.1989	-0.0912	-0.0204	1.3914	5.5381
1	0	1/2	1^-	5.33	0.0689	-0.0708	0.0137	0.8190	2.1590
2	0	1/2	1^-	5.87	0.1179	-0.0859	0.0093	1.0712	3.4610
1	2	3/2	1^-	5.97	0.1020	-0.0558	-0.0098	0.9966	3.4587
3	0	1/2	1^-	6.24	0.1590	-0.0893	0.0077	1.2442	4.5851
1	2	5/2	2^-	5.96	0.0993	-0.0399	-0.0066	0.9833	3.7330
1	2	3/2	2^-	5.98	0.1020	-0.0558	0.0059	0.9966	3.4587
2	2	5/2	2^-	6.31	0.1428	-0.0504	-0.0055	1.1790	4.7810
2	2	3/2	2^-	6.32	0.1457	-0.0637	0.0049	1.1910	4.6267
1	2	5/2	3^-	5.97	0.0993	-0.0399	0.0047	0.9833	3.7330
2	2	5/2	3^-	6.32	0.1428	-0.0504	0.0039	1.1790	4.7810
1	4	7/2	3^-	6.38	0.1356	-0.0412	-0.0042	1.1490	4.7048
1	4	9/2	4^-	6.36	0.1368	-0.0335	-0.0034	1.1542	4.8992
1	4	7/2	4^-	6.39	0.1356	-0.0412	0.0033	1.1490	4.7048
1	1	1/2	0^+	5.65	0.0923	-0.0804	-0.0310	0.9478	2.6664
2	1	1/2	0^+	6.06	0.1365	-0.0864	-0.0246	1.1530	3.9983
3	1	1/2	0^+	6.39	0.1775	-0.0892	-0.0212	1.3145	5.0550
1	1	1/2	1^+	5.69	0.0923	-0.0804	0.0103	0.9478	2.6664
1	1	3/2	1^+	5.69	0.0813	-0.0471	-0.0114	0.8898	3.0248
2	1	1/2	1^+	6.10	0.1365	-0.0864	0.0082	1.1530	3.9983
2	1	3/2	1^+	6.10	0.1269	-0.0603	-0.0089	1.1114	4.1834
3	1	1/2	1^+	6.42	0.1775	-0.0892	0.0071	1.3145	5.0550
3	1	3/2	1^+	6.43	0.1688	-0.0667	-0.0077	1.2817	5.1805
1	1	3/2	2^+	5.71	0.0813	-0.0471	0.0068	0.8898	3.0248
2	1	3/2	2^+	6.12	0.1269	-0.0603	0.0053	1.1114	4.1834
1	3	5/2	2^+	6.19	0.1182	-0.0465	-0.0059	1.0727	4.1214
3	1	3/2	2^+	6.44	0.1688	-0.0667	0.0046	1.2817	5.1805
2	3	5/2	2^+	6.49	0.1611	-0.0539	-0.0052	1.2522	5.1685
1	3	7/2	3^+	6.18	0.1180	-0.0360	-0.0045	1.0718	4.3484
1	3	5/2	3^+	6.20	0.1182	-0.0465	0.0042	1.0727	4.1214
2	3	7/2	3^+	6.48	0.1604	-0.0448	-0.0040	1.2495	5.3078
2	3	5/2	3^+	6.50	0.1611	-0.0539	0.0037	1.2522	5.1685
1	3	7/2	4^+	6.18	0.1180	-0.0360	0.0035	1.0718	4.3484
2	3	7/2	4^+	6.49	0.1604	-0.0448	0.0031	1.2495	5.3078
1	5	7/2	4^+	6.55	0.1539	-0.0379	-0.0032	1.2238	5.2290

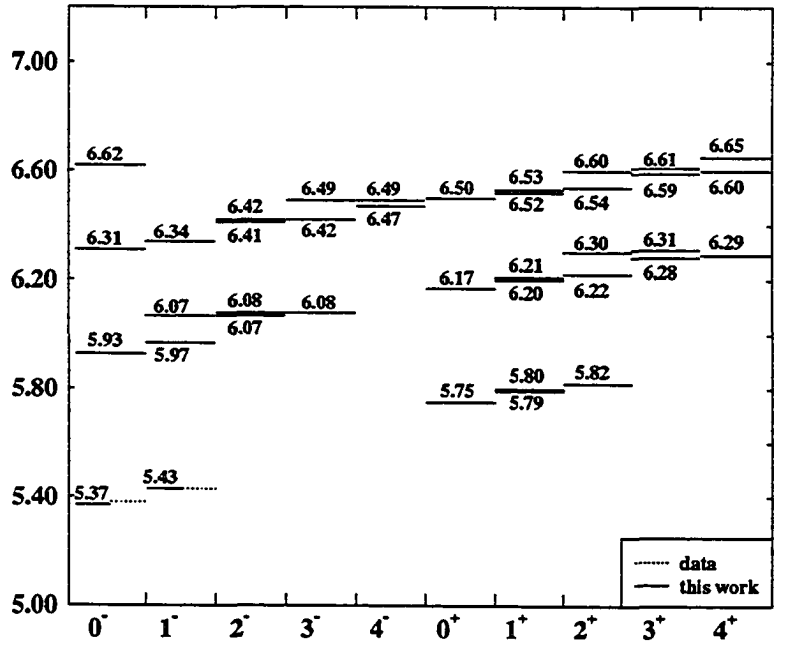

Figure 12: $b\bar{s}$ spectrum. See caption of Figure 9.

Table 11: Data for Figure 12. See caption of Table 8.

					(GeV)				(1/GeV)
n	ℓ	j_1	J^P	W_{bs}	ΔE_1	ΔE_2	ΔE_3	p_{rms}	r_{rms}
1	0	1/2	0^-	5.37	0.0777	-0.0765	-0.0439	0.8698	2.0134
2	0	1/2	0^-	5.93	0.1273	-0.0897	-0.0292	1.1131	3.3236
3	0	1/2	0^-	6.31	0.1690	-0.0924	-0.0238	1.2826	4.4419
4	0	1/2	0^-	6.62	0.2095	-0.0939	-0.0209	1.4281	5.3909
1	0	1/2	1^-	5.43	0.0777	-0.0765	0.0146	0.8698	2.0134
2	0	1/2	1^-	5.97	0.1273	-0.0897	0.0097	1.1131	3.3236
1	2	3/2	1^-	6.07	0.1107	-0.0581	-0.0101	1.0383	3.3304
3	0	1/2	1^-	6.34	0.1690	-0.0924	0.0079	1.2826	4.4419
1	2	5/2	2^-	6.07	0.1076	-0.0417	-0.0068	1.0237	3.5753
1	2	3/2	2^-	6.08	0.1107	-0.0581	0.0060	1.0383	3.3304
2	2	5/2	2^-	6.41	0.1521	-0.0522	-0.0056	1.2167	4.6289
2	2	3/2	2^-	6.42	0.1552	-0.0657	0.0050	1.2293	4.4878
1	2	5/2	3^-	6.08	0.1076	-0.0417	0.0049	1.0237	3.5753
2	2	5/2	3^-	6.42	0.1521	-0.0522	0.0040	1.2167	4.6289
1	4	7/2	3^-	6.49	0.1453	-0.0428	-0.0043	1.1892	4.5559
1	4	9/2	4^-	6.47	0.1461	-0.0348	-0.0035	1.1924	4.7347
1	4	7/2	4^-	6.49	0.1453	-0.0428	0.0034	1.1892	4.5559
1	1	1/2	0^+	5.75	0.1008	-0.0835	-0.0317	0.9908	2.5579
2	1	1/2	0^+	6.17	0.1459	-0.0890	-0.0250	1.1919	3.8675
3	1	1/2	0^+	6.50	0.1875	-0.0914	-0.0215	1.3512	4.9154
1	1	1/2	1^+	5.79	0.1008	-0.0835	0.0106	0.9908	2.5579
1	1	3/2	1^+	5.80	0.0893	-0.0498	-0.0119	0.9325	2.8728
2	1	1/2	1^+	6.20	0.1459	-0.0890	0.0083	1.1919	3.8675
2	1	3/2	1^+	6.21	0.1360	-0.0627	-0.0092	1.1505	4.0368
3	1	1/2	1^+	6.52	0.1875	-0.0914	0.0072	1.3512	4.9154
3	1	3/2	1^+	6.53	0.1786	-0.0689	-0.0079	1.3188	5.0322
1	1	3/2	2^+	5.82	0.0893	-0.0498	0.0071	0.9325	2.8728
2	1	3/2	2^+	6.22	0.1360	-0.0627	0.0055	1.1505	4.0368
1	3	5/2	2^+	6.30	0.1273	-0.0484	-0.0061	1.1132	3.9810
3	1	3/2	2^+	6.54	0.1786	-0.0689	0.0048	1.3188	5.0322
2	3	5/2	2^+	6.60	0.1709	-0.0556	-0.0053	1.2899	5.0238
1	3	7/2	3^+	6.28	0.1268	-0.0375	-0.0047	1.1109	4.1867
1	3	5/2	3^+	6.31	0.1273	-0.0484	0.0043	1.1132	3.9810
2	3	7/2	3^+	6.59	0.1700	-0.0463	-0.0041	1.2866	5.1516
2	3	5/2	3^+	6.61	0.1709	-0.0556	0.0038	1.2899	5.0238
1	3	7/2	4^+	6.29	0.1268	-0.0375	0.0037	1.1109	4.1867
2	3	7/2	4^+	6.60	0.1700	-0.0463	0.0032	1.2866	5.1516
1	5	9/2	4^+	6.65	0.1638	-0.0392	-0.0033	1.2627	5.0757

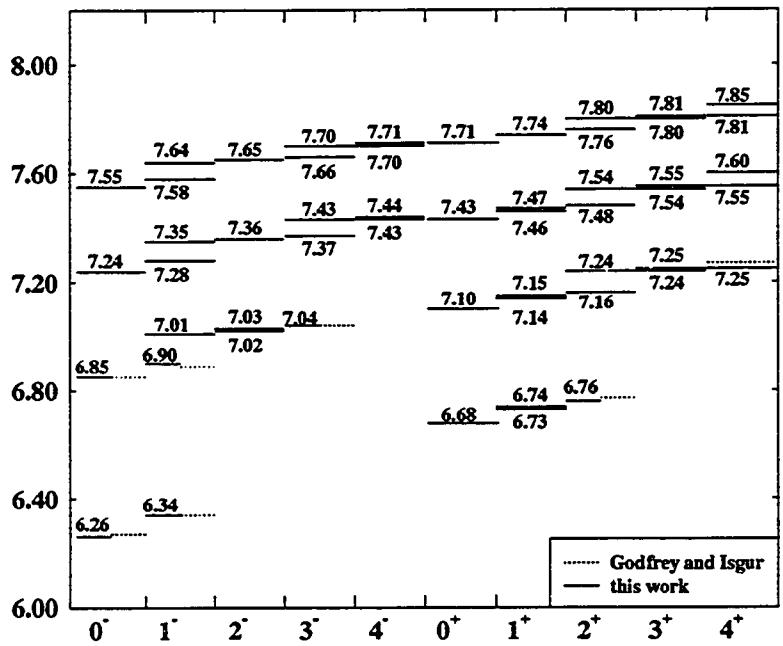

Figure 13: $b\bar{c}$ spectrum. See caption of Figure 9.

Table 12: Data for Figure 13. See caption of Table 8.

					(GeV)				(1/GeV)
n	ℓ	j_1	J^P	W_{bc}	ΔE_1	ΔE_2	ΔE_3	p_{rms}	r_{rms}
1	0	1/2	0^-	6.26	0.1563	-0.1134	-0.0633	1.2334	1.3657
2	0	1/2	0^-	6.85	0.2037	-0.1122	-0.0368	1.4083	2.5830
3	0	1/2	0^-	7.24	0.2494	-0.1104	-0.0286	1.5581	3.6155
4	0	1/2	0^-	7.55	0.2944	-0.1095	-0.0246	1.6931	4.5086
1	0	1/2	1^-	6.34	0.1563	-0.1134	0.0211	1.2334	1.3657
2	0	1/2	1^-	6.90	0.2037	-0.1122	0.0123	1.4083	2.5830
1	2	3/2	1^-	7.01	0.1807	-0.0701	-0.0113	1.3262	2.6413
3	0	1/2	1^-	7.28	0.2494	-0.1104	0.0095	1.5581	3.6155
2	2	3/2	1^-	7.35	0.2316	-0.0769	-0.0094	1.5015	3.6885
4	0	1/2	1^-	7.58	0.2944	-0.1095	0.0082	1.6931	4.5086
3	2	3/2	1^-	7.64	0.2795	-0.0810	-0.0082	1.6497	4.5787
1	2	5/2	2^-	7.02	0.1755	-0.0524	-0.0079	1.3073	2.7607
1	2	3/2	2^-	7.03	0.1807	-0.0701	0.0068	1.3262	2.6413
2	2	5/2	2^-	7.36	0.2270	-0.0625	-0.0064	1.4867	3.7674
2	2	3/2	2^-	7.36	0.2316	-0.0769	0.0056	1.5015	3.6885
3	2	5/2	2^-	7.65	0.2754	-0.0683	-0.0056	1.6375	4.6380
3	2	3/2	2^-	7.65	0.2795	-0.0810	0.0049	1.6497	4.5787
1	2	5/2	3^-	7.04	0.1755	-0.0524	0.0057	1.3073	2.7607
2	2	5/2	3^-	7.37	0.2270	-0.0625	0.0046	1.4867	3.7674
1	4	7/2	3^-	7.43	0.2212	-0.0514	-0.0050	1.4676	3.7253
3	2	5/2	3^-	7.66	0.2754	-0.0683	0.0040	1.6375	4.6380
2	4	7/2	3^-	7.70	0.2698	-0.0578	-0.0043	1.6206	4.6269
1	4	9/2	4^-	7.43	0.2206	-0.0423	-0.0041	1.4653	3.8225
1	4	7/2	4^-	7.44	0.2212	-0.0514	0.0039	1.4676	3.7253
2	4	9/2	4^-	7.70	0.2690	-0.0499	-0.0037	1.6184	4.6955
2	4	7/2	4^-	7.71	0.2698	-0.0578	0.0034	1.6206	4.6269
1	1	1/2	0^+	6.68	0.1711	-0.1006	-0.0358	1.2905	1.9819
2	1	1/2	0^+	7.10	0.2214	-0.1034	-0.0275	1.4683	3.1297
3	1	1/2	0^+	7.43	0.2679	-0.1040	-0.0233	1.6151	4.0917
4	1	1/2	0^+	7.71	0.3138	-0.1046	-0.0208	1.7477	4.9297
1	1	1/2	1^+	6.73	0.1711	-0.1006	0.0119	1.2905	1.9819
1	1	3/2	1^+	6.74	0.1560	-0.0648	-0.0143	1.2323	2.1287
2	1	1/2	1^+	7.14	0.2214	-0.1034	0.0092	1.4683	3.1297
2	1	3/2	1^+	7.15	0.2096	-0.0761	-0.0108	1.4285	3.2251
3	1	1/2	1^+	7.46	0.2679	-0.1040	0.0078	1.6151	4.0917
3	1	3/2	1^+	7.47	0.2579	-0.0809	-0.0090	1.5845	4.1645
4	1	1/2	1^+	7.74	0.3138	-0.1046	0.0069	1.7477	4.9297
4	1	3/2	1^+	7.74	0.3047	-0.0840	-0.0080	1.7223	4.9898
1	1	3/2	2^+	6.76	0.1560	-0.0648	0.0086	1.2323	2.1287
2	1	3/2	2^+	7.16	0.2096	-0.0761	0.0065	1.4285	3.2251
1	3	5/2	2^+	7.24	0.2000	-0.0583	-0.0069	1.3953	3.2111
3	1	3/2	2^+	7.48	0.2579	-0.0809	0.0054	1.5845	4.1645
2	3	5/2	2^+	7.54	0.2495	-0.0650	-0.0059	1.5584	4.1495
4	1	3/2	2^+	7.76	0.3047	-0.0840	0.0048	1.7223	4.9898
3	3	5/2	2^+	7.80	0.2973	-0.0697	-0.0053	1.7013	5.0133
1	3	7/2	3^+	7.24	0.1978	-0.0463	-0.0055	1.3878	3.3172
1	3	5/2	3^+	7.25	0.2000	-0.0583	0.0049	1.3953	3.2111
2	3	7/2	3^+	7.54	0.2474	-0.0549	-0.0046	1.5521	4.2519
2	3	5/2	3^+	7.55	0.2495	-0.0650	0.0042	1.5584	4.1495
3	3	7/2	3^+	7.80	0.2953	-0.0606	-0.0042	1.6955	5.0685
3	3	5/2	3^+	7.81	0.2973	-0.0697	0.0038	1.7013	5.0133
1	3	7/2	4^+	7.25	0.1978	-0.0463	0.0042	1.3878	3.3172
2	3	7/2	4^+	7.55	0.2474	-0.0549	0.0036	1.5521	4.2519
1	5	9/2	4^+	7.60	0.2430	-0.0468	-0.0038	1.5381	4.1986
3	3	7/2	4^+	7.81	0.2953	-0.0606	0.0032	1.6955	5.0685
2	5	9/2	4^+	7.85	0.2910	-0.0528	-0.0035	1.6831	5.0426

4.2 $Q\bar{Q}$ Sector

Figures 14 and 15 show the spectra for $c\bar{c}$ and $b\bar{b}$ mesons as calculated with (144). As before, the calculated masses are shown as solid lines and the experimental masses as dotted lines. The $D\bar{D}$ and $B\bar{B}$ thresholds are shown as horizontal dotdashed lines across the Figures 14 and 15, respectively. Ref. [48] has also listed states $h_c(1P)$ with mass 3.526 GeV and $\eta_c(2S)$ with mass 3.590 GeV. We believe they correspond to the states $2^1S_0(3.67)$ and $1^1P_1(3.51)$ in Figure 14, respectively.

The $b\bar{b}$ spectrum is in quite good agreement with the data for the states lying below the $B\bar{B}$ threshold. The agreement deteriorates as the masses approach and cross the $B\bar{B}$ threshold. As argued in the previous subsection, this may be the result of the absence of coupling to strong decay channels in our model. The agreement for the $c\bar{c}$ is less satisfactory. This may be an indication of the inadequacy of the truncation of the nonrelativistic expansion at order $\frac{1}{m_Q^2}$. In both cases the hyperfine splitting of the spin triplet states is too large.

Since the hyperfine tensor interaction has non-zero off diagonal matrix elements for states with spin 1 and with L differing by 0 or 2, there should be mixings of states such as $^3S_1$ with $^3D_1$ and $^3P_2$ with $^3F_2$. These mixings do not affect the spectrum to order $\frac{1}{m_Q^2}$ but should result in shifts in some states at higher order in both the $b\bar{b}$ and $c\bar{c}$ spectra.

Table 13 and Table 14 show the individual contributions to the masses W of a number of $c\bar{c}$ and $b\bar{b}$ states from $W^{(0)}$, E_c, E_{hyp}, E_{so}, E_{SR} and E_{VR}. The retardation contributions E_{SR} and E_{VR} are clearly gauge dependent since they would not appear in Coulomb gauge. E_c is also gauge dependent. These contributions may also be sensitive to the choice of quasipotential prescription. To this order, E_{hyp} and E_{so} should be independent of these factors. Note that the scalar and vector retardation contributions are of opposite sign and therefore tend to cancel. However the sum of these contributions is comparable with E_{hyp} and E_{so}. The assumption that the scalar retardation potential depends only on the square of the exchanged four-momentum, Q^2, is uncontrolled and it is possible to propose forms for this retardation potential which would eliminate the scalar term altogether.

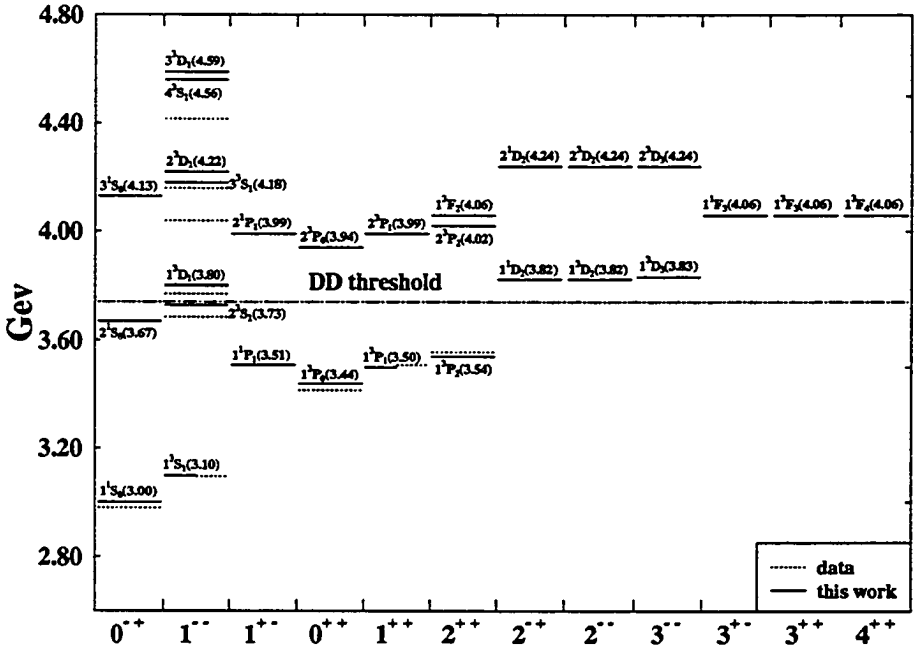

Figure 14: $c\bar{c}$ spectra. See caption of Figure 9.

Table 13: Zeroth order and various first order interaction energies in the $c\bar{c}$ spectrum. E_c, E_{hyp}, E_{so}, E_{SR} and E_{VR} are defined in (141) of Section 3.2.2. p_{rms} and r_{rms} are the root mean squared p and r, respectively.

			(GeV)							(1/GeV)
State	W	$W^{(0)}$	E_c	E_{hyp}	E_{so}	E_{SR}	E_{VR}	$E_{SR}+E_{VR}$	p_{rms}	r_{rms}
1^1S_0	3.00	3.2621	-0.1700	-0.0790	0.0000	0.0427	-0.0594	-0.0167	0.7392	2.0786
1^3S_1	3.10	3.2621	-0.1700	0.0263	0.0000	0.0427	-0.0594	-0.0167	0.7392	2.0786
2^1S_0	3.67	3.9063	-0.2614	-0.0485	0.0000	0.1142	-0.0444	0.0698	0.8479	4.0858
2^3S_1	3.73	3.9063	-0.2614	0.0162	0.0000	0.1142	-0.0444	0.0698	0.8479	4.0858
3^1S_0	4.13	4.3659	-0.3596	-0.0400	0.0000	0.2031	-0.0394	0.1637	0.9429	5.7599
3^3S_1	4.18	4.3659	-0.3596	0.0133	0.0000	0.2031	-0.0394	0.1637	0.9429	5.7599
4^1S_0	4.52	4.7520	-0.4691	-0.0357	0.0000	0.3051	-0.0369	0.2682	1.0250	7.2280
4^3S_1	4.56	4.7520	-0.4691	0.0119	0.0000	0.3051	-0.0369	0.2682	1.0250	7.2280
5^1S_0	4.86	5.0959	-0.5878	-0.0330	0.0000	0.4174	-0.0354	0.3820	1.0968	8.5616
5^3S_1	4.90	5.0959	-0.5878	0.0110	0.0000	0.4174	-0.0354	0.3820	1.0968	8.5616
6^1S_0	5.17	5.4115	-0.7143	-0.0311	0.0000	0.5384	-0.0344	0.5040	1.1608	9.7987
6^3S_1	5.21	5.4115	-0.7143	0.0104	0.0000	0.5384	-0.0344	0.5040	1.1608	9.7987
1^1P_1	3.51	3.7028	-0.2281	-0.0064	0.0000	0.0786	-0.0413	0.0373	0.7914	3.1910
1^3P_0	3.44	3.7028	-0.2281	-0.0209	-0.0521	0.0786	-0.0413	0.0373	0.7914	3.1910
1^3P_1	3.50	3.7028	-0.2281	0.0136	-0.0261	0.0786	-0.0413	0.0373	0.7914	3.1910
1^3P_2	3.54	3.7028	-0.2281	-0.0002	0.0261	0.0786	-0.0413	0.0373	0.7914	3.1910
2^1P_1	3.99	4.1948	-0.3196	-0.0048	0.0000	0.1600	-0.0364	0.1236	0.8962	5.0121
2^3P_0	3.94	4.1948	-0.3196	-0.0166	-0.0417	0.1600	-0.0364	0.1236	0.8962	5.0121
2^3P_1	3.99	4.1948	-0.3196	-0.0107	-0.0208	0.1600	-0.0364	0.1236	0.8962	5.0121
2^3P_2	4.02	4.1948	-0.3196	-0.0002	0.0208	0.1600	-0.0364	0.1236	0.8962	5.0121
1^1D_2	3.82	4.0196	-0.2830	-0.0019	0.0000	0.1182	-0.0359	0.0823	0.8496	4.1448
1^3D_1	3.80	4.0196	-0.2830	-0.0037	-0.0127	0.1182	-0.0359	0.0823	0.8496	4.1448
1^3D_2	3.82	4.0196	-0.2830	0.0049	-0.0042	0.1182	-0.0359	0.0823	0.8496	4.1448
1^3D_3	3.83	4.0196	-0.2830	-0.0006	0.0085	0.1182	-0.0359	0.0823	0.8496	4.1448
2^1D_2	4.24	4.4413	-0.3788	-0.0018	0.0000	0.2080	-0.0334	0.1746	0.9446	5.8275
2^3D_1	4.22	4.4413	-0.3788	-0.0030	-0.0116	0.2080	-0.0334	0.1746	0.9446	5.8275
2^3D_2	4.24	4.4413	-0.3788	0.0042	-0.0039	0.2080	-0.0334	0.1746	0.9446	5.8275
2^3D_3	4.24	4.4413	-0.3788	-0.0004	0.0077	0.2080	-0.0334	0.1746	0.9446	5.8275
3^1D_2	4.60	4.8088	-0.4865	-0.0017	0.0000	0.3104	-0.0322	0.2782	1.0263	7.2902
3^3D_1	4.59	4.8088	-0.4865	-0.0027	-0.0115	0.3104	-0.0322	0.2782	1.0263	7.2902
3^3D_2	4.60	4.8088	-0.4865	0.0039	-0.0038	0.3104	-0.0322	0.2782	1.0263	7.2902
3^3D_3	4.61	4.8088	-0.4865	-0.0003	0.0077	0.3104	-0.0322	0.2782	1.0263	7.2902
1^1F_3	4.06	4.2838	-0.3536	-0.0006	0.0000	0.1612	-0.0330	0.1282	0.9029	5.0048
1^3F_2	4.06	4.2838	-0.3536	-0.0017	0.0037	0.1612	-0.0330	0.1282	0.9029	5.0048
1^3F_3	4.06	4.2838	-0.3536	0.0025	0.0009	0.1612	-0.0330	0.1282	0.9029	5.0048
1^3F_4	4.06	4.2838	-0.3536	-0.0006	-0.0028	0.1612	-0.0330	0.1282	0.9029	5.0048

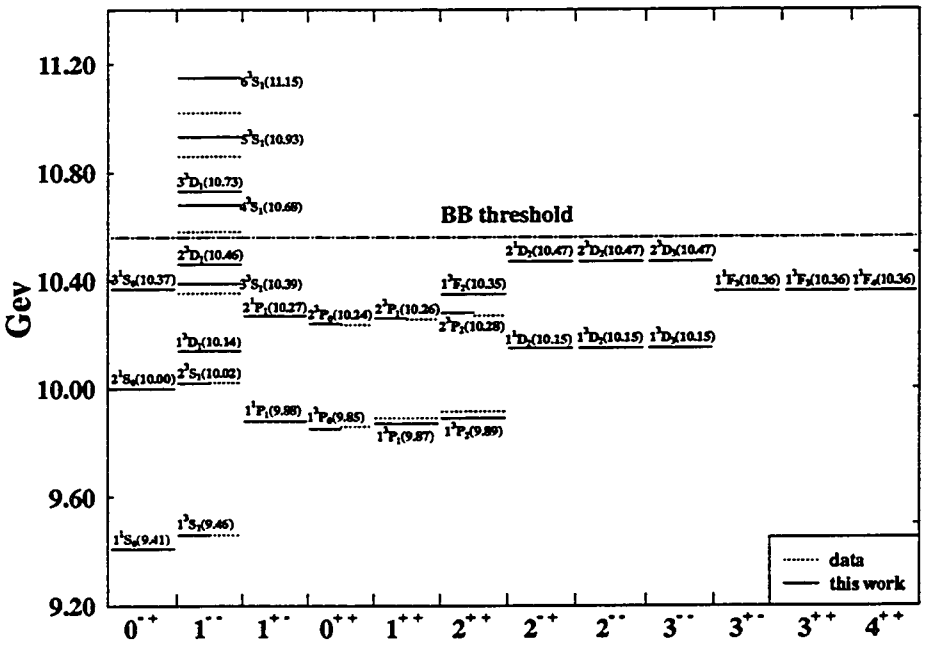

Figure 15: $b\bar{b}$ spectra. See caption of Figure 9.

Table 14: Zeroth order and various first order interaction energies in the $b\bar{b}$ spectrum. See caption of Table 13.

State	W	$W^{(0)}$	E_c	E_{hyp}	E_{so}	E_{SR}	E_{VR}	$E_{SR}+E_{VR}$	p_{rms}	r_{rms}
					(GeV)					(GeV)
1^1S_0	9.41	9.5315	-0.0602	-0.0367	0.0000	0.0072	-0.0297	-0.0224	1.3077	1.1930
1^3S_1	9.46	9.5315	-0.0602	0.0122	0.0000	0.0072	-0.0297	-0.0224	1.3077	1.1930
2^1S_0	10.00	10.0892	-0.0708	-0.0192	0.0000	0.0175	-0.0192	-0.0017	1.3719	2.5139
2^3S_1	10.02	10.0892	-0.0708	0.0064	0.0000	0.0175	-0.0192	-0.0017	1.3719	2.5139
3^1S_0	10.37	10.4511	-0.0839	-0.0146	0.0000	0.0302	-0.0160	0.0142	1.4771	3.6558
3^3S_1	10.39	10.4511	-0.0839	0.0049	0.0000	0.0302	-0.0160	0.0142	1.4771	3.6558
4^1S_0	10.66	10.7411	-0.0992	-0.0125	0.0000	0.0447	-0.0144	0.0303	1.5769	4.6722
4^3S_1	10.68	10.7411	-0.0992	0.0042	0.0000	0.0447	-0.0144	0.0303	1.5769	4.6722
5^1S_0	10.91	10.9928	-0.1162	-0.0113	0.0000	0.0608	-0.0135	0.0473	1.6697	5.5961
5^3S_1	10.93	10.9928	-0.1162	0.0038	0.0000	0.0608	-0.0135	0.0473	1.6697	5.5961
6^1S_0	11.14	11.2202	-0.1345	-0.0105	0.0000	0.0781	-0.0128	0.0653	1.7551	6.4520
6^3S_1	11.15	11.2202	-0.1345	0.0035	0.0000	0.0781	-0.0128	0.0653	1.7551	6.4520
1^1P_1	9.88	9.9438	-0.0610	-0.0023	0.0000	0.0126	-0.0169	-0.0043	1.2977	1.9561
1^3P_0	9.85	9.9438	-0.0610	-0.0074	-0.0243	0.0126	-0.0169	-0.0043	1.2977	1.9561
1^3P_1	9.87	9.9438	-0.0610	0.0049	-0.0121	0.0126	-0.0169	-0.0043	1.2977	1.9561
1^3P_2	9.89	9.9438	-0.0610	-0.0001	0.0121	0.0126	-0.0169	-0.0043	1.2977	1.9561
2^1P_1	10.27	10.3321	-0.0752	-0.0016	0.0000	0.0244	-0.0143	0.0101	1.4166	3.1728
2^3P_0	10.24	10.3321	-0.0752	-0.0056	-0.0182	0.0244	-0.0143	0.0101	1.4166	3.1728
2^3P_1	10.26	10.3321	-0.0752	0.0036	-0.0091	0.0244	-0.0143	0.0101	1.4166	3.1728
2^3P_2	10.28	10.3321	-0.0752	-0.0001	0.0091	0.0244	-0.0143	0.0101	1.4166	3.1728
1^1D_2	10.15	10.2072	-0.0637	-0.0008	0.0000	0.0186	-0.0139	0.0047	1.3535	2.6082
1^3D_1	10.14	10.2072	-0.0637	-0.0011	-0.0097	0.0186	-0.0139	0.0047	1.3535	2.6082
1^3D_2	10.15	10.2072	-0.0637	0.0016	-0.0032	0.0186	-0.0139	0.0047	1.3535	2.6082
1^3D_3	10.15	10.2072	-0.0637	-0.0001	0.0064	0.0186	-0.0139	0.0047	1.3535	2.6082
2^1D_2	10.47	10.5277	-0.0792	-0.0006	0.0000	0.0315	-0.0125	0.0190	1.4696	3.7489
2^3D_1	10.46	10.5277	-0.0792	-0.0009	-0.0080	0.0315	-0.0125	0.0190	1.4696	3.7489
2^3D_2	10.47	10.5277	-0.0792	0.0013	-0.0027	0.0315	-0.0125	0.0190	1.4696	3.7489
2^3D_3	10.47	10.5277	-0.0792	-0.0001	0.0053	0.0315	-0.0125	0.0190	1.4696	3.7489
3^1D_2	10.74	10.7982	-0.0955	-0.0005	0.0000	0.0461	-0.0117	0.0344	1.5729	4.7553
3^3D_1	10.73	10.7982	-0.0955	-0.0008	-0.0071	0.0461	-0.0117	0.0344	1.5729	4.7553
3^3D_2	10.74	10.7982	-0.0955	0.0012	-0.0024	0.0461	-0.0117	0.0344	1.5729	4.7553
3^3D_3	10.74	10.7982	-0.0955	-0.0001	0.0048	0.0461	-0.0117	0.0344	1.5729	4.7553
1^1F_3	10.36	10.4164	-0.0717	-0.0004	0.0000	0.0250	-0.0124	0.0126	1.4160	3.1965
1^3F_2	10.35	10.4164	-0.0717	-0.0004	-0.0047	0.0250	-0.0124	0.0126	1.4160	3.1965
1^3F_3	10.36	10.4164	-0.0717	0.0008	-0.0012	0.0250	-0.0124	0.0126	1.4160	3.1965
1^3F_4	10.36	10.4164	-0.0717	-0.0001	0.0035	0.0250	-0.0124	0.0126	1.4160	3.1965

Chapter 5

Conclusion and Outlook

5.1 Conclusion

We have constructed a model for heavy mesons based on a relativistic bound state equation - the spectator or Gross equation. The kernel used in the equation is the one-gluon-exchange interaction for the asymptotic region plus a scalar linear potential for the confining region. Using this model, we have calculated the heavy meson spectra. By choosing a reasonable set of model parameters, we are able to obtain a respectable fit to the observed heavy meson masses and to predict the approximate masses of heavy mesons which have not yet been observed.

For $Q\bar{q}$ and $q\bar{Q}$ mesons, we have studied the meson spectra in the approach to the heavy quark symmetry limit. By expanding the Gross equation in $1/m_Q$, we have obtained the meson Hamiltonian to the order of $1/m_Q$. While solving the Hamiltonian, to observe the $1/m_Q$ effects consistently, the meson masses and wave functions are calculated using perturbative techniques and the first order corrections to the unperturbed masses are obtained. We have found that our results agree with the predictions from HQET. In particular, in the limit $m_Q \to \infty$, the one-body limit — Dirac equation for the light quark q is obtained, and the spectra of B and D mesons, B^* and D^* mesons etc. are very much alike, modulo $1/m_b$ and $1/m_c$ effects.

$Q\bar{Q}$ mesons are studied for the purpose of separating the scalar potential shift c from the light quark mass m_1. One can see from the zeroth-order Hamiltonian of the $Q\bar{q}$ mesons (89) that m_1 and c cannot be distinguished in the $Q\bar{q}$, $q\bar{Q}$ sector. However, the separation of c and m_1 can be obtained by studying the $1/m_Q^2$ effects in the $Q\bar{Q}$ sector. By using a similar technique to that used in the $Q\bar{q}$, $q\bar{Q}$ sector, we have calculated the masses and wave functions for $Q\bar{Q}$ mesons and found that the retardation contributions to the $Q\bar{Q}$ mesons, which are missing in most other quark models, have noticeable effects.

While $1/m_Q$ expansion has been used in obtaining meson Hamiltonians and calculating meson masses and wave functions, our model should give better results for b-flavored mesons than for c-flavored mesons since in c-flavored mesons, $v \sim \frac{1}{2}c$, but in b-flavored mesons, $v \sim \frac{1}{5}c$.

5.2 Outlook

The goal of constructing this model is to study electroweak interactions and ultimately to extract some properties, such as V_{cb} — one of the parameters in the standard model, with little model dependence. The model is therefore constructed so that the weak decay amplitudes for semileptonic decays $B \to D\ell\bar{\nu}$ and $B \to D^*\ell\bar{\nu}$ can be calculated in the framework of HQET. In particular, the universal Isgur-Wise functions in the decay current matrix elements can be calculated using the wave functions obtained in this model. Such a calculation is underway.

In addition, the slope of the Isgur-Wise function for the elastic decays can also be calculated in this model, weak decay constants may be evaluated and a number of HQET sum rules may be tested. Furthermore, the strong and electromagnetic decays can also be treated with the wave functions that we have obtained here. Thus, the wave functions obtained in this model may be applied to a number of different calculations.

Appendix A

Notation

1. The units are chosen such that $\hbar = c = 1$.

2. A four-vector A is represented by:

$$A = \left(A^0, A^1, A^2, A^3\right) = \left(A^0, A_x, A_y, A_z\right) = \left(A^0, \mathbf{A}\right) .$$

examples :

a) coordinates : $x = (x^0, x^1, x^2, x^3) = (t, x, y, z) = (t,\ \mathbf{x})$,

b) four − momentum : $p = (p^0, p^1, p^2, p^3) = (E, p_x, p_y, p_z) = (E,\ \mathbf{p})$.

3. The metric is chosen such that the inner product of two four-vectors is

$$A \cdot B = A^0 B^0 - \mathbf{A} \cdot \mathbf{B}.$$

4. The $\boldsymbol{\alpha}$, β matrices are defined as

$$\boldsymbol{\alpha} = \begin{pmatrix} 0 & \boldsymbol{\sigma} \\ \boldsymbol{\sigma} & 0 \end{pmatrix}, \qquad \beta = \begin{pmatrix} I & 0 \\ 0 & -I \end{pmatrix},$$

where I is the unit matrix, $\boldsymbol{\sigma}$ are the Pauli matrices:

$$I = \begin{pmatrix} 1 & 0 \\ 0 & 1 \end{pmatrix}, \ \sigma_x = \begin{pmatrix} 0 & 1 \\ 1 & 0 \end{pmatrix}, \ \sigma_y = \begin{pmatrix} 0 & -i \\ i & 0 \end{pmatrix}, \ \sigma_z = \begin{pmatrix} 1 & 0 \\ 0 & -1 \end{pmatrix}.$$

5. The γ matrices are defined as

$$\gamma = \left(\gamma^0,\ \boldsymbol{\gamma}\right) = \left(\beta,\ \beta\boldsymbol{\alpha}\right) .$$

We use the standard form of the γ matrices:

$$\gamma^0 = \begin{pmatrix} I & 0 \\ 0 & -I \end{pmatrix} , \qquad \boldsymbol{\gamma} = \begin{pmatrix} 0 & \boldsymbol{\sigma} \\ -\boldsymbol{\sigma} & 0 \end{pmatrix} .$$

6. The matrix γ^5 is defined as

$$\gamma^5 = i\gamma^0\gamma^1\gamma^2\gamma^3 = \gamma_5 .$$

7. The Dirac spinors are defined as

$$u(\mathbf{p},\ m_s) = \sqrt{\frac{E(\mathbf{p},\ m)+m}{2m}} \begin{pmatrix} 1 \\ \frac{\boldsymbol{\sigma}\cdot\mathbf{p}}{E(\mathbf{p},\ m)+m} \end{pmatrix} \chi_{m_s} ,$$

$$v(\mathbf{p},\ m_s) = \sqrt{\frac{E(\mathbf{p},\ m)+m}{2m}} \begin{pmatrix} \frac{\boldsymbol{\sigma}\cdot\mathbf{p}}{E(\mathbf{p},\ m)+m} \\ 1 \end{pmatrix} \chi_{-m_s} ,$$

where m is the mass of the particle, $E(\mathbf{p},\ m) = \sqrt{\mathbf{p}^2 + m^2}$ and χ_{m_s} is the Pauli spinor.

8. The Dirac conjugate is defined as

$$\bar{\psi} = \psi^\dagger\gamma^0 .$$

9. The free Dirac propagator $S_F(p,m)$ is given by

$$S_F(p,m) = (\gamma\cdot p - m)^{-1} .$$

Appendix B

Solving the Coupled Equations

The coupled equations for G_{nlj_1} and F_{nlj_1} in $Q\bar{q}$ sector are given by (106) and (107). Operating $\left(\frac{d}{dr}-\frac{\kappa_1}{r}\right)$ on (106), using $\left(\frac{d}{dr}-\frac{\kappa_1}{r}\right)F_{nlj_1}(r)$ from (107) and $F_{nlj_1}(r)$ from (106), the coupled radial wave equations can be written as a second order differential equation for $G_{nlj_1}(r)$,

$$\begin{aligned}
&\frac{d^2G_{n\ell j_1}(r)}{dr^2}+\frac{dG_{n\ell j_1}(r)}{dr}\left(\frac{V_v'(r)-V_s'(r)}{m_1+V_s(r)-V_v(r)+E^{(0)}_{n\ell j_1}}\right)\\
&+G_{n\ell j_1}(r)\left\{\left(\frac{\kappa_1}{r}\right)\frac{V_v'(r)-V_s'(r)}{m_1+V_s(r)-V_v(r)+E^{(0)}_{n\ell j_1}}-\frac{\kappa_1}{r^2}\left(\kappa_1+1\right)\right.\\
&\qquad-\left(m_1+V_s(r)-V_v(r)+E^{(0)}_{n\ell j_1}\right)\\
&\qquad\left.\times\left(m_1+V_s(r)+V_v(r)-E^{(0)}_{n\ell j_1}\right)\right\}=0\,,
\end{aligned}\tag{147}$$

with

$$F_{n\ell j_1}(r)=\frac{1}{m_1+V_s(r)-V_v(r)+E^{(0)}_{n\ell j_1}}\left(\frac{dG_{n\ell j_1}(r)}{dr}+\frac{\kappa_1}{r}G_{n\ell j_1}(r)\right).\tag{148}$$

A direct integration numerical method has been used to obtain the solution of (147). This approach uses stepping techniques to obtain solutions to the differential equations. Such techniques are much more efficient if any large asymptotic

damping of the radial wave functions can be extracted and reduced radial wave equations can then be integrated.

When examing this equation, we found that for $V_s(r)$, $V_v(r)$ being determined by (91) and (92), at $r \to \infty$, $G_{nlj_1}(r) \to e^{-br^2/2-(m_1+c)r}$. We therefore define a reduced wave function $\bar{g}(\rho)$ by

$$G_{nlj_1}(r) = \bar{g}(\rho)\rho^s e^{-(\rho^2+\gamma\rho)/2}, \tag{149}$$

where $\gamma = 2(m_1 + c)/\sqrt{b}$, $\rho = \sqrt{b}\, r$ is a dimensionless radial variable and s will be determined while solving the equation.

By (147), the equation for the reduced wave function $\bar{g}(\rho)$ is

$$\frac{d^2\bar{g}(\rho)}{d\rho^2} = \frac{1}{\alpha_+ + \rho - V_v(\rho)/\sqrt{b}} \times \left\{ \mathcal{F}_1(\rho)\frac{d\bar{g}(\rho)}{d\rho} - \left[\mathcal{F}_2(\rho) + \mathcal{F}_3(\rho) + \mathcal{F}_4(\rho) + \mathcal{F}_5(\rho)\right]\bar{g}(\rho) \right\}, \tag{150}$$

where

$$\alpha_+ = \frac{1}{\sqrt{b}}\left(m_1 + c + E^{(0)}_{n\ell j_1}\right), \tag{151}$$

$$\alpha_- = \frac{1}{\sqrt{b}}\left(m_1 + c - E^{(0)}_{n\ell j_1}\right), \tag{152}$$

$$V_v(\rho) = V_v(r) = -\frac{4\sqrt{b}}{3\rho}\sum_{k=1}^{3}\alpha_k erf\left(\frac{\gamma_k\rho}{\sqrt{b}}\right), \tag{153}$$

$$V_v'(\rho) = \frac{dV_v(\rho)}{d\rho} = \frac{dr}{d\rho}\frac{dV_v(r)}{dr} = \frac{V_v'(r)}{\sqrt{b}} = -\frac{V_v(\rho)}{\rho} - \frac{8}{3\sqrt{\pi}\rho}\sum_{k=1}^{3}\alpha_k\gamma_k e^{-\gamma_k^2\rho^2/b}, \tag{154}$$

and

$$\mathcal{F}_1(\rho) = 2\rho^2 + \left(2\alpha_+ + \gamma\right)\rho + \alpha_+\gamma - 2s + 1 - \frac{2\alpha_+ s}{\rho} + \frac{V_v(\rho)}{\sqrt{b}}\left(\frac{2s}{\rho} - 2\rho - \gamma\right) - \frac{V_v'(\rho)}{\sqrt{b}},$$

$$\mathcal{F}_2(\rho) = \frac{\alpha_+}{\rho^2}\left(s^2 - s - \kappa_1^2 - \kappa_1\right) + \frac{1}{\rho}\left(s^2 - 2s - \kappa_1^2 - 2\kappa_1 - \gamma s\alpha_+\right)$$

$$
\begin{aligned}
&-\gamma s + \frac{1}{4}\alpha_+\gamma^2 - 2\alpha_+ s - \alpha_+ - \alpha_+^2\alpha_- + \frac{1}{2}\gamma \\
&+\rho\left(\frac{1}{4}\gamma^2 - 2s - \alpha_+\alpha_-\right), \\
\mathcal{F}_3(\rho) = &-\frac{V_v(\rho)}{\sqrt{b}}\left\{\frac{1}{\rho^2}\left(s^2 - s - \kappa_1^2 - \kappa_1\right) - \frac{1}{\rho}\gamma s\right. \\
&\left.+\frac{1}{4}\gamma^2 - 2s - 1 - 2\alpha_+\alpha_- + \alpha_+^2 + \rho\left(\alpha_+ - \alpha_-\right)\right\}, \\
\mathcal{F}_4(\rho) = &\frac{V_v'(\rho)}{\sqrt{b}}\left[\frac{1}{\rho}\left(s + \kappa_1\right) - \frac{1}{2}\gamma - \rho\right], \\
\mathcal{F}_5(\rho) = &\frac{V_v^2(\rho)}{b}\left[2\alpha_+ - \alpha_- + \rho\right] - \frac{1}{b\sqrt{b}}V_v^3(\rho).
\end{aligned}
$$

In order to integrate the differential equation (150) , it is necessary to know the values of the function $\bar{g}(\rho)$ and its derivative $\frac{d\bar{g}(\rho)}{d\rho}$ at some point and then to have a stepping algorithm that predicts the values of the functions and their derivatives at subsequent points. The value of the function and its first derivative at $\rho = 0$ are obtained by construction of a series solution for the functions for small ρ. An adaptive Runge-Kutte routine [69] is used to integrate the differential equation for increasing values of ρ. Energy eigenvalues are found by adjusting the value of the energy until the functions have the correct asymptotic behavior as determined by an asymptotic expansion of the functions at some large finite ρ. This process of finding the eigenenergies is called the shooting method [69]. In the calculations shown here, the accuracy of the eigenvalues is increased by integrating up from $\rho = 0$ and down from some large finite ρ to some intermediate point where the values of $\bar{g}(\rho)$ and $\frac{d\bar{g}(\rho)}{d\rho}$ are required to match. Our meson spectra varies less than 1 MeV as the matching point is changed.

(*a*) The series solution for $\bar{g}(\rho)$ at small ρ

Since

$$
\mathrm{erf}(x) = \frac{2}{\sqrt{\pi}}\int_0^x e^{-t^2}\,dt = \frac{2}{\sqrt{\pi}}\sum_{n=0}^{\infty}\frac{(-1)^n}{n!\,(2n+1)}\,x^{2n+1}, \tag{155}
$$

at small ρ, (153) and (154) are reduced to

$$V_v(\rho) = V_0 = -\frac{8}{3\sqrt{\pi}}\sum_{k=1}^{3}\alpha_k\gamma_k, \tag{156}$$

$$V_v'(\rho) = 0. \tag{157}$$

Thus, for small ρ, (150) therefore can be written as

$$\left(\rho+\alpha_+-\frac{V_0}{\sqrt{b}}\right)\frac{d^2\bar{g}(\rho)}{d\rho^2}-\left(\mathcal{B}_1\rho^2+\mathcal{B}_2\rho+\mathcal{B}_3+\mathcal{B}_4\frac{1}{\rho}\right)\frac{d\bar{g}(\rho)}{d\rho}$$
$$+\left(\mathcal{D}_1\rho+\mathcal{D}_2+\mathcal{D}_3\frac{1}{\rho}+\mathcal{D}_4\frac{1}{\rho^2}\right)\bar{g}(\rho)=0. \tag{158}$$

where

$$\begin{aligned}
\mathcal{B}_1 &= 2,\\
\mathcal{B}_2 &= \gamma-2\frac{V_0}{\sqrt{b}}+2\alpha_+,\\
\mathcal{B}_3 &= \alpha_+\gamma-2s+1-\frac{V_0\gamma}{\sqrt{b}},\\
\mathcal{B}_4 &= -2\alpha_+s+\frac{2sV_0}{\sqrt{b}},\\
\\
\mathcal{D}_1 &= \frac{1}{4}\gamma^2-2s-\alpha_+\alpha_--\frac{V_0}{\sqrt{b}}\left(\alpha_+-\alpha_-\right)+\frac{V_0^2}{b},\\
\mathcal{D}_2 &= -\gamma s+\frac{1}{4}\alpha_+\gamma^2-2\alpha_+s-\alpha_+-\alpha_+^2\alpha_-+\frac{1}{2}\gamma\\
&\quad-\frac{V_0}{\sqrt{b}}\left(\frac{1}{4}\gamma^2-2s-1-2\alpha_+\alpha_-+\alpha_+^2\right)\\
&\quad+\frac{V_0^2}{b}\left(2\alpha_+-\alpha_-\right)-\frac{V_0^3}{b\sqrt{b}},\\
\mathcal{D}_3 &= s^2-2s-\kappa_1^2-2\kappa_1-\gamma s\alpha_++\frac{V_0}{\sqrt{b}}\gamma s,\\
\mathcal{D}_4 &= \left(s^2-s-\kappa_1^2-\kappa_1\right)\left(\alpha_+-\frac{V_0}{\sqrt{b}}\right),
\end{aligned} \tag{159}$$

Expanding $\bar{g}(\rho)$ as a power series for small ρ as

$$\bar{g}(\rho)=\sum_{k=0}^{\infty}\mathcal{A}_k\rho^k, \tag{160}$$

and substituting into the differential equation for small ρ , (158) , we have

$$\begin{aligned}
&\sum_{k=0}^{\infty}\left[\left(\alpha_+ - \frac{V_0}{\sqrt{b}}\right)k\left(k-1\right) - \mathcal{B}_4 k + \mathcal{D}_4\right]\mathcal{A}_k\,\rho^{k-2} \\
+\;&\sum_{k=1}^{\infty}\left[\left(k-1\right)\left(k-2\right) - \mathcal{B}_3\left(k-1\right) + \mathcal{D}_3\right]\mathcal{A}_{k-1}\,\rho^{k-2} \\
+\;&\sum_{k=2}^{\infty}\left[-\mathcal{B}_2\left(k-2\right) + \mathcal{D}_2\right]\mathcal{A}_{k-2}\,\rho^{k-2} \\
+\;&\sum_{k=3}^{\infty}\left[-\mathcal{B}_1\left(k-3\right) + \mathcal{D}_1\right]\mathcal{A}_{k-3}\,\rho^{k-2} = 0. \qquad (161)
\end{aligned}$$

Equating coefficients of equal powers of ρ gives

(*i*) $$s = \begin{cases} -\kappa_1 \\ \kappa_1 + 1 \end{cases},$$

$s < 0$ would be non-physical since this would result in, by (149), $G_{nlj_1}(r) \to \infty$ as $\rho \to 0$, we therefore have

$$s = \kappa_1 + 1\,,$$

(*ii*)
$$\mathcal{A}_1 = \frac{\mathcal{D}_3\mathcal{A}_0}{\mathcal{D}_4 - \mathcal{B}_4},$$

$$\mathcal{A}_2 = \frac{-1}{2\left(\alpha_+ - \frac{V_0}{\sqrt{b}} - \mathcal{B}_4\right) + \mathcal{D}_4}\left[\left(-\mathcal{B}_3 + \mathcal{D}_3\right)\mathcal{A}_1 + \mathcal{D}_2\mathcal{A}_0\right],$$

$$\begin{aligned}
\mathcal{A}_3 = &\frac{-1}{6\left(\alpha_+ - \frac{V_0}{\sqrt{b}} - \frac{1}{2}\mathcal{B}_4\right) + \mathcal{D}_4} \\
&\left[\left(2 - 2\mathcal{B}_3 + \mathcal{D}_3\right)\mathcal{A}_2 + \left(-\mathcal{B}_2 + \mathcal{D}_2\right)\mathcal{A}_1 + \mathcal{D}_1\mathcal{A}_0\right],
\end{aligned}$$

$$\begin{aligned}
\mathcal{A}_{k>3} = &\frac{-1}{\left(\alpha_+ - \frac{V_0}{\sqrt{b}}\right)k\left(k-1\right) - \mathcal{B}_4 k + \mathcal{D}_4} \\
&\left\{\left[\left(k-1\right)\left(k-2\right) - \mathcal{B}_3\left(k-1\right) + \mathcal{D}_3\right]\mathcal{A}_{k-1}\right. \\
&+\left[-\mathcal{B}_2\left(k-2\right) + \mathcal{D}_2\right]\mathcal{A}_{k-2} \\
&\left.+\left[-\mathcal{B}_1\left(k-3\right) + \mathcal{D}_1\right]\mathcal{A}_{k-3}\right\}.
\end{aligned}$$

(*b*) The series solution for $\bar{g}(\rho)$ at large ρ

Since $\mathrm{erf}(x) \to 1$ at $r \to \infty$, at large ρ, (153) and (154) are reduced to

$$V_v(\rho) = -\beta\sqrt{b}\frac{1}{\rho}, \tag{162}$$

$$V_v'(\rho) = \beta\sqrt{b}\frac{1}{\rho^2}, \tag{163}$$

where

$$\beta = \frac{4}{3}\sum_{k=1}^{3}\alpha_k. \tag{164}$$

At large ρ, (150) therefore becomes

$$\begin{aligned}
&\left(\rho + \alpha_+ + \frac{\beta}{\rho}\right)\frac{d^2\bar{g}(\rho)}{d\rho^2} \\
&- \left(\mathcal{P}_1\rho^2 + \mathcal{P}_2\rho + \mathcal{P}_3 + \mathcal{P}_4\frac{1}{\rho} + \mathcal{P}_5\frac{1}{\rho^2}\right)\frac{d\bar{g}(\rho)}{d\rho} \\
&+ \left(\mathcal{Q}_1\rho + \mathcal{Q}_2 + \mathcal{Q}_3\frac{1}{\rho} + \mathcal{Q}_4\frac{1}{\rho^2} + \mathcal{Q}_5\frac{1}{\rho^3}\right)\bar{g}(\rho) = 0.
\end{aligned} \tag{165}$$

where

$$\begin{aligned}
\mathcal{P}_1 &= 2, \\
\mathcal{P}_2 &= 2\alpha_+ + \gamma, \\
\mathcal{P}_3 &= \alpha_+\gamma - 2s + 1 + 2\beta, \\
\mathcal{P}_4 &= \beta\gamma - 2\alpha_+ s, \\
\mathcal{P}_5 &= -2\beta s - \beta,
\end{aligned}$$

$$\begin{aligned}
\mathcal{Q}_1 &= \frac{1}{4}\gamma^2 - 2s - \alpha_+\alpha_-, \\
\mathcal{Q}_2 &= -\gamma s + \frac{1}{4}\alpha_+\gamma^2 - 2\alpha_+ s - \alpha_+ - \alpha_+^2\alpha_- + \frac{1}{2}\gamma + \beta\left(\alpha_+ - \alpha_-\right), \\
\mathcal{Q}_3 &= s^2 - 2s - \kappa_1^2 - 2\kappa_1 - \gamma s\alpha_+ \\
&\quad + \beta\left(\frac{1}{4}\gamma^2 - 2s - 2 - 2\alpha_+\alpha_- + \alpha_+^2 + \beta\right),
\end{aligned}$$

$$\begin{aligned}
\mathcal{Q}_4 &= \alpha_+\left(s^2 - s - \kappa_1^2 - \kappa_1\right) - \beta\gamma s - \frac{1}{2}\beta\gamma + \beta^2\left(2\alpha_+ - \alpha_-\right), \\
\mathcal{Q}_5 &= \beta\left(s^2 - \kappa_1^2\right) + \beta^3 .
\end{aligned}$$

Expanding $\bar{g}(\rho)$ as

$$\bar{g}(\rho) = \sum_{k=0}^{\infty} \mathcal{C}_k \rho^{-k-\sigma}, \tag{166}$$

and substituting into the differential equation for large ρ, (165), we have

$$\begin{aligned}
&\sum_{k=0}^{\infty}\left[\mathcal{P}_1\left(k+\sigma\right) + \mathcal{Q}_1\right]\mathcal{C}_k\ \rho^{-k+1} \\
+\ &\sum_{k=1}^{\infty}\left[\mathcal{P}_2\left(k-1+\sigma\right) + \mathcal{Q}_2\right]\mathcal{C}_{k-1}\ \rho^{-k+1} \\
+\ &\sum_{k=2}^{\infty}\left[\left(k+\sigma-2\right)\left(k+\sigma-1\right) + \left(k+\sigma-2\right)\mathcal{P}_3 + \mathcal{Q}_3\right]\mathcal{C}_{k-2}\ \rho^{-k+1} \\
+\ &\sum_{k=3}^{\infty}\left[\alpha_+\left(k+\sigma-3\right)\left(k+\sigma-2\right) + \left(k+\sigma-3\right)\mathcal{P}_4 + \mathcal{Q}_4\right]\mathcal{C}_{k-3}\ \rho^{-k+1} \\
+\ &\sum_{k=4}^{\infty}\Big[\beta\left(k+\sigma-4\right)\left(k+\sigma-3\right) \\
&\qquad + \left(k+\sigma-4\right)\mathcal{P}_5 + \mathcal{Q}_5\Big]\mathcal{C}_{k-4}\ \rho^{-k+1} = 0 .
\end{aligned} \tag{167}$$

Equating coefficients of equal powers of ρ gives

$$\begin{aligned}
\sigma &= -\frac{\mathcal{Q}_1}{\mathcal{P}_1}, \\
\mathcal{C}_1 &= \frac{-1}{\mathcal{P}_1\left(\sigma+1\right) + \mathcal{Q}_1}\left(\mathcal{P}_2\sigma + \mathcal{Q}_2\right)\mathcal{C}_0 , \\
\mathcal{C}_2 &= \frac{-1}{\mathcal{P}_1\left(\sigma+2\right) + \mathcal{Q}_1}\Big\{\left[\mathcal{P}_2\left(\sigma+1\right) + \mathcal{Q}_2\right]\mathcal{C}_1 \\
&\qquad + \left[\sigma\left(\sigma+1+\mathcal{P}_3\right) + \mathcal{Q}_3\right]\mathcal{C}_0\Big\}, \\
\mathcal{C}_3 &= \frac{-1}{\mathcal{P}_1\left(\sigma+3\right) + \mathcal{Q}_1}\Big\{\left[\mathcal{P}_2\left(\sigma+2\right) + \mathcal{Q}_2\right]\mathcal{C}_2 \\
&\qquad + \left[\left(\sigma+1\right)\left(\sigma+2+\mathcal{P}_3\right) + \mathcal{Q}_3\right]\mathcal{C}_1
\end{aligned}$$

$$+\left[\sigma\left(\alpha_+\sigma+\alpha_++\mathcal{P}_4\right)+\mathcal{Q}_4\right]\mathcal{C}_0\Big\}\,,$$

$$\mathcal{C}_4=\frac{-1}{\mathcal{P}_1\left(\sigma+4\right)+\mathcal{Q}_1}\Big\{\left[\mathcal{P}_2\left(\sigma+3\right)+\mathcal{Q}_2\right]\mathcal{C}_3$$
$$+\left[\left(\sigma+2\right)\left(\sigma+3+\mathcal{P}_3\right)+\mathcal{Q}_3\right]\mathcal{C}_2$$
$$+\left[\left(\sigma+1\right)\left(\alpha_+\sigma+2\alpha_++\mathcal{P}_4\right)+\mathcal{Q}_4\right]\mathcal{C}_1$$
$$+\left[\sigma\left(\beta\sigma+\beta+\mathcal{P}_5\right)+\mathcal{Q}_5\right]\mathcal{C}_0\Big\}\,,$$

$$\mathcal{C}_{k>4}=\frac{-1}{\mathcal{P}_1\left(\sigma+k\right)+\mathcal{Q}_1}\Big\{\left[\mathcal{P}_2\left(\sigma+k-1\right)+\mathcal{Q}_2\right]\mathcal{C}_{k-1}$$
$$+\left[\left(\sigma+k-2\right)\left(\sigma+k-1+\mathcal{P}_3\right)+\mathcal{Q}_3\right]\mathcal{C}_{k-2}$$
$$+\left[\left(\sigma+k-3\right)\left(\alpha_+k+\alpha_+\sigma-2\alpha_++\mathcal{P}_4\right)+\mathcal{Q}_4\right]\mathcal{C}_{k-3}$$
$$+\left[\left(\sigma+k-4\right)\left(\beta k+\beta\sigma-3\beta+\mathcal{P}_5\right)+\mathcal{Q}_5\right]\mathcal{C}_{k-4}\Big\}\,.$$

(c) The relation of $\mathcal{A}_0$ and $\mathcal{C}_0$

$\mathcal{A}_0$ and $\mathcal{C}_0$ are normalization factors. However, for unnormalized $\bar{g}(\rho)$, only one of $\mathcal{A}_0$ and $\mathcal{C}_0$ is arbitrary. By using the series solutions of $\bar{g}(\rho)$ and $\frac{d\bar{g}(\rho)}{d\rho}$ at small ρ and setting $\mathcal{A}_0=1$, we are able to use the adaptive Runge-Kutte routine [69] to obtain the values of $\bar{g}(\rho)$ and $\frac{d\bar{g}(\rho)}{d\rho}$ at a point with larger ρ called ρ_{mid}

$$\bar{g}(\rho_{mid})\,|_{\mathcal{A}_0=1}=\bar{g}_-\,,$$
$$\frac{d\bar{g}(\rho_{mid})}{d\rho}\Big|_{\mathcal{A}_0=1}=\bar{g}'_-\,.$$

Similarly, by the series solution of $\bar{g}(\rho)$ and $\frac{d\bar{g}(\rho)}{d\rho}$ at large ρ and setting $\mathcal{C}_0=1$, we obtain

$$\bar{g}(\rho_{mid})\,|_{\mathcal{C}_0=1}=\bar{g}_+\,,$$
$$\frac{d\bar{g}(\rho_{mid})}{d\rho}\Big|_{\mathcal{C}_0=1}=\bar{g}'_+\,.$$

The condition of $\bar{g}(\rho)$ being continuous at $\rho=\rho_{mid}$ requires, for arbitrary $\mathcal{A}_0$

or C_0,

$$\mathcal{A}_0\,\bar{g}_- - C_0\,\bar{g}_+ = 0\,,$$
$$\mathcal{A}_0\,\bar{g}'_- - C_0\,\bar{g}'_+ = 0\,.$$

This gives us the relations

$$\bar{g}_+\,\bar{g}'_- - \bar{g}_-\,\bar{g}'_+ = 0\,, \tag{168}$$
$$C_0 = \mathcal{A}_0\left(\frac{\bar{g}'_-}{\bar{g}'_+}\right) = \mathcal{A}_0\left(\frac{\bar{g}_-}{\bar{g}_+}\right). \tag{169}$$

Appendix C

Matrix Elements in the $Q\bar{q}$ Sector

In this section, we evaluate the matrix element

$$\mathcal{I} = \int d^3r \; \Psi^{\dagger}_{n\ell j_1 JM_J}(\mathbf{r}) \, H_1 \, \Psi_{n\ell j_1 JM_J}(\mathbf{r}) \tag{170}$$

in the $Q\bar{q}$ and $q\bar{Q}$ sectors. To do so, we first consider the following integrals

$$\mathcal{I}_1 = \int d^3r \; f(r) \; \Psi^{\dagger}_{n\ell j_1 JM_J}(\mathbf{r}) \; \Psi_{n\ell j_1 JM_J}(\mathbf{r}) \,, \tag{171}$$

$$\mathcal{I}_2 = \int d^3r \; f(r) \; \Psi^{\dagger}_{n\ell j_1 JM_J}(\mathbf{r}) \; \beta^{(1)} \; \Psi_{n\ell j_1 JM_J}(\mathbf{r}) \,, \tag{172}$$

$$\mathcal{I}_3 = \int d^3r \; f(r) \; \Psi^{\dagger}_{n\ell j_1 JM_J}(\mathbf{r}) \boldsymbol{\sigma}^{(2)} \cdot (\boldsymbol{\alpha}^{(1)} \times \hat{\mathbf{r}}) \; \Psi_{n\ell j_1 JM_J}(\mathbf{r}) \,. \tag{173}$$

C.1 $\mathcal{I}_1$ and $\mathcal{I}_2$

By using (101), (102) and the explicit form of β matrix,

$$\begin{aligned}
\mathcal{I}'_1 &= \int d^3r \; f(r) \; \Psi^{\dagger}_{n'\ell' j'_1 JM_J}(\mathbf{r}) \; \Psi_{n\ell j_1 JM_J}(\mathbf{r}) \\
&= \sum_{m_{j_1} m'_{j_1} m_{s_2}} \left\langle j'_1 m'_{j_1} s_2 m_{s_2} \,\middle|\, j'_1 s_2 J M_J \right\rangle^{*} \left\langle j_1 m_{j_1} s_2 m_{s_2} \,\middle|\, j_1 s_2 J M_J \right\rangle \\
&\quad \int d^3r \; f(r) \; \frac{1}{r^2} \Big\{ G_{n'\ell' j'_1}(r) G_{n\ell j_1}(r) \mathcal{Y}^{m'_{j_1}\,\dagger}_{\ell' j'_1}(\Omega) \mathcal{Y}^{m_{j_1}}_{\ell j_1}(\Omega) \\
&\qquad + F_{n'\ell' j'_1}(r) F_{n\ell j_1}(r) \mathcal{Y}^{m'_{j_1}\,\dagger}_{\bar{\ell}' j'_1}(\Omega) \mathcal{Y}^{m_{j_1}}_{\bar{\ell} j_1}(\Omega) \Big\} \,,
\end{aligned} \tag{174}$$

$$\begin{aligned}
\mathcal{I}_2' &= \int d^3r\ f(r)\ \Psi^{\dagger}_{n'\ell' j_1' J M_J}(\mathbf{r})\ \beta^{(1)}\ \Psi_{n\ell j_1 J M_J}(\mathbf{r}) \\
&= \sum_{m_{j_1} m'_{j_1} m_{s_2}} \left\langle j_1' m'_{j_1} s_2 m_{s_2} \,\middle|\, j_1' s_2 J M_J \right\rangle^{*} \left\langle j_1 m_{j_1} s_2 m_{s_2} \,\middle|\, j_1 s_2 J M_J \right\rangle \\
&\quad \int d^3r\ f(r)\ \frac{1}{r^2} \Big\{ G_{n'\ell' j_1'}(r) G_{n\ell j_1}(r) \mathcal{Y}^{m'_{j_1}\,\dagger}_{\ell' j_1'}(\Omega) \mathcal{Y}^{m_{j_1}}_{\ell j_1}(\Omega) \\
&\qquad - F_{n'\ell' j_1'}(r) F_{n\ell j_1}(r) \mathcal{Y}^{m'_{j_1}\,\dagger}_{\bar{\ell}' j_1'}(\Omega) \mathcal{Y}^{m_{j_1}}_{\bar{\ell} j_1}(\Omega) \Big\}
\end{aligned} \tag{175}$$

Using the explicit form of $\mathcal{Y}^{m_{j_1}}_{\bar{\ell} j_1}(\Omega)$ by (103) and the orthogonality of $Y_{\ell m_\ell}(\Omega)$

$$\int d\Omega\ Y^{*}_{\ell' m'_\ell}(\Omega)\ Y_{\ell m_\ell}(\Omega) = \delta_{\ell',\ell}\ \delta_{m'_\ell, m_\ell}\,, \tag{176}$$

we have

$$\int d\Omega\ \mathcal{Y}^{m'_{j_1}\,\dagger}_{\ell' j_1'}(\Omega)\ \mathcal{Y}^{m_{j_1}}_{\ell j_1}(\Omega) = \ \delta_{\ell',\ell}\ \delta_{j_1', j_1}\ \delta_{m'_{j_1}, m_{j_1}}\,, \tag{177}$$

Putting (177) in (174) and (175), and by the orthogonality of the Clebsch-Gordan coefficients

$$\sum_{m_{j_1} m_{s_2}} \left\langle j_1 m_{j_1} s_2 m_{s_2} \,\middle|\, j_1 s_2 J M_J \right\rangle^{*} \left\langle j_1 m_{j_1} s_2 m_{s_2} \,\middle|\, j_1 s_2 J M_J \right\rangle = 1, \tag{178}$$

we obtain

$$\mathcal{I}_1' = \delta_{\ell',\ell}\ \delta_{j_1', j_1} \int dr\ f(r) \Big[\ G_{n'\ell j_1}(r) G_{n\ell j_1}(r) + F_{n'\ell j_1}(r) F_{n\ell j_1}(r)\ \Big]\,, \tag{179}$$

$$\mathcal{I}_2' = \delta_{\ell',\ell}\ \delta_{j_1', j_1} \int dr\ f(r) \Big[\ G_{n'\ell j_1}(r) G_{n\ell j_1}(r) - F_{n'\ell j_1}(r) F_{n\ell j_1}(r)\ \Big]\,. \tag{180}$$

We therefore have

$$\mathcal{I}_1 = \int d^3r\ f(r)\ \Psi^{\dagger}(\mathbf{r})\ \Psi(\mathbf{r}) = \int dr\ f(r) \Big[G^2_{n\ell j_1}(r) + F^2_{n\ell j_1}(r) \Big]\,, \tag{181}$$

$$\mathcal{I}_2 = \int d^3r\ f(r)\ \Psi^{\dagger}(\mathbf{r})\ \beta^{(1)}\ \Psi(\mathbf{r}) = \int dr\ f(r) \Big[G^2_{n\ell j_1}(r) - F^2_{n\ell j_1}(r) \Big]\,. \tag{182}$$

where $\Psi(\mathbf{r}) = \Psi_{n\ell j_1 J M_J}(\mathbf{r})$.

C.2 $\mathcal{I}_3$

By the definition of $\Psi_{n\ell j_1 JM_J}(\mathbf{r})$ in (101) , and the explicit form of $\boldsymbol{\alpha}$ matrices, we have

$$\begin{aligned}
\mathcal{I}_3' &= \int d^3r\, f(r)\, \Psi^{\dagger}_{n'\ell' j_1' JM_J}(\mathbf{r})\, \boldsymbol{\sigma}^{(2)}\cdot(\boldsymbol{\alpha}^{(1)}\times\hat{\mathbf{r}})\, \Psi_{n\ell j_1 JM_J}(\mathbf{r}) \\
&= \sum_{m_{j_1} m'_{j_1} m_{s_2} m'_{s_2}} \left\langle j_1' m'_{j_1} s_2 m'_{s_2} \,\middle|\, j_1' s_2 J M_J \right\rangle^{*} \left\langle j_1 m_{j_1} s_2 m_{s_2} \,\middle|\, j_1 s_2 J M_J \right\rangle \\
&\quad \cdot \left(\chi^{\dagger}_{m'_{s_2}} \cdot \boldsymbol{\sigma}^{(2)} \chi_{m_{s_2}}\right) \int d^3r \frac{f(r)}{r^2} \left[G_{n'\ell' j_1'}(r) F_{n\ell j_1}(r) + F_{n'\ell' j_1'}(r) G_{n\ell j_1}(r)\right] \\
&\quad \cdot \left[\mathcal{Y}^{m'_{j_1}\,\dagger}_{\ell' j_1'}(\Omega)\, \boldsymbol{\sigma}^{(1)}\, \mathcal{Y}^{m_{j_1}}_{\ell j_1}(\Omega) + \mathcal{Y}^{m'_{j_1}\,\dagger}_{\bar{\ell}' j_1'}(\Omega)\, \hat{\mathbf{r}}\, \mathcal{Y}^{m_{j_1}}_{\ell j_1}(\Omega)\right], \qquad (183)
\end{aligned}$$

where we have used (105) and the relation

$$-\left(i\boldsymbol{\sigma}\times\hat{\mathbf{r}}\right)\left(\boldsymbol{\sigma}\cdot\hat{\mathbf{r}}\right) = \left(\boldsymbol{\sigma}\cdot\hat{\mathbf{r}}\right)\left(i\boldsymbol{\sigma}\times\hat{\mathbf{r}}\right) = \boldsymbol{\sigma} - \left(\boldsymbol{\sigma}\cdot\hat{\mathbf{r}}\right)\hat{\mathbf{r}}. \qquad (184)$$

Using the explicit form of $\mathcal{Y}^{m_{j_1}}_{\ell j_1}(\Omega)$ by (103) and the orthogonality of $Y_{\ell m_\ell}(\Omega)$ (176), (183) becomes

$$\begin{aligned}
\mathcal{I}_3' = &\int dr\, f(r) \left[G_{n'\ell' j_1'}(r) F_{n\ell j_1}(r) + F_{n'\ell' j_1'}(r) G_{n\ell j_1}(r)\right] \\
&\times \Bigg\{ \sum_{m_{j_1} m'_{j_1} m_{s_2} m'_{s_2} m_{s_1} m'_{s_1} m_\ell} \left\langle j_1' m'_{j_1} s_2 m'_{s_2} \,\middle|\, j_1' s_2 J M_J \right\rangle^{*} \left\langle j_1 m_{j_1} s_2 m_{s_2} \,\middle|\, j_1 s_2 J M_J \right\rangle \\
&\qquad \left\langle \ell m_\ell s_1 m'_{s_1} \,\middle|\, \ell s_1 j_1' m'_{j_1} \right\rangle^{*} \left\langle \ell m_\ell s_1 m_{s_1} \,\middle|\, \ell s_1 j_1 m_{j_1} \right\rangle \\
&\qquad \left(\chi^{\dagger}_{m'_{s_2}} \boldsymbol{\sigma}^{(2)} \chi_{m_{s_2}}\right) \cdot \left(\chi^{\dagger}_{m'_{s_1}} \boldsymbol{\sigma}^{(1)} \chi_{m_{s_1}}\right) \delta_{\ell',\ell} \\
&+ \sum_{m_{j_1} m'_{j_1} m_{s_2} m'_{s_2} m_{s_1} m'_{s_1} m_\ell m'_{\bar{\ell}}} \left\langle j_1' m'_{j_1} s_2 m'_{s_2} \,\middle|\, j_1' s_2 J M_J \right\rangle^{*} \left\langle j_1 m_{j_1} s_2 m_{s_2} \,\middle|\, j_1 s_2 J M_J \right\rangle \\
&\qquad \left\langle \bar{\ell}' m'_{\bar{\ell}}\, s_1 m'_{s_1} \,\middle|\, \bar{\ell}' s_1 j_1' m'_{j_1} \right\rangle^{*} \left\langle \ell m_\ell s_1 m_{s_1} \,\middle|\, \ell j_1 s_1 m_{j_1} \right\rangle \\
&\qquad \times \int d\Omega\, Y^{*}_{\bar{\ell}' m'_{\bar{\ell}}}(\Omega)\, Y_{\ell m_\ell}(\Omega) \left(\chi^{\dagger}_{m'_{s_2}} \boldsymbol{\sigma}^{(2)} \chi_{m_{s_2}}\right) \cdot \left(\chi^{\dagger}_{m'_{s_1}} \hat{\mathbf{r}} \chi_{m_{s_1}}\right) \Bigg\}. \qquad (185)
\end{aligned}$$

We find $\left(\chi^{\dagger}_{m'_{s_2}} \boldsymbol{\sigma}^{(2)} \chi_{m_{s_2}}\right) \cdot \left(\chi^{\dagger}_{m'_{s_1}} \boldsymbol{\sigma}^{(1)} \chi_{m_{s_1}}\right)$ and $\left(\chi^{\dagger}_{m'_{s_2}} \boldsymbol{\sigma}^{(2)} \chi_{m_{s_2}}\right) \cdot \left(\chi^{\dagger}_{m'_{s_1}} \hat{\mathbf{r}} \chi_{m_{s_1}}\right)$ in

the spherical coordinate representation, in which a vector **A**, or a rank one tensor, is represented by the spherical components of the vector A_λ

$$A_\lambda = A(1,\lambda) = \begin{cases} A_1 = A(1,1) = -\frac{1}{\sqrt{2}}(A_x + iA_y) \\ A_0 = A(1,0) = A_z \\ A_{-1} = A(1,-1) = \frac{1}{\sqrt{2}}(A_x - iA_y) \end{cases} \tag{186}$$

and the product of two vectors, **A** and **B** is given by

$$\mathbf{A} \cdot \mathbf{B} = \sum_{\lambda=-1,0,1} (-1)^\lambda \, A_\lambda \, B_{-\lambda} \, . \tag{187}$$

Therefore, in spherical representation,

$$\hat{r}_\lambda = \hat{r}(1,\lambda) = \begin{cases} \hat{r}_1 = \hat{r}(1,1) = -\frac{1}{\sqrt{2}} \sin\theta \, e^{i\phi} \\ \hat{r}_0 = \hat{r}(1,0) = \cos\theta \\ \hat{r}_{-1} = \hat{r}(1,-1) = \frac{1}{\sqrt{2}} \sin\theta \, e^{-i\phi} \end{cases} \tag{188}$$

which can be written in terms of spherical harmonic $Y_{\ell,m_\ell}(\Omega)$ as

$$\hat{r}_\lambda = \sqrt{\frac{4\pi}{3}} Y_{1,\lambda}(\Omega) \, , \tag{189}$$

and

$$\sigma_\lambda = \sigma(1,\lambda) = \begin{cases} \sigma_1 = \sigma(1,1) = -\frac{1}{\sqrt{2}}(\sigma_x + i\sigma_y) \\ \sigma_0 = \sigma(1,0) = \sigma_z \\ \sigma_{-1} = \sigma(1,-1) = \frac{1}{\sqrt{2}}(\sigma_x - i\sigma_y) \, . \end{cases} \tag{190}$$

We therefore have

$$\begin{aligned} &\left(\chi^\dagger_{m'_{s_2}} \boldsymbol{\sigma}^{(2)} \chi_{m_{s_2}}\right) \cdot \left(\chi^\dagger_{m'_{s_1}} \hat{r} \chi_{m_{s_1}}\right) \\ &= \sum_{\lambda=-1,0,1} (-1)^\lambda \sqrt{\frac{4\pi}{3}} Y_{1,-\lambda}(\Omega) \left(\chi^\dagger_{m'_{s_2}} \sigma^{(2)}_\lambda \chi_{m_{s_2}}\right) \chi^\dagger_{m'_{s_1}} \chi_{m_{s_1}} \, . \end{aligned} \tag{191}$$

The Wigner-Eckart theorem [70, 71, 72] for the q component of a rank k tensor $T(k,q)$ is

$$\left\langle j' m'_j \middle| T(k,q) \middle| j m_j \right\rangle = (-1)^{k-j+j'} \frac{\left\langle kqjm_j \middle| kjj'm'_j \right\rangle}{\sqrt{2j'+1}} \left\langle j' \middle\| T(k) \middle\| j \right\rangle \, , \tag{192}$$

where $\left\langle j' \left\| T(k) \right\| j \right\rangle$ is called the reduced matrix element which is independent of m'_j , m_j and q. Applying the theorem to the case $T(k,q) = \sigma^{(i)}(1,\lambda)$, we have

$$\begin{aligned} \chi^{\dagger}_{m'_{s_i}} \sigma^{(i)}_{\lambda} \chi_{m_{s_i}} &= \left\langle \frac{1}{2} m'_{s_i} \left| \sigma^{(i)}(1,\lambda) \right| \frac{1}{2} m_{s_i} \right\rangle \\ &= (-1)^{1-\frac{1}{2}+\frac{1}{2}} \frac{\left\langle 1\lambda\frac{1}{2} m_{s_i} \left| 1\frac{1}{2}\frac{1}{2} m'_{s_i} \right\rangle}{\sqrt{2\times\frac{1}{2}+1}} \left\langle \frac{1}{2} \left\| \sigma^{(i)}(1) \right\| \frac{1}{2} \right\rangle , \end{aligned} \tag{193}$$

where we have used the fact that $s_i = \frac{1}{2}$ for i being either 1 or 2.

Consider the case of $\lambda = 0$ in (193), this gives

$$\left\langle \frac{1}{2} \left\| \sigma^{(i)}(1) \right\| \frac{1}{2} \right\rangle = -2\sqrt{2}\ m_{s_i} \frac{1}{\left\langle 10\frac{1}{2} m_{s_i} \left| 1\frac{1}{2}\frac{1}{2} m_{s_i} \right\rangle} , \tag{194}$$

which is independent of m_{s_i}. We can therefore set $m_{s_i} = \frac{1}{2}$, and find that

$$\left\langle \frac{1}{2} \left\| \sigma^{(i)}(1) \right\| \frac{1}{2} \right\rangle = \sqrt{6} . \tag{195}$$

Putting (195) back in (193), we have

$$\chi^{\dagger}_{m'_{s_i}} \sigma^{(i)}_{\lambda} \chi_{m_{s_i}} = -\sqrt{3} \left\langle 1\lambda\frac{1}{2} m_{s_i} \left| 1\frac{1}{2}\frac{1}{2} m'_{s_i} \right\rangle . \tag{196}$$

Using (196) and (191) , we find

$$\begin{aligned} &\left(\chi^{\dagger}_{m'_{s_2}} \boldsymbol{\sigma}^{(2)} \chi_{m_{s_2}} \right) \cdot \left(\chi^{\dagger}_{m'_{s_1}} \boldsymbol{\sigma}^{(1)} \chi_{m_{s_1}} \right) \\ &= \sum_{\lambda=-1,0,1} (-1)^{\lambda}\, 3 \left\langle 1\lambda\frac{1}{2} m_{s_2} \left| 1\frac{1}{2}\frac{1}{2} m'_{s_2} \right\rangle \left\langle 1\ -\lambda\ \frac{1}{2}\ m_{s_1} \left| 1\ \frac{1}{2}\ \frac{1}{2}\ m'_{s_1} \right\rangle \right. , \end{aligned} \tag{197}$$

$$\begin{aligned} &\left(\chi^{\dagger}_{m'_{s_2}} \boldsymbol{\sigma}^{(2)} \chi_{m_{s_2}} \right) \cdot \left(\chi^{\dagger}_{m'_{s_1}} \hat{\mathbf{r}} \chi_{m_{s_1}} \right) \\ &= \sum_{\lambda=-1,0,1} \delta_{m'_{s_1}, m_{s_1}} (-1)^{\lambda+1} \sqrt{4\pi}\ Y_{1,-\lambda}(\Omega) \left\langle 1\lambda\frac{1}{2} m_{s_2} \left| 1\frac{1}{2}\frac{1}{2} m'_{s_2} \right\rangle . \end{aligned} \tag{198}$$

Putting (197) and (198) in (185) and by [73]

$$\begin{aligned} &\int d\Omega\ Y_{\ell_1 m_{\ell_1}}(\Omega)\ Y_{\ell_2 m_{\ell_2}}(\Omega)\ Y_{\ell_3 m_{\ell_3}}(\Omega) \\ &= \left[\frac{(2\ell_1+1)(2\ell_2+1)(2\ell_3+1)}{4\pi} \right]^{\frac{1}{2}} \begin{pmatrix} \ell_1 & \ell_2 & \ell_3 \\ 0 & 0 & 0 \end{pmatrix} \begin{pmatrix} \ell_1 & \ell_2 & \ell_3 \\ m_{\ell_1} & m_{\ell_2} & m_{\ell_2} \end{pmatrix} , \end{aligned} \tag{199}$$

with

$$Y^{*}_{\ell m_\ell}(\Omega) = (-1)^{m_\ell} Y_{\ell\ -m_\ell}(\Omega)\,, \tag{200}$$

we obtain

$$\begin{aligned}
\mathcal{I}'_3 \;=\; & \int dr\; f(r)\left[G_{n'\ell' j'_1}(r)F_{n\ell j_1}(r) + F_{n'\ell' j'_1}(r)G_{n\ell j_1}(r)\right] \\
\times\; & \Bigg\{ \sum_{m_{j_1} m'_{j_1}} \sum_{m_{s_2} m'_{s_2}} \sum_{m_{s_1} m'_{s_1}} \sum_{m_\ell \lambda} \delta_{\ell',\ell}\; 3\;(-1)^{\lambda} \\
& \left\langle j'_1 m'_{j_1} \tfrac{1}{2} m'_{s_2} \,\middle|\, j'_1 \tfrac{1}{2} J M_J \right\rangle^{*} \left\langle j_1 m_{j_1} \tfrac{1}{2} m_{s_2} \,\middle|\, j_1 \tfrac{1}{2} J M_J \right\rangle \\
& \left\langle \ell m_\ell \tfrac{1}{2} m'_{s_1} \,\middle|\, \ell \tfrac{1}{2} j'_1 m'_{j_1} \right\rangle^{*} \left\langle \ell m_\ell \tfrac{1}{2} m_{s_1} \,\middle|\, \ell \tfrac{1}{2} j_1 m_{j_1} \right\rangle \\
& \left\langle 1\lambda \tfrac{1}{2} m_{s_2} \,\middle|\, 1 \tfrac{1}{2} \tfrac{1}{2} m'_{s_2} \right\rangle \left\langle 1\ -\lambda\ \tfrac{1}{2}\ m_{s_1} \,\middle|\, 1\ \tfrac{1}{2}\ \tfrac{1}{2}\ m'_{s_1} \right\rangle \\
& + \sum_{m_{j_1} m'_{j_1} m_{s_2} m'_{s_2} m_\ell m'_{\bar{\ell}} m_{s_1} \lambda} (-1)^{1+\lambda-m'_{\bar{\ell}}} \sqrt{3\;(2\ell+1)(2\bar{\ell}'+1)} \\
& \begin{pmatrix} \bar{\ell}' & \ell & 1 \\ 0 & 0 & 0 \end{pmatrix} \begin{pmatrix} \bar{\ell}' & \ell & 1 \\ -m'_{\bar{\ell}} & m_\ell & -\lambda \end{pmatrix} \left\langle j'_1 m'_{j_1} \tfrac{1}{2} m'_{s_2} \,\middle|\, j'_1 \tfrac{1}{2} J M_J \right\rangle^{*} \\
& \left\langle j_1 m_{j_1} \tfrac{1}{2} m_{s_2} \,\middle|\, j_1 \tfrac{1}{2} J M_J \right\rangle \left\langle \bar{\ell}' m'_{\bar{\ell}} \tfrac{1}{2} m_{s_1} \,\middle|\, \bar{\ell}' \tfrac{1}{2} j'_1 m'_{j_1} \right\rangle^{*} \\
& \left\langle \ell m_\ell \tfrac{1}{2} m_{s_1} \,\middle|\, \ell \tfrac{1}{2} j_1 m_{j_1} \right\rangle \left\langle 1\lambda \tfrac{1}{2} m_{s_2} \,\middle|\, 1 \tfrac{1}{2} \tfrac{1}{2} m'_{s_2} \right\rangle \Bigg\}\,.
\end{aligned} \tag{201}$$

Using the symmetry properties of the $3-j$ symbols and using the $6-j$ symbols to represent the Clebsch-Gordan coefficients, this equation becomes

$$\begin{aligned}
\mathcal{I}'_3 \;=\; & \int dr\; f(r)\left[G_{n'\ell' j'_1}(r)F_{n\ell j_1}(r) + F_{n'\ell' j'_1}(r)G_{n\ell j_1}(r)\right] \\
\times\; & \Bigg\{ \delta_{\ell',\ell}\,(-1)^{J+j_1+j'_1+\ell} \times\; 6\,\sqrt{2j_1+1}\sqrt{2j'_1+1} \begin{Bmatrix} j'_1 & \frac{1}{2} & J \\ \frac{1}{2} & j_1 & 1 \end{Bmatrix} \begin{Bmatrix} j'_1 & 1 & j_1 \\ \frac{1}{2} & \ell & \frac{1}{2} \end{Bmatrix} \\
+\; & (-1)^{1+J+2j_1+2j'_1} \sqrt{2j_1+1}\sqrt{2j'_1+1}\sqrt{2\ell+1}\sqrt{2\bar{\ell}'+1}\;\sqrt{6} \\
& \begin{Bmatrix} j'_1 & \frac{1}{2} & J \\ \frac{1}{2} & j_1 & 1 \end{Bmatrix} \begin{Bmatrix} j'_1 & 1 & j_1 \\ \ell & \frac{1}{2} & \bar{\ell}' \end{Bmatrix} \begin{pmatrix} \bar{\ell}' & 1 & \ell \\ 0 & 0 & 0 \end{pmatrix} \Bigg\}\,.
\end{aligned} \tag{202}$$

By finding the values of the $6-j$ symbols and the $3-j$ symbol, and using

their symmetry properties, (202) can be reduced to

$$\begin{aligned}
\mathcal{I}_3' &= \int dr\ f(r)\left[G_{n'\ell'j_1'}(r)F_{n\ell j_1}(r)+F_{n'\ell'j_1'}(r)G_{n\ell j_1}(r)\right] \\
&\times\Big\{\delta_{\ell',\ell}\,\delta_{j_1',j_1}\left[\delta_{\ell,J+1}\,\delta_{j_1,J+\frac{1}{2}}\left(\frac{2J+2}{2J+1}\right)+\delta_{\ell,J-1}\,\delta_{j_1,J-\frac{1}{2}}\left(\frac{2J}{2J+1}\right)\right. \\
&\qquad\left.+\delta_{\ell,J}\,\delta_{j_1,J+\frac{1}{2}}\left(-\frac{2J+2}{2J+1}\right)+\delta_{\ell,J}\,\delta_{j_1,J-\frac{1}{2}}\left(-\frac{2J}{2J+1}\right)\right] \\
&\quad+\delta_{\ell',\ell}\,\delta_{\ell,J}\left[\delta_{j_1,J+\frac{1}{2}}\,\delta_{j_1',J-\frac{1}{2}}+\delta_{j_1,J-\frac{1}{2}}\,\delta_{j_1',J+\frac{1}{2}}\right]\left(\frac{2\sqrt{J(J+1)}}{2J+1}\right) \\
&\quad+\Big(\delta_{\ell,J-1}\,\delta_{\ell',J+1}\,\delta_{j_1,J-\frac{1}{2}}\,\delta_{j_1',J+\frac{1}{2}} \\
&\qquad+\delta_{\ell,J+1}\,\delta_{\ell',J-1}\,\delta_{j_1,J+\frac{1}{2}}\,\delta_{j_1',J-\frac{1}{2}}\Big)\left(\frac{-2\sqrt{J(J+1)}}{2J+1}\right)\Big\}\,, \qquad (203)
\end{aligned}$$

we therefore have

$$\begin{aligned}
\mathcal{I}_3 &= \int d^3r\, f(r)\,\Psi^{\dagger}_{n\ell j_1 JM_J}(\mathbf{r})\,\boldsymbol{\sigma}^{(2)}\cdot\left(\boldsymbol{\alpha}^{(1)}\times\hat{\mathbf{r}}\right)\Psi_{n\ell j_1 JM_J}(\mathbf{r}) \\
&= \int dr\, 2\, f(r)\, G_{n\ell j_1}(r)F_{n\ell j_1}(r) \\
&\times\ \Big\{\delta_{\ell,J+1}\,\delta_{j_1,J+\frac{1}{2}}\left(\frac{2J+2}{2J+1}\right)+\delta_{\ell,J-1}\,\delta_{j_1,J-\frac{1}{2}}\left(\frac{2J}{2J+1}\right) \\
&\quad+\delta_{\ell,J}\left[\delta_{j_1,J+\frac{1}{2}}\left(-\frac{2J+2}{2J+1}\right)+\delta_{j_1,J-\frac{1}{2}}\left(-\frac{2J}{2J+1}\right)\right]\Big\}. \qquad (204)
\end{aligned}$$

C.3 $\mathcal{I}$

Using (90), and

$$\left\{V_v(r),\boldsymbol{\alpha}^{(1)}\cdot\boldsymbol{\nabla}\right\}\Psi = V_v(r)\boldsymbol{\alpha}^{(1)}\cdot\boldsymbol{\nabla}\Psi+\boldsymbol{\alpha}^{(1)}\cdot\boldsymbol{\nabla}\left[V_v(r)\Psi\right], \qquad (205)$$

we find

$$\begin{aligned}
&H_1\,\psi_{n\ell j_1 JM_J}(\mathbf{r}) \\
&=\frac{1}{2m_2}\Big\{-\boldsymbol{\nabla}^2\Psi_{n\ell j_1 JM_J}(\mathbf{r})+V_v(r)\boldsymbol{\alpha}^{(1)}\cdot\frac{1}{i}\boldsymbol{\nabla}\Psi_{n\ell j_1 JM_J}(\mathbf{r}) \\
&+\boldsymbol{\alpha}^{(1)}\cdot\frac{1}{i}\boldsymbol{\nabla}\left[V_v(r)\Psi_{n\ell j_1 JM_J}(\mathbf{r})\right]+\boldsymbol{\alpha}^{(1)}\cdot\boldsymbol{\sigma}^{(2)}\times\hat{\mathbf{r}}V_v'(r)\Psi_{n\ell j_1 JM_J}(\mathbf{r})\Big\}\,. \qquad (206)
\end{aligned}$$

This gives us

$$\mathcal{I} = \int d^3r\ \Psi^{\dagger}_{n\ell j_1 JM_J}(\mathbf{r})\ H_1\ \Psi_{n\ell j_1 JM_J}(\mathbf{r}) = \triangle E_1 + \triangle E_2 + \triangle E_3\,, \tag{207}$$

with

$$\triangle E_1 = \frac{1}{2m_2}\int d^3r\ \Psi^{\dagger}(\mathbf{r})\left(-\boldsymbol{\nabla}^2\right)\ \Psi(\mathbf{r})\,, \tag{208}$$

$$\triangle E_2 = \frac{1}{2m_2}\int d^3r\,\Psi^{\dagger}(\mathbf{r})\left\{V_v(r)\boldsymbol{\alpha}^{(1)}\cdot\frac{1}{i}\boldsymbol{\nabla}\Psi(\mathbf{r}) + \boldsymbol{\alpha}^{(1)}\cdot\frac{1}{i}\boldsymbol{\nabla}\left[V_v(r)\Psi(\mathbf{r})\right]\right\}, \tag{209}$$

$$\triangle E_3 = \frac{-1}{2m_2}\int d^3r\,\Psi^{\dagger}(\mathbf{r})\,\boldsymbol{\sigma}^{(2)}\cdot\boldsymbol{\alpha}^{(1)}\times\hat{\mathbf{r}}V_v'(r)\,\Psi(\mathbf{r}), \tag{210}$$

where

$$\Psi(\mathbf{r}) = \Psi_{n\ell j_1 JM_J}(\mathbf{r})$$

and we have used the relations $\boldsymbol{\alpha}^{(1)}\cdot\boldsymbol{\sigma}^{(2)}\times\hat{\mathbf{r}} = -\boldsymbol{\sigma}^{(2)}\cdot\boldsymbol{\alpha}^{(1)}\times\hat{\mathbf{r}}$ to obtain (210).

(a) $\triangle E_1$

Using the relation

$$\left(\boldsymbol{\alpha}^{(1)}\cdot\frac{1}{i}\boldsymbol{\nabla}\right)\left(\boldsymbol{\alpha}^{(1)}\cdot\frac{1}{i}\boldsymbol{\nabla}\right) = -\boldsymbol{\nabla}^2$$

and considering the fact that $\boldsymbol{\alpha}^{(1)}\cdot\frac{1}{i}\boldsymbol{\nabla}$ is a hermitian operator, (208) leads to

$$\triangle E_1 = \frac{1}{2m_2}\int d^3r\ \left[\boldsymbol{\alpha}^{(1)}\cdot\frac{1}{i}\boldsymbol{\nabla}\Psi(\mathbf{r})\right]^{\dagger}\left[\boldsymbol{\alpha}^{(1)}\cdot\frac{1}{i}\boldsymbol{\nabla}\Psi(\mathbf{r})\right]. \tag{211}$$

Using (95) and (89),

$$\boldsymbol{\alpha}^{(1)}\cdot\frac{1}{i}\boldsymbol{\nabla}\Psi(\mathbf{r}) = \left\{E^{(0)}_{nlj_1} - V_v(r) - \beta^{(1)}\left[m_1 + V_s(r)\right]\right\}\Psi(\mathbf{r})\,, \tag{212}$$

$$\left[\boldsymbol{\alpha}^{(1)}\cdot\frac{\boldsymbol{\nabla}}{i}\Psi(\mathbf{r})\right]^{\dagger} = \Psi^{\dagger}(\mathbf{r})\ \left\{E^{(0)}_{nlj_1} - V_v(r) - \beta^{(1)}\left[m_1 + V_s(r)\right]\right\}, \tag{213}$$

where $E^{(0)}_{nlj_1}$ is defined as $W^{(0)}_{nlj_1} - m_2$ by (108). Putting (212) and (213) in (211),

$$\triangle E_1 = \frac{1}{2m_2}\int d^3r\left\{\left[\left(E^{(0)}_{nlj_1} - V_v(r)\right)^2 + \left(m_1 + V_s(r)\right)^2\right]\Psi^{\dagger}(\mathbf{r})\,\Psi(\mathbf{r})\right.$$
$$\left. -2\left[E^{(0)}_{nlj_1} - V_v(r)\right]\left[m_1 + V_s(r)\right]\ \Psi^{\dagger}(\mathbf{r})\,\beta^{(1)}\,\Psi(\mathbf{r})\right\}. \tag{214}$$

Using (181) and (182), (214) gives

$$\triangle E_1 = \frac{1}{2m_2}\int dr \left\{ \left[\left(E^{(0)}_{nlj_1} - V_v(r)\right)^2 + \left(m_1 + V_s(r)\right)^2 \right] \left(G^2_{n\ell j_1}(r) + F^2_{n\ell j_1}(r)\right) \right.$$
$$\left. - 2\left[E^{(0)}_{nlj_1} - V_v(r)\right]\left[m_1 + V_s(r)\right]\left(G^2_{n\ell j_1}(r) - F^2_{n\ell j_1}(r)\right)\right\}. \quad (215)$$

(b) $\triangle \mathbf{E_2}$

Since $\boldsymbol{\alpha}^{(1)} \cdot \frac{1}{i}\boldsymbol{\nabla}$ is an hermitian operator, we have

$$\int d^3r \Psi^\dagger(\mathbf{r}) \left(\boldsymbol{\alpha}^{(1)} \cdot \frac{1}{i}\boldsymbol{\nabla}\right) V_v(r)\Psi(\mathbf{r}) = \int d^3r \left(\boldsymbol{\alpha}^{(1)} \cdot \frac{1}{i}\boldsymbol{\nabla}\Psi(\mathbf{r})\right)^\dagger V_v(r)\Psi(\mathbf{r}). \quad (216)$$

Using (212), (216) with (213), (209) gives

$$\triangle E_2 = \frac{1}{2m_2}\int d^3r \left\{ 2V_v(r)\left(E^{(0)}_{nlj_1} - V_v(r)\right)\Psi^\dagger(\mathbf{r})\Psi(\mathbf{r}) \right.$$
$$\left. -2V_v(r)\left[m_1 + V_s(r)\right]\Psi^\dagger(\mathbf{r})\beta^{(1)}\Psi(\mathbf{r})\right\}. \quad (217)$$

Using (181) and (182), (217) gives

$$\triangle E_2 = \frac{1}{2m_2}\int dr \left\{ 2V_v(r)\left(E^{(0)}_{nlj_1} - V_v(r)\right)\left(G^2_{n\ell j_1}(r) + F^2_{n\ell j_1}(r)\right) \right.$$
$$\left. -2V_v(r)\left[m_1 + V_s(r)\right]\left(G^2_{n\ell j_1}(r) - F^2_{n\ell j_1}(r)\right)\right\}. \quad (218)$$

(c) $\triangle \mathbf{E_3}$

Using (204) , (210) gives

$$\triangle E_3 = \frac{-1}{2m_2}\int dr\ 2V_v'(r)\ G_{n\ell j_1}(r)F_{n\ell j_1}(r)$$
$$\times \left\{ \delta_{\ell,J+1}\ \delta_{j_1,J+\frac{1}{2}}\ \left(\frac{2J+2}{2J+1}\right) + \delta_{\ell,J-1}\ \delta_{j_1,J-\frac{1}{2}}\ \left(\frac{2J}{2J+1}\right) \right.$$
$$\left. +\delta_{\ell,J}\left[\delta_{j_1,J+\frac{1}{2}}\ \left(-\frac{2J+2}{2J+1}\right) + \delta_{j_1,J-\frac{1}{2}}\ \left(-\frac{2J}{2J+1}\right)\right]\right\}. \quad (219)$$

Appendix D

Channel Potentials for $Q\bar{Q}$

Using (12) for the kernel $V(\check{p},\check{k};P)$ and the explicit form of the Dirac spinors defined in Appendix A, U^{++},U^{+-},U^{-+} and U^{--}, (117) $\sim$ (120), can be reduced to the Pauli spinor space as

$$
\begin{aligned}
&U^{++}_{m_{s_1}m_{s_2}m'_{s_1}m'_{s_2}}(\check{p},\check{k};P) \\
&= \sqrt{\Big(E(\mathbf{p}_1,m_1)+m_1\Big)\Big/2E(\mathbf{p}_1,m_1)}\sqrt{\Big(E(\mathbf{p}_2,m_2)+m_2\Big)\Big/2E(\mathbf{p}_2,m_2)} \\
&\times\sqrt{\Big(E(\mathbf{k}_1,m_1)+m_1\Big)\Big/2E(\mathbf{k}_1,m_1)}\sqrt{\Big(E(\mathbf{k}_2,m_2)+m_2\Big)\Big/2E(\mathbf{k}_2,m_2)} \\
&\chi^{\dagger}_{m_{s_1}}\chi^{\dagger}_{m_{s_2}}\Bigg\{V_s(Q^2)\Bigg[1-\frac{\boldsymbol{\sigma}^{(1)}\cdot\mathbf{p}_1\;\boldsymbol{\sigma}^{(1)}\cdot\mathbf{k}_1}{\Big(E(\mathbf{p}_1,m_1)+m_1\Big)\Big(E(\mathbf{k}_1,m_1)+m_1\Big)} \\
&\qquad -\frac{\boldsymbol{\sigma}^{(2)}\cdot\mathbf{p}_2\;\boldsymbol{\sigma}^{(2)}\cdot\mathbf{k}_2}{\Big(E(\mathbf{p}_2,m_2)+m_2\Big)\Big(E(\mathbf{k}_2,m_2)+m_2\Big)} \\
&\qquad +\frac{\boldsymbol{\sigma}^{(1)}\cdot\mathbf{p}_1\;\boldsymbol{\sigma}^{(1)}\cdot\mathbf{k}_1}{\Big(E(\mathbf{p}_1,m_1)+m_1\Big)\Big(E(\mathbf{k}_1,m_1)+m_1\Big)} \\
&\qquad \times\frac{\boldsymbol{\sigma}^{(2)}\cdot\mathbf{p}_2\;\boldsymbol{\sigma}^{(2)}\cdot\mathbf{k}_2}{\Big(E(\mathbf{p}_2,m_2)+m_2\Big)\Big(E(\mathbf{k}_2,m_2)+m_2\Big)}\Bigg] \\
&\quad +V_v(Q^2)\Bigg[1+\frac{\boldsymbol{\sigma}^{(1)}\cdot\mathbf{p}_1\;\boldsymbol{\sigma}^{(1)}\cdot\mathbf{k}_1}{\Big(E(\mathbf{p}_1,m_1)+m_1\Big)\Big(E(\mathbf{k}_1,m_1)+m_1\Big)}
\end{aligned}
$$

$$
\begin{aligned}
&+\frac{\boldsymbol{\sigma}^{(2)}\cdot\mathbf{p}_2\,\boldsymbol{\sigma}^{(2)}\cdot\mathbf{k}_2}{\Big(E(\mathbf{p}_2,m_2)+m_2\Big)\Big(E(\mathbf{k}_2,m_2)+m_2\Big)}\\
&+\frac{\boldsymbol{\sigma}^{(1)}\cdot\mathbf{p}_1\boldsymbol{\sigma}^{(1)}\cdot\mathbf{k}_1}{\Big(E(\mathbf{p}_1,m_1)+m_1\Big)\Big(E(\mathbf{k}_1,m_1)+m_1\Big)}\\
&\times\frac{\boldsymbol{\sigma}^{(2)}\cdot\mathbf{p}_2\boldsymbol{\sigma}^{(2)}\cdot\mathbf{k}_2}{\Big(E(\mathbf{p}_2,m_2)+m_2\Big)\Big(E(\mathbf{k}_2,m_2)+m_2\Big)}\Bigg]\\
&-V_v(Q^2)\left(\frac{\boldsymbol{\sigma}^{(1)}\cdot\mathbf{p}_1\,\boldsymbol{\sigma}^{(1)}}{E(\mathbf{p}_1,m_1)+m_1}+\frac{\boldsymbol{\sigma}^{(1)}\boldsymbol{\sigma}^{(1)}\cdot\mathbf{k}_1}{E(\mathbf{k}_1,m_1)+m_1}\right)\\
&\cdot\left(\frac{\boldsymbol{\sigma}^{(2)}\cdot\mathbf{p}_2\,\boldsymbol{\sigma}^{(2)}}{E(\mathbf{p}_2,m_2)+m_2}+\frac{\boldsymbol{\sigma}^{(2)}\boldsymbol{\sigma}^{(2)}\cdot\mathbf{k}_2}{E(\mathbf{k}_2,m_2)+m_2}\right)\Bigg\}\chi_{m'_{s_1}}\chi_{m'_{s_2}},
\end{aligned}
\tag{220}
$$

$$
\begin{aligned}
&U^{+-}_{m_{s_1}m_{s_2}m'_{s_1}m'_{s_2}}(\check{p},\check{k};P)\\
&=\sqrt{\Big(E(\mathbf{p}_1,m_1)+m_1\Big)\Big/2E(\mathbf{p}_1,m_1)}\sqrt{\Big(E(\mathbf{p}_2,m_2)+m_2\Big)\Big/2E(\mathbf{p}_2,m_2)}\\
&\times\sqrt{\Big(E(\mathbf{k}_1,m_1)+m_1\Big)\Big/2E(\mathbf{k}_1,m_1)}\sqrt{\Big(E(\mathbf{k}_2,m_2)+m_2\Big)\Big/2E(\mathbf{k}_2,m_2)}\\
&\chi^{\dagger}_{m_{s_1}}\chi^{\dagger}_{m_{s_2}}\Bigg\{V_s(Q^2)\Bigg[-\frac{\boldsymbol{\sigma}^{(1)}\cdot\mathbf{p}_1}{E(\mathbf{p}_1,m_1)+m_1}-\frac{\boldsymbol{\sigma}^{(1)}\cdot\mathbf{k}_1}{E(\mathbf{k}_1,m_1)+m_1}\\
&\qquad+\left(\frac{\boldsymbol{\sigma}^{(1)}\cdot\mathbf{p}_1}{E(\mathbf{p}_1,m_1)+m_1}+\frac{\boldsymbol{\sigma}^{(1)}\cdot\mathbf{k}_1}{E(\mathbf{k}_1,m_1)+m_1}\right)\\
&\qquad\times\left(\frac{\boldsymbol{\sigma}^{(2)}\cdot\mathbf{p}_2\,\boldsymbol{\sigma}^{(2)}\cdot\mathbf{k}_2}{\Big(E(\mathbf{p}_2,m_2)+m_2\Big)\Big(E(\mathbf{k}_2,m_2)+m_2\Big)}\right)\Bigg]\\
&\quad+V_v(Q^2)\Bigg[\frac{\boldsymbol{\sigma}^{(1)}\cdot\mathbf{p}_1}{E(\mathbf{p}_1,m_1)+m_1}-\frac{\boldsymbol{\sigma}^{(1)}\cdot\mathbf{k}_1}{E(\mathbf{k}_1,m_1)+m_1}\\
&\qquad+\left(\frac{\boldsymbol{\sigma}^{(1)}\cdot\mathbf{p}_1}{E(\mathbf{p}_1,m_1)+m_1}-\frac{\boldsymbol{\sigma}^{(1)}\cdot\mathbf{k}_1}{E(\mathbf{k}_1,m_1)+m_1}\right)\\
&\qquad\times\left(\frac{\boldsymbol{\sigma}^{(2)}\cdot\mathbf{p}_2\,\boldsymbol{\sigma}^{(2)}\cdot\mathbf{k}_2}{\Big(E(\mathbf{p}_2,m_2)+m_2\Big)\Big(E(\mathbf{k}_2,m_2)+m_2\Big)}\right)\Bigg]\\
&\quad-V_v(Q^2)\Bigg[\boldsymbol{\sigma}^{(1)}\cdot\left(\frac{\boldsymbol{\sigma}^{(2)}\cdot\mathbf{p}_2\,\boldsymbol{\sigma}^{(2)}}{E(\mathbf{p}_2,m_2)+m_2}+\frac{\boldsymbol{\sigma}^{(2)}\,\boldsymbol{\sigma}^{(2)}\cdot\mathbf{k}_2}{E(\mathbf{k}_2,m_2)+m_2}\right)\\
&\qquad-\frac{\boldsymbol{\sigma}^{(1)}\cdot\mathbf{p}_1\,\boldsymbol{\sigma}^{(1)}\,\boldsymbol{\sigma}^{(1)}\cdot\mathbf{k}_1}{\Big(E(\mathbf{p}_1,m_1)+m_1\Big)\Big(E(\mathbf{k}_1,m_1)+m_1\Big)}
\end{aligned}
$$

$$\cdot\left(\frac{\boldsymbol{\sigma}^{(2)}\cdot\mathbf{p}_2\,\boldsymbol{\sigma}^{(2)}}{E(\mathbf{p}_2,m_2)+m_2}+\frac{\boldsymbol{\sigma}^{(2)}\,\boldsymbol{\sigma}^{(2)}\cdot\mathbf{k}_2}{E(\mathbf{k}_2,m_2)+m_2}\right)\Bigg]\Bigg\}\chi_{-m'_{s_1}}\chi_{m'_{s_2}}\,, \quad (221)$$

$$\begin{aligned}
&U^{-+}_{m_{s_1}m_{s_2}m'_{s_1}m'_{s_2}}(\check{p},\check{k};P)\\
&=\sqrt{\Big(E(\mathbf{p}_1,m_1)+m_1\Big)\Big/2E(\mathbf{p}_1,m_1)}\sqrt{\Big(E(\mathbf{p}_2,m_2)+m_2\Big)\Big/2E(\mathbf{p}_2,m_2)}\\
&\times\sqrt{\Big(E(\mathbf{k}_1,m_1)+m_1\Big)\Big/2E(\mathbf{k}_1,m_1)}\sqrt{\Big(E(\mathbf{k}_2,m_2)+m_2\Big)\Big/2E(\mathbf{k}_2,m_2)}\\
&\chi^{\dagger}_{-m_{s_1}}\chi^{\dagger}_{m_{s_2}}\Bigg\{V_s(Q^2)\Bigg[-\frac{\boldsymbol{\sigma}^{(1)}\cdot\mathbf{p}_1}{E(\mathbf{p}_1,m_1)+m_1}-\frac{\boldsymbol{\sigma}^{(1)}\cdot\mathbf{k}_1}{E(\mathbf{k}_1,m_1)+m_1}\\
&\qquad+\left(\frac{\boldsymbol{\sigma}^{(1)}\cdot\mathbf{p}_1}{E(\mathbf{p}_1,m_1)+m_1}+\frac{\boldsymbol{\sigma}^{(1)}\cdot\mathbf{k}_1}{E(\mathbf{k}_1,m_1)+m_1}\right)\\
&\qquad\times\left(\frac{\boldsymbol{\sigma}^{(2)}\cdot\mathbf{p}_2\,\boldsymbol{\sigma}^{(2)}\cdot\mathbf{k}_2}{\Big(E(\mathbf{p}_2,m_2)+m_2\Big)\Big(E(\mathbf{k}_2,m_2)+m_2\Big)}\right)\Bigg]\\
&\quad+V_v(Q^2)\Bigg[\frac{-\boldsymbol{\sigma}^{(1)}\cdot\mathbf{p}_1}{E(\mathbf{p}_1,m_1)+m_1}+\frac{\boldsymbol{\sigma}^{(1)}\cdot\mathbf{k}_1}{E(\mathbf{k}_1,m_1)+m_1}\\
&\qquad+\left(\frac{-\boldsymbol{\sigma}^{(1)}\cdot\mathbf{p}_1}{E(\mathbf{p}_1,m_1)+m_1}+\frac{\boldsymbol{\sigma}^{(1)}\cdot\mathbf{k}_1}{E(\mathbf{k}_1,m_1)+m_1}\right)\\
&\qquad\times\left(\frac{\boldsymbol{\sigma}^{(2)}\cdot\mathbf{p}_2\,\boldsymbol{\sigma}^{(2)}\cdot\mathbf{k}_2}{\Big(E(\mathbf{p}_2,m_2)+m_2\Big)\Big(E(\mathbf{k}_2,m_2)+m_2\Big)}\right)\Bigg]\\
&\quad-V_v(Q^2)\Bigg[\boldsymbol{\sigma}^{(1)}\cdot\left(\frac{\boldsymbol{\sigma}^{(2)}\cdot\mathbf{p}_2\,\boldsymbol{\sigma}^{(2)}}{E(\mathbf{p}_2,m_2)+m_2}+\frac{\boldsymbol{\sigma}^{(2)}\,\boldsymbol{\sigma}^{(2)}\cdot\mathbf{k}_2}{E(\mathbf{k}_2,m_2)+m_2}\right)\\
&\qquad-\frac{\boldsymbol{\sigma}^{(1)}\cdot\mathbf{p}_1\,\boldsymbol{\sigma}^{(1)}\,\boldsymbol{\sigma}^{(1)}\cdot\mathbf{k}_1}{\Big(E(\mathbf{p}_1,m_1)+m_1\Big)\Big(E(\mathbf{k}_1,m_1)+m_1\Big)}\\
&\qquad\cdot\left(\frac{\boldsymbol{\sigma}^{(2)}\cdot\mathbf{p}_2\,\boldsymbol{\sigma}^{(2)}}{E(\mathbf{p}_2,m_2)+m_2}+\frac{\boldsymbol{\sigma}^{(2)}\,\boldsymbol{\sigma}^{(2)}\cdot\mathbf{k}_2}{E(\mathbf{k}_2,m_2)+m_2}\right)\Bigg]\Bigg\}\chi_{m'_{s_1}}\chi_{m'_{s_2}}\,, \quad (222)
\end{aligned}$$

$$\begin{aligned}
&U^{--}_{m_{s_1}m_{s_2}m'_{s_1}m'_{s_2}}(\check{p},\check{k};P)\\
&=\sqrt{\Big(E(\mathbf{p}_1,m_1)+m_1\Big)\Big/2E(\mathbf{p}_1,m_1)}\sqrt{\Big(E(\mathbf{p}_2,m_2)+m_2\Big)\Big/2E(\mathbf{p}_2,m_2)}\\
&\times\sqrt{\Big(E(\mathbf{k}_1,m_1)+m_1\Big)\Big/2E(\mathbf{k}_1,m_1)}\sqrt{\Big(E(\mathbf{k}_2,m_2)+m_2\Big)\Big/2E(\mathbf{k}_2,m_2)}
\end{aligned}$$

$$\chi^{\dagger}_{-m_{s_1}}\chi^{\dagger}_{m_{s_2}}\Bigg\{V_s(Q^2)\Bigg[-1+\frac{\boldsymbol{\sigma}^{(1)}\cdot\mathbf{p_1}\;\boldsymbol{\sigma}^{(1)}\cdot\mathbf{k_1}}{\Big(E(\mathbf{p_1},m_1)+m_1\Big)\;\Big(E(\mathbf{k_1},m_1)+m_1\Big)}$$
$$+\frac{\boldsymbol{\sigma}^{(2)}\cdot\mathbf{p_2}\;\boldsymbol{\sigma}^{(2)}\cdot\mathbf{k_2}}{\Big(E(\mathbf{p_2},m_2)+m_2\Big)\;\Big(E(\mathbf{k_2},m_2)+m_2\Big)}$$
$$-\frac{\boldsymbol{\sigma}^{(1)}\cdot\mathbf{p_1}\;\boldsymbol{\sigma}^{(1)}\cdot\mathbf{k_1}}{\Big(E(\mathbf{p_1},m_1)+m_1\Big)\;\Big(E(\mathbf{k_1},m_1)+m_1\Big)}$$
$$\times\frac{\boldsymbol{\sigma}^{(2)}\cdot\mathbf{p_2}\;\boldsymbol{\sigma}^{(2)}\cdot\mathbf{k_2}}{\Big(E(\mathbf{p_2},m_2)+m_2\Big)\;\Big(E(\mathbf{k_2},m_2)+m_2\Big)}\Bigg]$$
$$+V_v(Q^2)\Bigg[1+\frac{\boldsymbol{\sigma}^{(1)}\cdot\mathbf{p_1}\;\boldsymbol{\sigma}^{(1)}\cdot\mathbf{k_1}}{\Big(E(\mathbf{p_1},m_1)+m_1\Big)\;\Big(E(\mathbf{k_1},m_1)+m_1\Big)}$$
$$+\frac{\boldsymbol{\sigma}^{(2)}\cdot\mathbf{p_2}\;\boldsymbol{\sigma}^{(2)}\cdot\mathbf{k_2}}{\Big(E(\mathbf{p_2},m_2)+m_2\Big)\;\Big(E(\mathbf{k_2},m_2)+m_2\Big)}$$
$$+\frac{\boldsymbol{\sigma}^{(1)}\cdot\mathbf{p_1}\;\boldsymbol{\sigma}^{(1)}\cdot\mathbf{k_1}}{\Big(E(\mathbf{p_1},m_1)+m_1\Big)\;\Big(E(\mathbf{k_1},m_1)+m_1\Big)}$$
$$\times\frac{\boldsymbol{\sigma}^{(2)}\cdot\mathbf{p_2}\;\boldsymbol{\sigma}^{(2)}\cdot\mathbf{k_2}}{\Big(E(\mathbf{p_2},m_2)+m_2\Big)\;\Big(E(\mathbf{k_2},m_2)+m_2\Big)}\Bigg]$$
$$-V_v(Q^2)\left(\frac{-\boldsymbol{\sigma}^{(1)}\cdot\mathbf{p_1}\;\boldsymbol{\sigma}^{(1)}}{E(\mathbf{p_1},m_1)+m_1}+\frac{-\boldsymbol{\sigma}^{(1)}\;\boldsymbol{\sigma}^{(1)}\cdot\mathbf{k_1}}{E(\mathbf{k_1},m_1)+m_1}\right)$$
$$\cdot\left(\frac{\boldsymbol{\sigma}^{(2)}\cdot\mathbf{p_2}\;\boldsymbol{\sigma}^{(2)}}{E(\mathbf{p_2},m_2)+m_2}+\frac{\boldsymbol{\sigma}^{(2)}\;\boldsymbol{\sigma}^{(2)}\cdot\mathbf{k_2}}{E(\mathbf{k_2},m_2)+m_2}\right)\Bigg\}\chi_{-m'_{s_1}}\chi_{m'_{s_2}}. \quad (223)$$

Expanding in powers of $1/m_1$ and $1/m_2$, and keeping to the order of $1/(m_i m_j)$, (220-223) become

$$U^{++}_{m_{s_1}m_{s_2}m'_{s_1}m'_{s_2}}(\check{p},\check{k};P)$$
$$=\chi^{\dagger}_{m_{s_1}}\chi^{\dagger}_{m_{s_2}}\Bigg\{\left(1-\frac{\mathbf{p_1}^2}{8m_1^2}-\frac{\mathbf{p_2}^2}{8m_2^2}-\frac{\mathbf{k_1}^2}{8m_1^2}-\frac{\mathbf{k_2}^2}{8m_2^2}\right)\Big[V_s(\mathbf{q}^2)+V_v(\mathbf{q}^2)\Big]$$
$$-\frac{1}{4m_2^2}\Big[V'_s(\mathbf{q}^2)+V'_v(\mathbf{q}^2)\Big]\Big(\mathbf{p_2}^2-\mathbf{k_2}^2\Big)^2$$
$$-V_s(\mathbf{q}^2)\left(\frac{1}{4m_1^2}\boldsymbol{\sigma}^{(1)}\cdot\mathbf{p_1}\;\boldsymbol{\sigma}^{(1)}\cdot\mathbf{k_1}+\frac{1}{4m_2^2}\boldsymbol{\sigma}^{(2)}\cdot\mathbf{p_2}\;\boldsymbol{\sigma}^{(2)}\cdot\mathbf{k_2}\right)$$

$$+V_v(\mathbf{q}^2)\left(\frac{1}{4m_1^2}\boldsymbol{\sigma}^{(1)}\cdot\mathbf{p}_1\,\boldsymbol{\sigma}^{(1)}\cdot\mathbf{k}_1+\frac{1}{4m_2^2}\boldsymbol{\sigma}^{(2)}\cdot\mathbf{p}_2\,\boldsymbol{\sigma}^{(2)}\cdot\mathbf{k}_2\right)$$
$$-V_v(\mathbf{q}^2)\frac{1}{4m_1m_2}\left(\boldsymbol{\sigma}^{(1)}\cdot\mathbf{p}_1\,\boldsymbol{\sigma}^{(1)}+\boldsymbol{\sigma}^{(1)}\,\boldsymbol{\sigma}^{(1)}\cdot\mathbf{k}_1\right)$$
$$\cdot\left(\boldsymbol{\sigma}^{(2)}\cdot\mathbf{p}_2\,\boldsymbol{\sigma}^{(2)}+\boldsymbol{\sigma}^{(2)}\,\boldsymbol{\sigma}^{(2)}\cdot\mathbf{k}_2\right)\Big\}\,\chi_{m'_{s_1}}\chi_{m'_{s_2}}, \quad (224)$$

$$U^{+-}_{m_{s_1}m_{s_2}m'_{s_1}m'_{s_2}}(\check{p},\check{k};P)$$
$$=\chi^\dagger_{m_{s_1}}\chi^\dagger_{m_{s_2}}\Big\{\frac{1}{2m_1}\boldsymbol{\sigma}^{(1)}\cdot\mathbf{p}_1\left[V_v(\mathbf{q}^2)-V_s(\mathbf{q}^2)\right]$$
$$-\frac{1}{2m_1}\boldsymbol{\sigma}^{(1)}\cdot\mathbf{k}_1\left[V_v(\mathbf{q}^2)+V_s(\mathbf{q}^2)\right]$$
$$-\frac{1}{2m_2}\boldsymbol{\sigma}^{(1)}\cdot\left(\boldsymbol{\sigma}^{(2)}\cdot\mathbf{p}_2\,\boldsymbol{\sigma}^{(2)}+\boldsymbol{\sigma}^{(2)}\,\boldsymbol{\sigma}^{(2)}\cdot\mathbf{k}_2\right)V_v(\mathbf{q}^2)\Big\}\,\chi_{-m'_{s_1}}\chi_{m'_{s_2}}, \quad (225)$$

$$U^{-+}_{m_{s_1}m_{s_2}m'_{s_1}m'_{s_2}}(\check{p},\check{k};P)$$
$$=\chi^\dagger_{-m_{s_1}}\chi^\dagger_{m_{s_2}}\Big\{-\frac{1}{2m_1}\boldsymbol{\sigma}^{(1)}\cdot\mathbf{p}_1\left[V_v(\mathbf{q}^2)+V_s(\mathbf{q}^2)\right]$$
$$+\frac{1}{2m_1}\boldsymbol{\sigma}^{(1)}\cdot\mathbf{k}_1\left[V_v(\mathbf{q}^2)-V_s(\mathbf{q}^2)\right]$$
$$-\frac{1}{2m_2}\boldsymbol{\sigma}^{(1)}\cdot\left(\boldsymbol{\sigma}^{(2)}\cdot\mathbf{p}_2\,\boldsymbol{\sigma}^{(2)}+\boldsymbol{\sigma}^{(2)}\,\boldsymbol{\sigma}^{(2)}\cdot\mathbf{k}_2\right)V_v(\mathbf{q}^2)\Big\}\,\chi_{m'_{s_1}}\chi_{m'_{s_2}}, \quad (226)$$

$$U^{--}_{m_{s_1}m_{s_2}m'_{s_1}m'_{s_2}}(\check{p},\check{k};P)$$
$$=\chi^\dagger_{-m_{s_1}}\chi^\dagger_{m_{s_2}}\Big\{\left(1-\frac{\mathbf{p}_1{}^2}{8m_1^2}-\frac{\mathbf{p}_2{}^2}{8m_2^2}-\frac{\mathbf{k}_1{}^2}{8m_1^2}-\frac{\mathbf{k}_2{}^2}{8m_2^2}\right)\left[V_v(\mathbf{q}^2)-V_s(\mathbf{q}^2)\right]$$
$$-\frac{1}{4m_2^2}\left[V'_s(\mathbf{q}^2)+V'_v(\mathbf{q}^2)\right]\left(\mathbf{p}_2{}^2-\mathbf{k}_2{}^2\right)^2$$
$$+V_s(\mathbf{q}^2)\left(\frac{1}{4m_1^2}\boldsymbol{\sigma}^{(1)}\cdot\mathbf{p}_1\,\boldsymbol{\sigma}^{(1)}\cdot\mathbf{k}_1+\frac{1}{4m_2^2}\boldsymbol{\sigma}^{(2)}\cdot\mathbf{p}_2\,\boldsymbol{\sigma}^{(2)}\cdot\mathbf{k}_2\right)$$
$$+V_v(\mathbf{q}^2)\left(\frac{1}{4m_1^2}\boldsymbol{\sigma}^{(1)}\cdot\mathbf{p}_1\,\boldsymbol{\sigma}^{(1)}\cdot\mathbf{k}_1+\frac{1}{4m_2^2}\boldsymbol{\sigma}^{(2)}\cdot\mathbf{p}_2\,\boldsymbol{\sigma}^{(2)}\cdot\mathbf{k}_2\right)$$
$$+V_v(\mathbf{q}^2)\frac{1}{4m_1m_2}\left(\boldsymbol{\sigma}^{(1)}\cdot\mathbf{p}_1\,\boldsymbol{\sigma}^{(1)}+\boldsymbol{\sigma}^{(1)}\,\boldsymbol{\sigma}^{(1)}\cdot\mathbf{k}_1\right)$$
$$\cdot\left(\boldsymbol{\sigma}^{(2)}\cdot\mathbf{p}_2\,\boldsymbol{\sigma}^{(2)}+\boldsymbol{\sigma}^{(2)}\,\boldsymbol{\sigma}^{(2)}\cdot\mathbf{k}_2\right)\Big\}\,\chi_{-m'_{s_1}}\chi_{m'_{s_2}}, \quad (227)$$

To solve the coupled equations, (115) and (116), we obtain $\Psi^{(-)}_{m'_{s_1} m'_{s_2}}(\check{k}, P)$ from (116) as

$$\begin{aligned}
&\Psi^{(-)}_{m'_{s_1} m'_{s_2}}(\check{k}, P) \\
&= \sum_{m''_{s_1} m''_{s_2}} \int \frac{d^3k'}{(2\pi)^3} \left[\frac{U^{-+}_{m'_{s_1} m'_{s_2} m''_{s_1} m''_{s_2}}(\check{k}, \check{k}'; P)}{W + E(\mathbf{k}_1, m_1) - E(\mathbf{k}_2, m_2)} \Psi^{(+)}_{m''_{s_1} m''_{s_2}}(\check{k}', P) \right. \\
&\qquad \left. + \frac{U^{--}_{m'_{s_1} m'_{s_2} m''_{s_1} m''_{s_2}}(\check{k}, \check{k}'; P)}{W + E(\mathbf{k}_1, m_1) - E(\mathbf{k}_2, m_2)} \Psi^{(-)}_{m''_{s_1} m''_{s_2}}(\check{k}', P) \right]. \qquad (228)
\end{aligned}$$

For the binding energy $E_b = W - m_1 - m_2$ of the order $1/m_i$, we have

$$\frac{1}{W + E(\mathbf{k}_1, m_1) - E(\mathbf{k}_2, m_2)} = \frac{1}{2m_1} + \mathcal{O}(1/m_i^3). \qquad (229)$$

Using this with (226) and (227), we can see

$$\frac{U^{-+}_{m'_{s_1} m'_{s_2} m''_{s_1} m''_{s_2}}(\check{k}, \check{k}'; P)}{W + E(\mathbf{k}_1, m_1) - E(\mathbf{k}_2, m_2)} = \mathcal{O}[1/(m_i m_j)], \qquad (230)$$

$$\frac{U^{--}_{m'_{s_1} m'_{s_2} m''_{s_1} m''_{s_2}}(\check{k}, \check{k}'; P)}{W + E(\mathbf{k}_1, m_1) - E(\mathbf{k}_2, m_2)} = \mathcal{O}(1/m_i). \qquad (231)$$

Equation (228) can therefore be written as

$$\begin{aligned}
\Psi^{(-)}_{m'_{s_1} m'_{s_2}}(\check{k}, P) = \sum_{m''_{s_1} m''_{s_2}} \int \frac{d^3k'}{(2\pi)^3} \Big[&\mathcal{O}[1/(m_i m_j)] \, \Psi^{(+)}_{m''_{s_1} m''_{s_2}}(\check{k}', P) \\
&+ \mathcal{O}(1/m_i) \, \Psi^{(-)}_{m''_{s_1} m''_{s_2}}(\check{k}', P) \Big]. \qquad (232)
\end{aligned}$$

Substituting (232) into (115), and using $U^{+-}_{m_{s_1} m_{s_2} m'_{s_1} m'_{s_2}} = \mathcal{O}(1/m_i)$ from (225), we have

$$\begin{aligned}
&\Big[W - E(\mathbf{p}_1, m_1) - E(\mathbf{p}_2, m_2) \Big] \, \Psi^{(+)}_{m_{s_1} m_{s_2}}(\check{p}, P) \\
&= \sum_{m'_{s_1} m'_{s_2}} \int \frac{d^3k}{(2\pi)^3} \, U^{++}_{m_{s_1} m_{s_2} m'_{s_1} m'_{s_2}}(\check{p}, \check{k}; P) \, \Psi^{(+)}_{m'_{s_1} m'_{s_2}}(\check{k}, P) \\
&+ \sum_{m'_{s_1} m'_{s_2}} \sum_{m''_{s_1} m''_{s_2}} \int \frac{d^3k}{(2\pi)^3} \int \frac{d^3k'}{(2\pi)^3} \Big[\mathcal{O}(1/m_i^3) \, \Psi^{(+)}_{m''_{s_1} m''_{s_2}}(\check{k}', P) \\
&\qquad + \mathcal{O}(1/m_i^2) \, \Psi^{(-)}_{m''_{s_1} m''_{s_2}}(\check{k}', P) \Big]. \qquad (233)
\end{aligned}$$

Using (232) for $\Psi^{(-)}_{m''_{s_1} m''_{s_2}}(\check{k}', P)$, and substituting into (233), we get

$$\begin{aligned}
&\Big[W - E(\mathbf{p}_1, m_1) - E(\mathbf{p}_2, m_2) \Big] \, \Psi^{(+)}_{m_{s_1} m_{s_2}}(\check{p}, P) \\
&= \sum_{m'_{s_1} m'_{s_2}} \int \frac{d^3k}{(2\pi)^3} U^{++}_{m_{s_1} m_{s_2} m'_{s_1} m'_{s_2}}(\check{p}, \check{k}; P) \, \Psi^{(+)}_{m'_{s_1} m'_{s_2}}(\check{k}, P) \\
&+ \sum_{m'_{s_1} m'_{s_2}} \sum_{m''_{s_1} m''_{s_2}} \int \frac{d^3k}{(2\pi)^3} \int \frac{d^3k'}{(2\pi)^3} \mathcal{O}(1/m_i^3) \, \Psi^{(+)}_{m''_{s_1} m''_{s_2}}(\check{k}', P) \\
&+ \sum_{m'_{s_1} m'_{s_2}} \sum_{m''_{s_1} m''_{s_2}} \sum_{m'''_{s_1} m'''_{s_2}} \int \frac{d^3k}{(2\pi)^3} \int \frac{d^3k'}{(2\pi)^3} \int \frac{d^3k''}{(2\pi)^3} \Big[\mathcal{O}(1/m_i^4) \, \Psi^{(+)}_{m'''_{s_1} m'''_{s_2}}(\check{k}'', P) \\
&\qquad + \mathcal{O}(1/m_i^3) \Psi^{(-)}_{m'''_{s_1} m'''_{s_2}}(\check{k}'', P) \Big] . \qquad (234)
\end{aligned}$$

One can see that to the order of $1/(m_i m_j)$, only the term with $U^{++}\Psi^{(+)}$ contributes. Equation (234) becomes

$$\begin{aligned}
&\left(W - m_1 - m_2 - \frac{\mathbf{p_1}^2}{2m_1} - \frac{\mathbf{p_2}^2}{2m_2} \right) \Psi^{(+)}_{m_{s_1} m_{s_2}}(\check{p}, P) \\
&= \sum_{m'_{s_1} m'_{s_2}} \int \frac{d^3k}{(2\pi)^3} U^{++}_{m_{s_1} m_{s_2} m'_{s_1} m'_{s_2}}(\check{p}, \check{k}; P) \, \Psi^{(+)}_{m'_{s_1} m'_{s_2}}(\check{k}, P) \, . \qquad (235)
\end{aligned}$$

This equation can be reduced to (122) by defining Ψ as in (121) . $\mathcal{U}(\mathbf{p}, \mathbf{k})$ in (123) is obtained from (224) using (86) and the relations

$$(\boldsymbol{\sigma} \cdot \mathbf{a})(\boldsymbol{\sigma} \cdot \mathbf{b}) = \mathbf{a} \cdot \mathbf{b} + i(\mathbf{a} \times \mathbf{b}), \qquad (236)$$

$$\left(\mathbf{q} \times \boldsymbol{\sigma}^{(1)} \right) \cdot \left(\mathbf{q} \times \boldsymbol{\sigma}^{(2)} \right) = \mathbf{q}^2 \left(\boldsymbol{\sigma}^{(1)} \cdot \boldsymbol{\sigma}^{(2)} \right) - \left(\boldsymbol{\sigma}^{(1)} \cdot \mathbf{q} \right) \left(\boldsymbol{\sigma}^{(2)} \cdot \mathbf{q} \right) . \qquad (237)$$

Appendix E

$H_{\mathrm{S(V)R}}$ for $Q\bar{Q}$ Mesons

Let

$$\begin{aligned} I &= \int \frac{d^3k}{(2\pi)^3}\left(-\frac{1}{4m_2^2}\right)\left(\mathbf{p}^2-\mathbf{k}^2\right)^2 V'(\mathbf{q}^2)\,\Psi(\mathbf{k}) \\ &= \int d^3r e^{-i\mathbf{p}\cdot\mathbf{r}}\, H_{\mathrm{R}}(\mathbf{r})\,\Psi(\mathbf{r})\,. \end{aligned} \tag{238}$$

Letting $F_{\mathrm{R}}(\mathbf{r})$ represent the Fourier transform of $V'(\mathbf{q}^2)$, and using

$$\left(\mathbf{p}^2-\mathbf{k}^2\right)^2 = \mathbf{p}^4-2\mathbf{p}^2\mathbf{k}^2+\mathbf{k}^4,$$

we have

$$\mathrm{I} = -\frac{1}{4\mathrm{m}_2^2}\int\frac{\mathrm{d}^3\mathrm{k}}{(2\pi)^3}\left(\mathbf{p}^4-2\mathbf{p}^2\mathbf{k}^2+\mathbf{k}^4\right)\int\mathrm{d}^3\mathrm{r}\,\mathrm{e}^{i\mathbf{q}\cdot\mathbf{r}}\,\mathrm{F_R}(\mathbf{r})\int\mathrm{d}^3\mathrm{r}'\,\mathrm{e}^{-i\mathbf{k}\cdot\mathbf{r}'}\,\Psi(\mathbf{r}')\,, \tag{239}$$

where $k = |\mathbf{k}|$, $r = |\mathbf{r}|$. Using

$$e^{i\mathbf{q}\cdot\mathbf{r}-i\mathbf{k}\cdot\mathbf{r}'} = e^{i\mathbf{k}\cdot(\mathbf{r}-\mathbf{r}')}e^{-i\mathbf{p}\cdot\mathbf{r}},$$

since $\mathbf{q}=\mathbf{k}-\mathbf{p}$, and

$$\int\frac{d^3k}{(2\pi)^3}\,e^{i\mathbf{k}\cdot(\mathbf{r}-\mathbf{r}')} = \delta(\mathbf{r}'-\mathbf{r})\,, \tag{240}$$

I can be written as

$$\begin{aligned} \mathrm{I} = -\frac{1}{4\mathrm{m}_2^2}\Bigg\{&\int\mathrm{d}^3\mathrm{r}\,\mathbf{p}^4\,\mathrm{e}^{-i\mathbf{p}\cdot\mathbf{r}}\,\mathrm{F_R}(\mathbf{r})\,\Psi(\mathbf{r}) \\ &+\int\frac{\mathrm{d}^3\mathrm{k}}{(2\pi)^3}\int\mathrm{d}^3\mathrm{r}\int\mathrm{d}^3\mathrm{r}'\left(-2\mathbf{p}^2\mathbf{k}^2+\mathbf{k}^4\right)\mathrm{e}^{-i\mathbf{p}\cdot\mathbf{r}}\,\mathrm{e}^{i\mathbf{k}\cdot(\mathbf{r}-\mathbf{r}')}\mathrm{F_R}(\mathbf{r})\,\Psi(\mathbf{r}')\Bigg\}. \end{aligned}$$

Using $\mathbf{p}^2 e^{-i\mathbf{p}\cdot\mathbf{r}} = -\nabla^2\left(e^{-i\mathbf{p}\cdot\mathbf{r}}\right)$ and the divergence theorem, we get

$$\mathrm{I} = -\frac{1}{4\mathrm{m}_2^2}\int \mathrm{d}^3\mathrm{r}\, \mathrm{e}^{-i\mathbf{p}\cdot\mathbf{r}}\left\{\nabla^4 \mathrm{F}_{\mathrm{R}}(\mathbf{r}) - 2\nabla^2 \mathrm{F}_{\mathrm{R}}(\mathbf{r})\nabla^2 + \mathrm{F}_{\mathrm{R}}(\mathbf{r})\nabla^4\right\}\Psi(\mathbf{r}). \tag{241}$$

This can be written as

$$I = -\frac{1}{4m_2^2}\int d^3r\, e^{-i\mathbf{p}\cdot\mathbf{r}}\left[\nabla^2, \left[\nabla^2, F_{\mathrm{R}}(\mathbf{r})\right]\right]\Psi(\mathbf{r}). \tag{242}$$

Therefore, by (238) ,

$$H_{\mathrm{R}}(\mathbf{r}) = -\frac{1}{4m_2^2}\left[\nabla^2, \left[\nabla^2, F_{\mathrm{R}}(\mathbf{r})\right]\right]. \tag{243}$$

Note that

$$\left[\nabla^2,\ F_{\mathrm{R}}(\mathbf{r})\right] = \left[\frac{\partial^2}{\partial r^2} + \frac{2}{r}\frac{\partial}{\partial r} - \frac{\mathbf{L}^2}{r^2},\ F_{\mathrm{R}}(\mathbf{r})\right].$$

For $F_{\mathrm{R}}(\mathbf{r}) = F_{\mathrm{R}}(r)$, this becomes

$$\left[\nabla^2,\ F_{\mathrm{R}}(\mathbf{r})\right] = \left[\nabla^2,\ F_{\mathrm{R}}(r)\right] = F''_{\mathrm{R}}(r) + 2F'_{\mathrm{R}}(r)\frac{\partial}{\partial r} + \frac{2}{r}F'_{\mathrm{R}}(r)\,. \tag{244}$$

Equation (243) can therefore be written as

$$H_{\mathrm{R}}(\mathbf{r}) = -\frac{1}{4m_2^2}\left[\nabla^2,\ F''_{\mathrm{R}}(r) + 2F'_{\mathrm{R}}(r)\frac{\partial}{\partial r} + \frac{2}{r}F'_{\mathrm{R}}(r)\right]. \tag{245}$$

This can be simplified to

$$\begin{aligned} H_{\mathrm{R}}(\mathbf{r}) = -\frac{1}{m_2^2}\Bigg(&\frac{1}{4}\frac{d^4F_{\mathrm{R}}(r)}{dr^4} + \frac{1}{r}\frac{d^3F_{\mathrm{R}}(r)}{dr^3} + \frac{d^3F_{\mathrm{R}}(r)}{dr^3}\frac{\partial}{\partial r} \\ &+ \frac{2}{r}\frac{d^2F_{\mathrm{R}}(r)}{dr^2}\frac{\partial}{\partial r} + \frac{d^2F_{\mathrm{R}}(r)}{dr^2}\frac{\partial^2}{\partial r^2} - \frac{1}{r^3}\frac{dF_{\mathrm{R}}(r)}{dr}\mathbf{L}^2\Bigg). \end{aligned} \tag{246}$$

(*a*) $H_{\mathrm{VR}}(\mathbf{r})$, $H_{\mathrm{R}}(\mathbf{r})$ for vector potential $V_v(r)$

By the definition of $F_{\mathrm{R}}(\mathbf{r})$, for vector potential $V_v(r)$,

$$F_{\mathrm{R}}(\mathbf{r}) = F_{\mathrm{VR}}(\mathbf{r}) = \int \frac{d^3q}{(2\pi)^3}\, e^{-i\mathbf{q}\cdot\mathbf{r}}\, V'_v(\mathbf{q}^2)\,, \tag{247}$$

where $q = |\mathbf{q}|$. Since

$$V_v(\mathbf{q}^2) = -\frac{4}{3}\alpha_s(\mathbf{q}^2)\frac{4\pi}{\mathbf{q}^2}\,, \tag{248}$$

where

$$\alpha_s(\mathbf{q}^2) = \sum_{k=1}^{3} \alpha_k\, e^{-\mathbf{q}^2/(4\gamma_k^2)}\,, \tag{249}$$

we define

$$V_v(\mathbf{q}^2,\epsilon) = -\frac{4}{3}\left(\sum_{k=1}^{3}\alpha_k\, e^{-\mathbf{q}^2/(4\gamma_k^2)}\right)\left(\frac{4\pi}{\mathbf{q}^2+\epsilon^2}\right). \tag{250}$$

By this definition,

$$V_v(\mathbf{q}^2) \;=\; V_v(\mathbf{q}^2,\epsilon=0)\,, \tag{251}$$

and,

$$\frac{d\,V_v(\mathbf{q}^2,\epsilon)}{d\,\mathbf{q}^2} = -\frac{16\pi}{3}\sum_{k=1}^{3}\alpha_k\; e^{-\mathbf{q}^2/(4\gamma_k^2)}\left(-\frac{1}{4\gamma_k^2}+\frac{d}{d\epsilon^2}\right)\left(\frac{1}{\mathbf{q}^2+\epsilon^2}\right), \tag{252}$$

where we have used

$$\frac{d}{d\,\mathbf{q}^2}\left(\frac{1}{\mathbf{q}^2+\epsilon^2}\right) = \frac{d}{d\epsilon^2}\left(\frac{1}{\mathbf{q}^2+\epsilon^2}\right)\,. \tag{253}$$

Define $F_{\rm VR}(\mathbf{r},\epsilon)$ as the Fourier transform of $dV_v(\mathbf{q}^2,\epsilon)/d\mathbf{q}^2$,

$$F_{\rm VR}(\mathbf{r},\epsilon) = \int \frac{d^3q}{(2\,\pi)^3}\, e^{-i\mathbf{q}\cdot\mathbf{r}}\,\frac{d\,V_v(\mathbf{q}^2,\epsilon)}{d\mathbf{q}^2}\,. \tag{254}$$

Using (252), this can be written as

$$\begin{aligned} F_{\rm VR}(\mathbf{r},\epsilon) = -\frac{16\pi}{3}\sum_{k=1}^{3}\alpha_k\left(-\frac{1}{4\gamma_k^2}+\frac{d}{d\epsilon^2}\right) \\ \cdot\int\frac{d^3q}{(2\pi)^3}\, e^{-i\mathbf{q}\cdot\mathbf{r}}\, e^{-\mathbf{q}^2/(4\gamma_k^2)}\left(\frac{1}{\mathbf{q}^2+\epsilon^2}\right). \end{aligned} \tag{255}$$

Using

$$\int\frac{\mathrm{d}^3\mathrm{q}}{(2\pi)^3}\,\mathrm{e}^{-i\mathbf{q}\cdot\mathbf{r}}\,\mathrm{e}^{-\mathbf{q}^2/(4\gamma_k^2)}\left(\frac{1}{\mathbf{q}^2+\epsilon^2}\right) = \frac{1}{2\pi^2\mathrm{r}}\int_0^\infty \mathrm{dq}\,\frac{\mathrm{q}\sin(\mathrm{qr})}{\mathbf{q}^2+\epsilon^2}\,\mathrm{e}^{-\mathbf{q}^2/(4\gamma_k^2)}\,, \tag{256}$$

and [74]

$$\int_0^\infty dq \frac{q\sin(qr)}{q^2+\epsilon^2} e^{-q^2/(4\gamma_k^2)}$$
$$= -\frac{\pi}{4} e^{\epsilon^2/(4\gamma_k^2)} \left[e^{\epsilon r} - e^{-\epsilon r} + e^{-\epsilon r}\mathrm{erf}(-) - e^{\epsilon r}\mathrm{erf}(+) \right], \quad (257)$$

where

$$erf(+) = erf\left(\frac{\epsilon}{2\gamma_k} + \gamma_k r\right),$$
$$erf(-) = erf\left(\frac{\epsilon}{2\gamma_k} - \gamma_k r\right), \quad (258)$$

(255) becomes

$$\mathrm{F_{VR}(r,\epsilon)} = \mathrm{F_{VR}(r,\epsilon)}$$
$$= \frac{1}{3\epsilon}\sum_{k=1}^{3} \alpha_k\, e^{\epsilon^2/(4\gamma_k^2)} \left[e^{\epsilon r} + e^{-\epsilon r} - e^{-\epsilon r}\mathrm{erf}(-) - e^{\epsilon r}\mathrm{erf}(+) \right]$$
$$+ \frac{1}{3\epsilon\sqrt{\pi}\,r}\sum_{k=1}^{3} \frac{\alpha_k}{\gamma_k}\, e^{\epsilon^2/(4\gamma_k^2)} \left[e^{-\epsilon r}\exp(-) - e^{\epsilon r}\exp(+) \right]$$
$$+ \frac{2\alpha}{3\epsilon} e^{-\epsilon r}, \quad (259)$$

where

$$exp(+) = e^{-\left(\frac{\epsilon}{2\gamma_k} + \gamma_k r\right)^2},$$
$$exp(-) = e^{-\left(\frac{\epsilon}{2\gamma_k} - \gamma_k r\right)^2}. \quad (260)$$

We can therefore find

$$\frac{d^i F_{\mathrm{VR}}(r)}{dr^i} = \lim_{\epsilon\to 0} \frac{d^i F_{\mathrm{VR}}(r,\epsilon)}{dr^i}, \quad (261)$$

and $H_{\mathrm{VR}}(\mathbf{r})$ can be obtained from (246).

(*b*) $H_{\mathrm{SR}}(\mathbf{r})$, $H_{\mathrm{R}}(\mathbf{r})$ for scalar potential $V_s(r)$

Define

$$V_s(r,\epsilon) = (b\,r + c)\, e^{-\epsilon r}, \quad (262)$$
$$V_c(r,\epsilon) = \frac{1}{r}\, e^{-\epsilon r}, \quad (263)$$

and denote $V_s(\mathbf{q}^2,\epsilon)$, $V_c(\mathbf{q}^2,\epsilon)$ as the Fourier transformation of $V_s(r,\epsilon)$, $V_c(r,\epsilon)$. Therefore,

$$V_s(r,\epsilon) = \left(b\,\frac{d^2}{d\epsilon^2} - c\frac{d}{d\epsilon}\right) V_c(r,\epsilon)\,, \tag{264}$$

$$V_s(\mathbf{q}^2,\epsilon) = \left(b\,\frac{d^2}{d\epsilon^2} - c\frac{d}{d\epsilon}\right) V_c(\mathbf{q}^2,\epsilon)\,, \tag{265}$$

$$\frac{dV_s(\mathbf{q}^2,\epsilon)}{d\mathbf{q}^2} = \left(b\frac{d^2}{d\epsilon^2} - c\frac{d}{d\epsilon}\right)\frac{dV_c(\mathbf{q}^2,\epsilon)}{d\mathbf{q}^2}\,, \tag{266}$$

$$F_{SR}(\mathbf{r},\epsilon) = \left(b\frac{d^2}{d\epsilon^2} - c\frac{d}{d\epsilon}\right) F_{CR}(\mathbf{r},\epsilon)\,, \tag{267}$$

where $F_{SR}(\mathbf{r},\epsilon)$ and $F_{CR}(\mathbf{r},\epsilon)$ are the Fourier transform of $dV_s(\mathbf{q}^2,\epsilon)/d\mathbf{q}^2$ and $dV_c(\mathbf{q}^2,\epsilon)/d\mathbf{q}^2$ respectively. Making Fourier transformation of (263), we have

$$V_c(\mathbf{q}^2,\epsilon) = \int d^3r\, e^{i\mathbf{q}\cdot\mathbf{r}}\frac{1}{r}e^{-\epsilon r} = \frac{4\pi}{\mathbf{q}^2+\epsilon}. \tag{268}$$

This gives,

$$\frac{dV_c(\mathbf{q}^2,\epsilon)}{d\mathbf{q}^2} = \frac{dV_c(\mathbf{q}^2,\epsilon)}{d\epsilon^2} = \int d^3r\, e^{i\mathbf{q}\cdot\mathbf{r}}\frac{d}{d\epsilon^2}\left(\frac{1}{r}e^{-\epsilon r}\right)\,. \tag{269}$$

We therefore have

$$F_{CR}(\mathbf{r},\epsilon) = \frac{d}{d\epsilon^2}\left(\frac{1}{r}e^{-\epsilon r}\right) = -\frac{1}{2\epsilon}e^{-\epsilon r}\,. \tag{270}$$

Putting (270) in (267), we can find $F_{SR}(\mathbf{r},\epsilon)$ as

$$\mathrm{F_{SR}(r,\epsilon)} = \mathrm{F_{SR}(r,\epsilon)} = -\frac{b}{2}\left(\frac{2}{\epsilon^3}+\frac{2r}{\epsilon^2}+\frac{r^2}{\epsilon}\right)e^{-\epsilon r} - \frac{c}{2}\left(\frac{r}{\epsilon}+\frac{1}{\epsilon^2}\right)e^{-\epsilon r}\,. \tag{271}$$

We can therefore find

$$\frac{d^i F_{SR}(r)}{dr^i} = \lim_{\epsilon\to 0}\frac{d^i F_{SR}(r,\epsilon)}{dr^i}\,, \tag{272}$$

and $H_{SR}(\mathbf{r})$ can be obtained from (246).

Appendix F

Other Quasipotential Equations

To compare the results from the spectator or Gross equation, we have investigated two other quasipotential equations. They are the Wallace-Mandelzweig [62] and the Cooper-Jennings [63] equations.

F.1 The Wallace-Mandelzweig Equation

In the center of mass frame (CM frame) of the quark and antiquark, the Wallace-Mandelzweig propagator [62] is

$$G^{(WM)}(k;P) = (-2\pi i)\,\delta\left(k^0 - \frac{m_1^2 - m_2^2}{2W}\right)\hat{g}^{(WM)}(k;P)\,, \tag{273}$$

where

$$\begin{aligned}\hat{g}^{(WM)}(k;P) = \frac{m_1 m_2}{E(\mathbf{k}_1,m_1)\,E(\mathbf{k}_2,m_2)} \\ \times\left\{\frac{\Lambda^{+(1)}\Lambda^{+(2)}}{\varepsilon_1+\varepsilon_2-E(\mathbf{k}_1,m_1)-E(\mathbf{k}_2,m_2)}\right. \\ +\frac{\Lambda^{+(1)}\Lambda^{-(2)}}{\varepsilon_1-\varepsilon_2-E(\mathbf{k}_1,m_1)-E(\mathbf{k}_2,m_2)} \\ +\frac{\Lambda^{-(1)}\Lambda^{+(2)}}{-\varepsilon_1+\varepsilon_2-E(\mathbf{k}_1,m_1)-E(\mathbf{k}_2,m_2)} \\ \left.+\frac{\Lambda^{-(1)}\Lambda^{-(2)}}{-\varepsilon_1-\varepsilon_2-E(\mathbf{k}_1,m_1)-E(\mathbf{k}_2,m_2)}\right\}\end{aligned} \tag{274}$$

where $\varepsilon_1+\varepsilon_2=W$, $\varepsilon_1-\varepsilon_2=(m_1^2-m_2^2)/W$ and $\Lambda^{\pm(i)}$ are positive- and negative-energy projection operators,

$$\Lambda^{+(i)}=\frac{\mathrm{E(k_i,m_i)}\gamma^{(i)0}-\gamma^{(i)}\cdot\mathrm{k_i}+\mathrm{m_i}}{2\mathrm{m_i}}=\sum_{m'_{s_i}}\mathrm{u}^{(i)}(\mathrm{k_i},m'_{s_i})\bar{\mathrm{u}}^{(i)}(\mathrm{k_i},m'_{s_i}), \tag{275}$$

$$\Lambda^{-(i)}=\frac{-\mathrm{E(k_i,m_i)}\gamma^{(i)0}-\gamma^{(i)}\cdot\mathrm{k_i}+\mathrm{m_i}}{2\mathrm{m_i}}=-\sum_{m'_{s_i}}\mathrm{v}^{(i)}(-\mathrm{k_i},m'_{s_i})\bar{\mathrm{v}}^{(i)}(-\mathrm{k_i},m'_{s_i}), \tag{276}$$

The three-dimensional Wallace-Mandelzweig equation for the vertex function in the CM frame is

$$\Gamma(\check{p};P)=\int\frac{d^3k}{(2\pi)^3}V(\check{p},\check{k};P)\,\hat{g}^{(WM)}(\check{k};P)\,\Gamma(\check{k};P), \tag{277}$$

where $\check{p}$ and $\check{k}$ indicate that the constraint of $p^0=k^0=(m_1^2-m_2^2)/(2W)$, has been imposed on p and k.

F.1.1 $Q\bar{q}$ and $q\bar{Q}$ Mesons

For $Q\bar{q}$ and $q\bar{Q}$ mesons with $m_1=m_q$, $m_2=m_Q$, we expand $\Lambda^{\pm(2)}$ by (275) and (276) and then multiply the resulting Wallace-Mandelzweig equation for the vertex function from the left respectively by $\sqrt{m_2/E(\mathbf{p_2},m_2)}\,\lambda_+(\check{p})\,\bar{u}^{(2)}(\mathbf{p_2},m_{s_2})$ and $\sqrt{m_2/E(\mathbf{p_2},m_2)}\,\lambda_-(\check{p})\,\bar{v}^{(2)}(-\mathbf{p_2},m_{s_2})$, where

$$\lambda_+(\check{p})=\left\{\frac{\varepsilon_2-E(\mathbf{p_1},m_1)-E(\mathbf{p_2},m_2)}{E(\mathbf{p_1},m_1)\left[\varepsilon_1^2-\left(\varepsilon_2-E(\mathbf{p_1},m_1)-E(\mathbf{p_2},m_2)\right)^2\right]}\right\}\cdot\left(\frac{-E(\mathbf{p_1},m_1)\,\varepsilon_1\,\gamma^{(1)0}}{\varepsilon_2-E(\mathbf{p_1},m_1)-E(\mathbf{p_2},m_2)}-\gamma^{(1)}\cdot\mathbf{p_1}+m_1\right), \tag{278}$$

$$\lambda_-(\check{p})=\left\{\frac{\varepsilon_2+E(\mathbf{p_1},m_1)+E(\mathbf{p_2},m_2)}{E(\mathbf{p_1},m_1)\left[\varepsilon_1^2-\left(\varepsilon_2+E(\mathbf{p_1},m_1)+E(\mathbf{p_2},m_2)\right)^2\right]}\right\}\cdot\left(\frac{E(\mathbf{p_1},m_1)\,\varepsilon_1\,\gamma^{(1)0}}{\varepsilon_2+E(\mathbf{p_1},m_1)+E(\mathbf{p_2},m_2)}-\gamma^{(1)}\cdot\mathbf{p_1}+m_1\right). \tag{279}$$

As a result, we obtain a pair of coupled equations

$$\lambda_+^{-1}(\check{p})\,\Psi^{(+)}_{m_{s_2}}(\check{p},P) = -\sum_{m'_{s_2}}\int\frac{d^3k}{(2\pi)^3}\left[U^{++}_{m_{s_2}m'_{s_2}}\,\Psi^{(+)}_{m'_{s_2}} + U^{+-}_{m_{s_2}m'_{s_2}}\,\Psi^{(-)}_{m'_{s_2}}\right], \quad (280)$$

$$\lambda_-^{-1}(\check{p})\,\Psi^{(-)}_{m_{s_2}}(\check{p},P) = -\sum_{m'_{s_2}}\int\frac{d^3k}{(2\pi)^3}\left[U^{-+}_{m_{s_2}m'_{s_2}}\,\Psi^{(+)}_{m'_{s_2}} + U^{--}_{m_{s_2}m'_{s_2}}\,\Psi^{(-)}_{m'_{s_2}}\right], \quad (281)$$

where

$$\Psi^{(+)}_{m'_{s_2}} = \Psi^{(+)}_{m'_{s_2}}(\check{k},P) = \left(\frac{m_2}{E(\mathbf{k}_2,m_2)}\right)^{1/2}\lambda_+(\check{k})\,\bar{u}^{(2)}(\mathbf{k}_2,m'_{s_2})\,\Gamma(\check{k};P), \quad (282)$$

$$\Psi^{(-)}_{m'_{s_2}} = \Psi^{(-)}_{m'_{s_2}}(\check{k},P) = \left(\frac{m_2}{E(\mathbf{k}_2,m_2)}\right)^{1/2}\lambda_-(\check{k})\,\bar{v}^{(2)}(-\mathbf{k}_2,m'_{s_2})\,\Gamma(\check{k};P), \quad (283)$$

and

$$U^{++}_{m_{s_2}m'_{s_2}} = U^{++}_{m_{s_2}m'_{s_2}}(\check{p},\check{k};P)$$
$$= \left(m_2\Big/\sqrt{E(\mathbf{p}_2,m_2)E(\mathbf{k}_2,m_2)}\right)\bar{u}^{(2)}(\mathbf{p}_2,m_{s_2})\,V(\check{p},\check{k};P)\,u^{(2)}(\mathbf{k}_2,m'_{s_2}), \quad (284)$$

$$U^{+-}_{m_{s_2}m'_{s_2}} = U^{+-}_{m_{s_2}m'_{s_2}}(\check{p},\check{k};P)$$
$$= \left(m_2\Big/\sqrt{E(\mathbf{p}_2,m_2)E(\mathbf{k}_2,m_2)}\right)\bar{u}^{(2)}(\mathbf{p}_2,m_{s_2})\,V(\check{p},\check{k};P)\,v^{(2)}(-\mathbf{k}_2,m'_{s_2}), \quad (285)$$

$$U^{-+}_{m_{s_2}m'_{s_2}} = U^{-+}_{m_{s_2}m'_{s_2}}(\check{p},\check{k};P)$$
$$= \left(m_2\Big/\sqrt{E(\mathbf{p}_2,m_2)E(\mathbf{k}_2,m_2)}\right)\bar{v}^{(2)}(-\mathbf{p}_2,m_{s_2})\,V(\check{p},\check{k};P)\,u^{(2)}(\mathbf{k}_2,m'_{s_2}), \quad (286)$$

$$U^{--}_{m_{s_2}m'_{s_2}} = U^{--}_{m_{s_2}m'_{s_2}}(\check{p},\check{k};P)$$
$$= \left(m_2\Big/\sqrt{E(\mathbf{p}_2,m_2)E(\mathbf{k}_2,m_2)}\right)\bar{v}^{(2)}(-\mathbf{p}_2,m_{s_2})\,V(\check{p},\check{k};P)\,v^{(2)}(-\mathbf{k}_2,m'_{s_2}), \quad (287)$$

Using (12) for the kernel $V(\check{p},\check{k};P)$ and the explicit form of the Dirac spinors defined in Appendix A, U^{++}, U^{+-}, U^{-+} and U^{--} can be reduced to the Pauli spin space of particle 2 and expanded in powers of $1/m_2$. Keeping to the order of $1/m_2$,

$$U^{++}_{m_{s_2}m'_{s_2}} = \chi^{\dagger}_{m_{s_2}}\left[V_s(\mathbf{q}^2) + \gamma^{(1)^0}V_v(\mathbf{q}^2)\right.$$
$$\left.-\frac{V_v(\mathbf{q}^2)}{2m_2}\gamma^{(1)}\cdot\left(\boldsymbol{\sigma}^{(2)}\cdot\mathbf{p}_2\,\boldsymbol{\sigma}^{(2)} + \boldsymbol{\sigma}^{(2)}\,\boldsymbol{\sigma}^{(2)}\cdot\mathbf{k}_2\right)\right]\chi_{m'_{s_2}}, \quad (288)$$

$$U^{+-}_{m_{s_2}m'_{s_2}} = \chi^{\dagger}_{m_{s_2}}\left[-\gamma^{(1)}\cdot\sigma^{(2)}V_v(\mathbf{q}^2)+\frac{V_s(\mathbf{q}^2)}{2m_2}(-\sigma^{(2)}\cdot\mathbf{p}_2-\sigma^{(2)}\cdot\mathbf{k}_2)\right.$$
$$\left.+\frac{V_v(\mathbf{q}^2)}{2m_2}\gamma^{(1)^0}(\sigma^{(2)}\cdot\mathbf{p}_2-\sigma^{(2)}\cdot\mathbf{k}_2)\right]\chi_{-m'_{s_2}}, \tag{289}$$

$$U^{-+}_{m_{s_2}m'_{s_2}} = \chi^{\dagger}_{-m_{s_2}}\left[-\gamma^{(1)}\cdot\sigma^{(2)}V_v(\mathbf{q}^2)+\frac{V_s(\mathbf{q}^2)}{2m_2}(-\sigma^{(2)}\cdot\mathbf{p}_2-\sigma^{(2)}\cdot\mathbf{k}_2)\right.$$
$$\left.+\frac{V_v(\mathbf{q}^2)}{2m_2}\gamma^{(1)^0}(-\sigma^{(2)}\cdot\mathbf{p}_2+\sigma^{(2)}\cdot\mathbf{k}_2)\right]\chi_{m'_{s_2}}, \tag{290}$$

$$U^{--}_{m_{s_2}m'_{s_2}} = \chi^{\dagger}_{-m_{s_2}}\left[-V_s(\mathbf{q}^2)+\gamma^{(1)^0}V_v(\mathbf{q}^2)\right.$$
$$\left.+\frac{V_v(\mathbf{q}^2)}{2m_2}\gamma^{(1)}\cdot\left(\sigma^{(2)}\cdot\mathbf{p}_2\,\sigma^{(2)}+\sigma^{(2)}\sigma^{(2)}\cdot\mathbf{k}_2\right)\right]\chi_{-m'_{s_2}}, \tag{291}$$

By the same technique we used in Appendix D, the coupled equations (280) and (281) can be reduced to one equation. Keeping to the order of $1/m_2$, the wave equation is

$$\left\{\gamma^{(1)^0}\left(W-m_2\right)-\gamma^{(1)}\cdot\mathbf{p}-m_1\right.$$
$$\left.-\frac{1}{2m_2}\left[\gamma^{(1)^0}\omega_1+\omega_2(\mathbf{p})\left(\gamma^{(1)}\cdot\mathbf{p}+m_1\right)\right]\right\}\Psi(\mathbf{p})$$
$$=\int\frac{d^3k}{(2\pi)^3}U(\mathbf{p},\mathbf{k})\,\Psi(\mathbf{k})$$
$$-\int\frac{d^3k}{(2\pi)^3}\frac{d^3k'}{(2\pi)^3}\frac{1}{2m_2E(\mathbf{k}_1,m_1)}\tilde{U}(\mathbf{p},\mathbf{k},\mathbf{k}')\,\Psi(\mathbf{k}')\,, \tag{292}$$

where $U(\mathbf{p},\mathbf{k})$ is determined by (85) which is the potential derived from the spectator equation for $Q\bar{q}$, $q\bar{Q}$ mesons, and

$$\mathbf{q}'=\mathbf{k}'-\mathbf{k},$$
$$\omega_1=\left(W-m_2\right)^2-m_1^2,$$
$$\omega_2(\mathbf{p})=E(\mathbf{p},m_1)-\frac{\left(W-m_2\right)^2}{E(\mathbf{p},m_1)},$$
$$\tilde{U}(\mathbf{p},\mathbf{k},\mathbf{k}')=V_v(\mathbf{q}^2)\,V_v(\mathbf{q}'^2)\left(\gamma^{(1)}\cdot\sigma^{(2)}\right)\left(\gamma^{(1)}\cdot\mathbf{k}-m_1\right)\left(\gamma^{(1)}\cdot\sigma^{(2)}\right).$$

We can see that as $m_2\to\infty$, (292) is reduced to the one-body Dirac equation for particle 1 with the potential $U(\mathbf{p},\mathbf{k})$ which is the same as that derived from the

Gross equation. However, when contribution to the order of $1/m_2$ is considered, the equation becomes difficult to solve.

F.1.2 $Q\bar{Q}$ Mesons

For $Q\bar{Q}$ mesons, we expand both $\Lambda^{\pm(1)}$ and $\Lambda^{\pm(2)}$ by (275) and (276) and then multiply the resulting Wallace-Mandelzweig equation for the vertex function from the left respectively by

$$\sqrt{m_1 m_2 \Big/ \Big[E(\mathbf{p}_1, m_1)\, E(\mathbf{p}_2, m_2)\Big]}\ \bar{u}^{(1)}(\mathbf{p}_1, m_{s_1})\, \bar{u}^{(2)}(\mathbf{p}_2, m_{s_2}),$$

$$\sqrt{m_1 m_2 \Big/ \Big[E(\mathbf{p}_1, m_1)\, E(\mathbf{p}_2, m_2)\Big]}\ \bar{u}^{(1)}(\mathbf{p}_1, m_{s_1})\, \bar{v}^{(2)}(-\mathbf{p}_2, m_{s_2}),$$

$$\sqrt{m_1 m_2 \Big/ \Big[E(\mathbf{p}_1, m_1)\, E(\mathbf{p}_2, m_2)\Big]}\ \bar{v}^{(1)}(-\mathbf{p}_1, m_{s_1})\, \bar{u}^{(2)}(\mathbf{p}_2, m_{s_2}),$$

$$\sqrt{m_1 m_2 \Big/ \Big[E(\mathbf{p}_1, m_1)\, E(\mathbf{p}_2, m_2)\Big]}\ \bar{v}^{(1)}(-\mathbf{p}_1, m_{s_1})\, \bar{v}^{(2)}(-\mathbf{p}_2, m_{s_2}).$$

As a result, we obtain four equations

$$\Big[W - E(\mathbf{p}_1, m_1) - E(\mathbf{p}_2, m_2)\Big]\ \Psi^{++}_{m_{s_1} m_{s_2}}(\check{p}, P)$$
$$= \int \Big(U^{++,++}\, \Psi^{++} + U^{++,+-}\, \Psi^{+-} + U^{++,-+}\, \Psi^{-+} + U^{++,--}\, \Psi^{--} \Big), \quad (293)$$

$$\Big\{ \Big[(m_1^2 - m_2^2)\,/\,W\Big] - E(\mathbf{p}_1, m_1) - E(\mathbf{p}_2, m_2) \Big\}\ \Psi^{+-}_{m_{s_1} m_{s_2}}(\check{p}, P)$$
$$= - \int \Big(U^{+-,++}\, \Psi^{++} + U^{+-,+-}\, \Psi^{+-} + U^{+-,-+}\, \Psi^{-+} + U^{+-,--}\, \Psi^{--} \Big), \quad (294)$$

$$\Big\{ - \Big[(m_1^2 - m_2^2)\,/\,W\Big] - E(\mathbf{p}_1, m_1) - E(\mathbf{p}_2, m_2) \Big\}\ \Psi^{-+}_{m_{s_1} m_{s_2}}(\check{p}, P)$$
$$= - \int \Big(U^{-+,++}\, \Psi^{++} + U^{-+,+-}\, \Psi^{+-} + U^{-+,-+}\, \Psi^{-+} + U^{-+,--}\, \Psi^{--} \Big), \quad (295)$$

$$\Big[- W - E(\mathbf{p}_1, m_1) - E(\mathbf{p}_2, m_2) \Big]\ \Psi^{--}_{m_{s_1} m_{s_2}}(\check{p}, P)$$

$$= \int \left(U^{--,++}\,\Psi^{++} + U^{--,+-}\,\Psi^{+-} + U^{--,-+}\,\Psi^{-+} + U^{--,--}\,\Psi^{--} \right), \quad (296)$$

where

$$\int = \sum_{m'_{s_1}\, m'_{s_2}} \int \frac{\mathrm{d}^3\mathrm{k}}{(2\pi)^3},$$

$$\Psi^{\rho\rho} = \Psi^{\rho\rho}_{m'_{s_1}\, m'_{s_2}}(\check{\mathrm{k}}, \mathrm{P}),$$

$$\Psi^{++}_{m'_{s_1}\, m'_{s_2}}(\check{\mathrm{k}}, \mathrm{P}) = \sqrt{\frac{\mathrm{m_1 m_2}}{\mathrm{E(k_1, m_1) E(k_2, m_2)}}}\, \frac{\bar{\mathrm{u}}^{(1)}(\mathbf{k_1}, m'_{s_1})\, \bar{\mathrm{u}}^{(2)}(\mathbf{k_2}, m'_{s_2})\Gamma(\check{\mathrm{k}}, \mathrm{P})}{\mathrm{W - E(k_1, m_1) - E(k_2, m_2)}},$$

$$\Psi^{+-}_{m'_{s_1}\, m'_{s_2}}(\check{\mathrm{k}}, \mathrm{P}) = \sqrt{\frac{\mathrm{m_1 m_2}}{\mathrm{E(k_1, m_1) E(k_2, m_2)}}}\, \frac{\bar{\mathrm{u}}^{(1)}(\mathbf{k_1}, m'_{s_1})\, \bar{\mathrm{v}}^{(2)}(-\mathbf{k_2}, m'_{s_2})\Gamma(\check{\mathrm{k}}, \mathrm{P})}{\left(\frac{\mathrm{m_1^2 - m_2^2}}{\mathrm{W}}\right) - \mathrm{E(k_1, m_1) - E(k_2, m_2)}},$$

$$\Psi^{-+}_{m'_{s_1}\, m'_{s_2}}(\check{\mathrm{k}}, \mathrm{P}) = \sqrt{\frac{\mathrm{m_1 m_2}}{\mathrm{E(k_1, m_1) E(k_2, m_2)}}}\, \frac{\bar{\mathrm{v}}^{(1)}(-\mathbf{k_1}, m'_{s_1})\, \bar{\mathrm{u}}^{(2)}(\mathbf{k_2}, m'_{s_2})\Gamma(\check{\mathrm{k}}, \mathrm{P})}{\left(\frac{\mathrm{m_2^2 - m_1^2}}{\mathrm{W}}\right) - \mathrm{E(k_1, m_1) - E(k_2, m_2)}},$$

$$\Psi^{--}_{m'_{s_1}\, m'_{s_2}}(\check{\mathrm{k}}, \mathrm{P}) = \sqrt{\frac{\mathrm{m_1 m_2}}{\mathrm{E(k_1, m_1) E(k_2, m_2)}}}\, \frac{\bar{\mathrm{v}}^{(1)}(-\mathbf{k_1}, m'_{s_1})\, \bar{\mathrm{v}}^{(2)}(-\mathbf{k_2}, m'_{s_2})\Gamma(\check{\mathrm{k}}, \mathrm{P})}{\mathrm{-W - E(k_1, m_1) - E(k_2, m_2)}},$$

$$\mathrm{U}^{\rho_1\rho_2,\tau_1\tau_2} = \mathrm{U}^{\rho_1\rho_2,\tau_1\tau_2}_{m_{s_1}\, m_{s_2}\, m'_{s_1}\, m'_{s_2}}(\check{\mathrm{p}}, \check{\mathrm{k}}; \mathrm{P})$$

$$= (\rho_1\, \rho_2\, \tau_1\, \tau_2)\, (\mathrm{m_1\, m_2}) \Big/ \sqrt{\mathrm{E(p_1, m_1)\, E(p_2, m_2)\, E(k_1, m_1)\, E(k_2, m_2)}}$$

$$\bar{\varphi}^{(\rho_1)}(\mathbf{p_1}, m_{s_1})\, \bar{\varphi}^{(\rho_2)}(\mathbf{p_2}, m_{s_2})\, \mathrm{V}(\check{\mathrm{p}}, \check{\mathrm{k}}; \mathrm{P})\, \varphi^{(\tau_1)}(\mathbf{k_1}, m'_{s_1})\, \varphi^{(\tau_2)}(\mathbf{k_2}, m'_{s_2}), \quad (297)$$

with $\rho_1,\ \rho_2,\ \tau_1,\ \tau_2 = +, -$; $\varphi^{(+)}(\mathbf{p}, m_s) = u(\mathbf{p}, m_s)$; $\varphi^{(-)}(\mathbf{p}, m_s) = v(-\mathbf{p}, m_s)$.

Using the same method as in the $Q\bar{q}$ and $q\bar{Q}$ sector, $U^{\rho_1\rho_2,\tau_1\tau_2}$ can be reduced to the Pauli spin space and the four equations can be reduced to one. When keeping only to the order of $1/(m_i m_j)$, this equation is

$$\left(W - m_1 - m_2 - \frac{\mathbf{p}^2}{2m_1} - \frac{\mathbf{p}^2}{2m_2}\right) \Psi(\mathbf{p})$$

$$= \int \frac{d^3k}{(2\pi)^3}\, V^{(WM)}(\mathbf{p}, \mathbf{k})\, \Psi(\mathbf{k})$$

$$- \int \frac{d^3k}{(2\pi)^3} \frac{d^3k'}{(2\pi)^3} \left(3 - 2\boldsymbol{\sigma}^{(1)} \cdot \boldsymbol{\sigma}^{(2)}\right) \frac{V_s(\mathbf{q}^2)\, V_v(\mathbf{q}'^2)}{W + m_1 + m_2}\, \Psi(\mathbf{k}')$$

$$+\int \frac{d^3k}{(2\pi)^3}\frac{d^3k'}{(2\pi)^3}\frac{d^3k''}{(2\pi)^3}\left(3-2\boldsymbol{\sigma}^{(1)}\cdot\boldsymbol{\sigma}^{(2)}\right)$$
$$\times\frac{V_v(\mathbf{q}^2)\left[V_s(\mathbf{q}'^2)+V_v(\mathbf{q}'^2)\right]V_v(\mathbf{q}''^2)}{(W+m_1+m_2)^2}\,\Psi(\mathbf{k}''), \qquad (298)$$

where we have used the relation $(\boldsymbol{\sigma}^{(1)}\cdot\boldsymbol{\sigma}^{(2)})(\boldsymbol{\sigma}^{(1)}\cdot\boldsymbol{\sigma}^{(2)}) = 3-2\boldsymbol{\sigma}^{(1)}\cdot\boldsymbol{\sigma}^{(2)}$. In this equation,

$$\mathbf{q}'' = \mathbf{k}'' - \mathbf{k}'$$
$$V^{(WM)}(\mathbf{p},\mathbf{k}) = \mathcal{U}(\mathbf{p},\mathbf{k}) + \frac{1}{4m_2^2}\left[V_s'(\mathbf{q}^2)+V_v'(\mathbf{q}^2)\right]\left(\mathbf{p}^2-\mathbf{k}^2\right)^2, \qquad (299)$$

where $\mathcal{U}(\mathbf{p},\mathbf{k})$ is determined by (123) which is the potential derived from the spectator equation for $Q\bar{Q}$ mesons.

Comparing to the result from the spectator equation (122), (298) gives rise to $1/m_Q$ order of spin-spin interaction which contradicts to experiments. In addition, (298) does not give the retardation effects.

F.2 The Cooper-Jennings Equation

In the CM frame of the quark and antiquark, the Cooper-Jennings propagator [63] is

$$G^{(CJ)}(k;P) = (-2\pi i)\,\delta\left(k^0 - \frac{m_1^2-m_2^2}{2W}\right)\hat{g}^{(CJ)}(k;P), \qquad (300)$$

where

$$\hat{g}^{(CJ)}(k;P) = \left(\frac{2W^2}{E(\mathbf{k}_1,m_1)+E(\mathbf{k}_2,m_2)}\right)$$
$$\times\left\{W^2-\left[E(\mathbf{k}_1,m_1)+E(\mathbf{k}_2,m_2)\right]^2\right\}^{-1}$$
$$\times\left\{W^2-\left[E(\mathbf{k}_1,m_1)-E(\mathbf{k}_2,m_2)\right]^2\right\}^{-1}$$
$$\times\left(\frac{\tilde{k}_1^{0^2}-E^2(\mathbf{k}_1,m_1)}{\left(\gamma^{(1)}\cdot\tilde{k}_1-m_1\right)}\right)\left(\frac{\tilde{k}_2^{0^2}-E^2(\mathbf{k}_2,m_2)}{\left(\gamma^{(2)}\cdot\tilde{k}_2-m_2\right)}\right), \qquad (301)$$

with

$$\tilde{k}_i = \left(\tilde{k}_i^0,\ \mathbf{k_i}\right),$$

$$\tilde{k}_1^0 = \frac{W^2 + m_1^2 - m_2^2}{2W^2}\left[E(\mathbf{k}_1, m_1) + E(\mathbf{k}_2, m_2)\right], \tag{302}$$

$$\tilde{k}_2^0 = \frac{W^2 - m_1^2 + m_2^2}{2W^2}\left[E(\mathbf{k}_1, m_1) + E(\mathbf{k}_2, m_2)\right]. \tag{303}$$

Note that $\left(\gamma^{(i)} \cdot \tilde{k}_i - m_i\right)^{-1}$ can be decomposed in terms of Dirac spinors by

$$\frac{1}{\left(\gamma^{(i)} \cdot \tilde{k}_i - m_i\right)} = \frac{m_i}{E(\mathbf{k_i}, m_i)} \sum_{m'_{s_i}} \left(\frac{u^{(i)}(\mathbf{k_i}, m'_{s_i})\bar{u}^{(i)}(\mathbf{k_i}, m'_{s_i})}{\tilde{k}_i^0 - E(\mathbf{k_i}, m_i)} + \frac{v^{(i)}(-\mathbf{k_i}, m'_{s_i})\bar{v}^{(i)}(-\mathbf{k_i}, m'_{s_i})}{\tilde{k}_i^0 + E(\mathbf{k_i}, m_i)} \right). \tag{304}$$

The three dimensional Cooper-Jennings equation for the vertex function is

$$\Gamma(\check{p}; P) = \int \frac{d^3k}{(2\pi)^3} V(\check{p}, \check{k}; P)\, \hat{g}^{(CJ)}(\check{k}; P)\, \Gamma(\check{k}; P), \tag{305}$$

This equation was specificaly constructed to agree with the Blankenbecler-Sugar equation in the equal mass limit and also have the one-body limit for the unequal mass systems.

The procedures for solving this Cooper-Jennings equation are the same as those in solving the Wallace-Mandelzweig equation. Here, we expand $\left(\gamma^{(i)} \cdot \tilde{k}_i - m_i\right)^{-1}$ in terms of (304) and multiply (305) by certain factors. This results in a pair of coupled equations in the $Q\bar{q}$, $q\bar{Q}$ sector and a set of four equations in the $Q\bar{Q}$ sector. Solving these two sets of equation leads to a single wave equation for each sector respectively.

F.2.1 $Q\bar{q}$ and $q\bar{Q}$ Mesons

To get the coupled equations in this sector, we multiply (305) from the left by

$$\sqrt{m_2/E(\mathbf{p_2}, m_2)}\,\bar{u}^{(2)}(\mathbf{p_2}, m_{s_2}),$$

$$\sqrt{m_2/E(\mathbf{p_2}, m_2)}\,\bar{v}^{(2)}(-\mathbf{p_2}, m_{s_2}),$$

respectively. We define the wave functions as

$$\Psi^{(+)}_{m_{s_2}}(\tilde{p},P)$$
$$= \left(\frac{\bar{u}^{(2)}(\mathbf{p_2},m_{s_2})\,\Gamma(\tilde{p};P)}{\gamma^{(1)}\cdot\tilde{p}_1-m_1}\right)\cdot\left(\frac{m_2}{E(\mathbf{p_2},m_2)}\right)^{1/2}\cdot\left(\frac{2W^2}{E(\mathbf{p_1},m_1)+E(\mathbf{p_2},m_2)}\right)$$
$$\times\frac{\left(\tilde{p}_1^0-E(\mathbf{p_1},m_1)\right)\left(\tilde{p}_1^0+E(\mathbf{p_1},m_1)\right)\left(\tilde{p}_2^0+E(\mathbf{p_2},m_2)\right)}{\left(W^2-\left[E(\mathbf{p_1},m_1)+E(\mathbf{p_2},m_2)\right]^2\right)\left(W^2-\left[E(\mathbf{p_1},m_1)-E(\mathbf{p_2},m_2)\right]^2\right)},$$

$$\Psi^{(-)}_{m_{s_2}}(\tilde{p},P)$$
$$= \left(\frac{\bar{v}^{(2)}(-\mathbf{p_2},m_{s_2})\,\Gamma(\tilde{p};P)}{\gamma^{(1)}\cdot\tilde{p}_1-m_1}\right)\cdot\left(\frac{m_2}{E(\mathbf{p_2},m_2)}\right)^{1/2}\cdot\left(\frac{2W^2}{E(\mathbf{p_1},m_1)+E(\mathbf{p_2},m_2)}\right)$$
$$\times\frac{\left(\tilde{p}_1^0-E(\mathbf{p_1},m_1)\right)\left(\tilde{p}_1^0+E(\mathbf{p_1},m_1)\right)\left(\tilde{p}_2^0-E(\mathbf{p_2},m_2)\right)}{\left(W^2-\left[E(\mathbf{p_1},m_1)+E(\mathbf{p_2},m_2)\right]^2\right)\left(W^2-\left[E(\mathbf{p_1},m_1)-E(\mathbf{p_2},m_2)\right]^2\right)}.$$

Keeping only to the order of $1/m_2$, the wave equation in momentum space is

$$\begin{aligned}
&\left\{\gamma^{(1)^0}\left(W-m_2\right)-\boldsymbol{\gamma}^{(1)}\cdot\mathbf{p}-m_1\right.\\
&\left.+\frac{1}{2m_2}\left[\gamma^{(1)^0}\varpi_1-\varpi_2(\mathbf{p})\left(\boldsymbol{\gamma}^{(1)}\cdot\mathbf{p}+m_1\right)\right]\right\}\Psi(\mathbf{p})\\
&=\int\frac{d^3k}{(2\pi)^3}\,U(\mathbf{p},\mathbf{k})\,\Psi(\mathbf{k})\\
&-\int\frac{d^3k}{(2\pi)^3}\,\frac{d^3k'}{(2\pi)^3}\,\frac{1}{2m_2\left[W-m_2+E(\mathbf{k},m_1)\right]}\,\bar{U}(\mathbf{p},\mathbf{k},\mathbf{k}')\,\Psi(\mathbf{k}')\,, \qquad (306)
\end{aligned}$$

where $U(\mathbf{p},\mathbf{k})$ is determined by (85) which is the potential derived from the spectator equation, and

$$\varpi_1 = 3\,E(\mathbf{p},m_1)\left(W-m_2\right)+m_1^2+2\left(W-m_2\right)^2\left(\frac{W-m_2-E(\mathbf{p},m_1)}{W-m_2+E(\mathbf{p},m_1)}\right),$$

$$\varpi_2(\mathbf{p}) = E(\mathbf{p},m_1)+\left(W-m_2\right)\frac{5\left(W-m_2\right)+E(\mathbf{p},m_1)}{W-m_2+E(\mathbf{p},m_1)},$$

$$\begin{aligned}
\bar{U}(\mathbf{p},\mathbf{k},\mathbf{k}') &= V_v(\mathbf{q}^2)\,V_v(\mathbf{q}'^2)\\
&\times\left(\boldsymbol{\gamma}^{(1)}\cdot\boldsymbol{\sigma}^{(2)}\right)\left(\gamma^{(1)^0}(W-m_2)-\boldsymbol{\gamma}^{(1)}\cdot\mathbf{k}+m_1\right)\left(\boldsymbol{\gamma}^{(1)}\cdot\boldsymbol{\sigma}^{(2)}\right).
\end{aligned}$$

One can see that as $m_2 \to \infty$, (306) is reduced to the Dirac equation for particle 1 which is the same as that from Gross equation and that from Wallace-Mandelzweig equation. Similar to Wallace-Mandelzweig equation, to the order of $1/m_2$, this equation is difficult to solve.

F.2.2 $Q\bar{Q}$ Mesons

To get the set of four equations, we multiply (305) from the left respectively by

$$\sqrt{m_1 m_2 \Big/ \Big[E(\mathbf{p}_1, m_1)\, E(\mathbf{p}_2, m_2)\Big]}\ \bar{u}^{(1)}(\mathbf{p}_1, m_{s_1})\, \bar{u}^{(2)}(\mathbf{p}_2, m_{s_2}),$$

$$\sqrt{m_1 m_2 \Big/ \Big[E(\mathbf{p}_1, m_1)\, E(\mathbf{p}_2, m_2)\Big]}\ \bar{u}^{(1)}(\mathbf{p}_1, m_{s_1})\, \bar{v}^{(2)}(-\mathbf{p}_2, m_{s_2}),$$

$$\sqrt{m_1 m_2 \Big/ \Big[E(\mathbf{p}_1, m_1)\, E(\mathbf{p}_2, m_2)\Big]}\ \bar{v}^{(1)}(-\mathbf{p}_1, m_{s_1})\, \bar{u}^{(2)}(\mathbf{p}_2, m_{s_2}),$$

$$\sqrt{m_1 m_2 \Big/ \Big[E(\mathbf{p}_1, m_1)\, E(\mathbf{p}_2, m_2)\Big]}\ \bar{v}^{(1)}(-\mathbf{p}_1, m_{s_1})\, \bar{v}^{(2)}(-\mathbf{p}_2, m_{s_2}).$$

The wave functions are defined as

$$\Psi^{(++)}_{m_{s_2}}(\check{p}, P) = \left(\frac{m_1 m_2}{E(\mathbf{p}_1, m_1)\, E(\mathbf{p}_2, m_2)}\right)^{1/2} \cdot \left(\frac{2W^2}{E(\mathbf{p}_1, m_1) + E(\mathbf{p}_2, m_2)}\right)$$
$$\times \frac{\Big[\tilde{p}_1^0 + E(\mathbf{p}_1, m_1)\Big]\ \Big[\tilde{p}_2^0 + E(\mathbf{p}_2, m_2)\Big]\ \bar{u}^{(1)}(\mathbf{p}_1, m_{s_1})\, \bar{u}^{(2)}(\mathbf{p}_2, m_{s_2})\, \Gamma(\check{p}; P)}{\Big(W^2 - \Big[E(\mathbf{p}_1, m_1) + E(\mathbf{p}_2, m_2)\Big]^2\Big)\ \Big(W^2 - \Big[E(\mathbf{p}_1, m_1) - E(\mathbf{p}_2, m_2)\Big]^2\Big)},$$

$$\Psi^{(+-)}_{m_{s_2}}(\check{p}, P) = \left(\frac{m_1 m_2}{E(\mathbf{p}_1, m_1)\, E(\mathbf{p}_2, m_2)}\right)^{1/2} \cdot \left(\frac{2W^2}{E(\mathbf{p}_1, m_1) + E(\mathbf{p}_2, m_2)}\right)$$
$$\times \frac{\Big[\tilde{p}_1^0 + E(\mathbf{p}_1, m_1)\Big]\ \Big[\tilde{p}_2^0 - E(\mathbf{p}_2, m_2)\Big]\ \bar{u}^{(1)}(\mathbf{p}_1, m_{s_1})\, \bar{v}^{(2)}(-\mathbf{p}_2, m_{s_2})\, \Gamma(\check{p}; P)}{\Big(W^2 - \Big[E(\mathbf{p}_1, m_1) + E(\mathbf{p}_2, m_2)\Big]^2\Big)\ \Big(W^2 - \Big[E(\mathbf{p}_1, m_1) - E(\mathbf{p}_2, m_2)\Big]^2\Big)},$$

$$\Psi^{(-+)}_{m_{s_2}}(\check{p}, P) = \left(\frac{m_1 m_2}{E(\mathbf{p}_1, m_1)\, E(\mathbf{p}_2, m_2)}\right)^{1/2} \cdot \left(\frac{2W^2}{E(\mathbf{p}_1, m_1) + E(\mathbf{p}_2, m_2)}\right)$$

$$\times\frac{\left[\tilde{p}_1^0 - E(\mathbf{p}_1, m_1)\right]\left[\tilde{p}_2^0 + E(\mathbf{p}_2, m_2)\right]\bar{v}^{(1)}(-\mathbf{p}_1, m_{s_1})\,\bar{u}^{(2)}(\mathbf{p}_2, m_{s_2})\,\Gamma(\check{p}; P)}{\left(W^2 - \left[E(\mathbf{p}_1, m_1) + E(\mathbf{p}_2, m_2)\right]^2\right)\left(W^2 - \left[E(\mathbf{p}_1, m_1) - E(\mathbf{p}_2, m_2)\right]^2\right)},$$

$$\Psi^{(--)}_{m_{s_2}}(\check{p}, P) = \left(\frac{m_1 m_2}{E(\mathbf{p}_1, m_1)\,E(\mathbf{p}_2, m_2)}\right)^{1/2} \cdot \left(\frac{2W^2}{E(\mathbf{p}_1, m_1) + E(\mathbf{p}_2, m_2)}\right)$$
$$\times\frac{\left[\tilde{p}_1^0 - E(\mathbf{p}_1, m_1)\right]\left[\tilde{p}_2^0 - E(\mathbf{p}_2, m_2)\right]\bar{v}^{(1)}(-\mathbf{p}_1, m_{s_1})\,\bar{v}^{(2)}(-\mathbf{p}_2, m_{s_2})\,\Gamma(\check{p}; P)}{\left(W^2 - \left[E(\mathbf{p}_1, m_1) + E(\mathbf{p}_2, m_2)\right]^2\right)\left(W^2 - \left[E(\mathbf{p}_1, m_1) - E(\mathbf{p}_2, m_2)\right]^2\right)}.$$

For $m_1 = m_2 = m_Q$ and keeping only to the order of $1/m_Q^2$, the wave equation in momentum space is

$$\left(W - m_1 - m_2 - \frac{\mathbf{p}^2}{2m_1} - \frac{\mathbf{p}^2}{2m_2}\right)\Psi(\mathbf{p}) = \int \frac{d^3k}{(2\pi)^3}\, V^{(CJ)}(\mathbf{p}, \mathbf{k})\,\Psi(\mathbf{k}) \qquad (307)$$

where $V^{(CJ)}(\mathbf{p}, \mathbf{k}) = V^{(WM)}(\mathbf{p}, \mathbf{k})$ determined by (299) .

Note that the difference between $U(\mathbf{p}, \mathbf{k})$, and $V^{(CJ)}(\mathbf{p}, \mathbf{k})$ and $V^{(WM)}(\mathbf{p}, \mathbf{k})$ is the term that results from the retardation Hamiltonian, H_{SR} and H_{VR}. This is not surprising because both of the Cooper-Jennings equation and the Wallace-Mandelzweig equation describe systems with instantaneous interactions. For the case of $m_1 = m_2 = m_Q$, the Cooper-Jennings equation has the same solution as the spectator equation except for the retardation contributions. This is encouraging because the Cooper-Jennings equation in this case agrees with the Blankenbecler-Sugar equation.

F.3 Conclusion

By investigating the Wallace-Mandelzweig equation and the Cooper-Jennings equation, we find the following:

In the $Q\bar{q}$ sector, both the Wallace-Mandelzweig and the Cooper-Jennings equations give the correct one-body limit as does the Gross equation. However, when $1/m_Q$ corrections to this limit are considered, both the Wallace-Mandelzweig and the Cooper-Jennings equations are difficult to solve.

In the $Q\bar{Q}$ sector, the Hamiltonian derived from the Cooper-Jennings equation is the same as that from the Gross equation, to the order of $1/m_Q^2$, except for the retardation effects. The Wallace-Mandelzweig equation produces these same terms along with additional terms that are inconsistent with experiments.

Neither the Wallace-Mandelzweig nor the Cooper-Jennings equation includes the retardation effects since they describe instantaneously interacting systems.

We have, therefore, concluded that the Gross equation is easier to work with and the Hamiltonians derived from it have more reasonable physical interpretations.

Bibliography

[1] F. Gross, Phys. Rev. **186**, 1448 (1969).

[2] G. Zweig, CERN 8182/TH. 401 (1964).

[3] G. Zweig, CERN 8419/TH. 412 (1964).

[4] M. Gell-Mann, Phys. Lett. **8**, 214 (1964).

[5] O. W. Greenberg, Phys. Rev. Lett. **13**, 598 (1964).

[6] *see, for example*, D. H. Perkins, *Introduction to High Energy Physics* (Addison-Wesley, Reading, Massachusetts, 1982), pp. 305–310.

[7] S. L. Adler, Phys. Rev. **177**, 2426 (1969).

[8] J. S. Bell and R. Jackiw, Nuovo Cimento **60A**, 47 (1969).

[9] Review of Particle Properties, Phys. Rev. D 50, 1297 (1994).

[10] *for a review, see*: J. Hamber and G. Parisi, Phys. Rev. D **27**, 208 (1983).

[11] *for a review, see*: L. J. Reinders, J. Rubinstein and S.Yazaki, Phys. Rep. **127**, 1 (1985).

[12] T. Appelquist and J. D. Politzer, Phys. Rev. Lett. **34**, 43 (1975).

[13] A. De Rújula and S. L. Glashow, Phys. Rev. Lett. **34**, 46 (1975).

[14] T. Appelquist et al., Phys. Rev. Lett. **34**, 365 (1975).

[15] C. G. Callan et al., Phys. Rev. Lett. **34**, 52 (1975).

[16] K. G. Wilson, Phys. Rev. D **10**, 2445 (1974).

[17] K. G. Wilson, Phys. Rep. **23C**, 331 (1976).

[18] J. Kogut and L. Susskind, Phys. Rev. D **11**, 395 (1975).

[19] J. Kogut and L. Susskind, Phys. Rev. D **12**, 2821 (1975).

[20] A. De Rújula, H. Georgi, and S. L. Glashow, Phys. Rev. D **12**, 147 (1975).

[21] W. Heisenberg, Z. Phys. **39**, 499 (1926).

[22] G. Breit, Phys. Rev. **36**, 383 (1930).

[23] E. Fermi, Z. Phys. **60**, 320 (1930).

[24] T. Appelquist, R. M. Barnett and K. Lane, Ann. Rev. Nucl. Part. Sci. **28**, 387 (1978).

[25] S. Godfrey and N. Isgur, Phys. Rev. D **32**, 189 (1985).

[26] E. E. Salpeter and H. A. Bethe, Phys. Rev. **84**, 1232 (1951).

[27] D. Gromes, Nucl. Phys. **B131**, 80 (1977).

[28] *see, for example*, M. G. Olsson, S. Veseli and K. Williams , Phys. Rev. D **51**, 5079 (1995).

[29] J. D. Bjorken and S. D. Drell, *Relativisatic Quantum Mechanics* (McGraw-Hill, New York, 1964).

[30] S. L. Glashow, Nucl. Phys. **22**, 579 (1961).

[31] S. Weinberg, Phys. Rev. Lett. **19**, 1264 (1967).

[32] A. Salam, in *Elementary Particle Theory*, edited by N. Svartholm (Almqvist and Wiksell, Stockholm, 1968).

[33] J. L. Rosner, in *B Decays*, Revised 2nd ed., edited by Sheldon Stone (World Scientific, Singapore, 1994), p. 470.

[34] L. B. Okun, *Leptons and Quarks* (North-Holland, Amsterdam · Nwe York · Oxford, 1982), Chap. 2.

[35] M. Kobayashi and K. Maskawa, Prog. Theor. Phys. **49**, 652 (1973).

[36] N. Cabibbo, Phys. Rev. Lett. **10**, 531 (1963).

[37] J. J. Hernández et al. (Particle Data Group), Phys. Lett. **239B**, 1 (1990).

[38] G. Arnison et al. (UA1), Phys. Lett. **122B**, 103 (1983).

[39] M. Banner et al. (UA2), Phys. Lett. **122B**, 476 (1983).

[40] The LEP Collaborations and the LEP Electroweak Working Group, CERN/PPE/94 187 (1994).

[41] M. Demarteau et al., CEF/PHYS/CDF/PUBLIC/2552 and D0 NOTE 2115 .

[42] *see, for review, CP Violation*, edited by C. Jarlskog (World Scientific, Singapore, 1989).

[43] N. Isgur and M. B. Wise, Phys. Lett. **232B**, 113 (1989).

[44] N. Isgur and M. B. Wise, Phys. Lett. **237B**, 527 (1990).

[45] N. Isgur and M. B. Wise, in *B Decays*, Revised 2nd ed., edited by Sheldon Stone (World Scientific, Singapore, 1994), p. 231.

[46] M. Neubert, Phys. Rep. **245**, 259 (1994).

[47] W. Roberts, in *Proceedings of the 14th Physics in Collision Conference at Tallahassee Florida*, edited by S. Keller and J. D. Wahl (Editions Frontieres, France, 1994), p. 295.

[48] Review of Particle Properties, Phys. Rev. D 50 (1994).

[49] F. J. Gilman and R. L. Singleton, Jr., Phys. Rev. D **41**, 142 (1990).

[50] M. E. Luke, Phys. Lett. **252B**, 447 (1990).

[51] N. Isgur, D. Scora, B. Grinstein and M. B. Wise , Phys. Rev. D **39**, 799 (1989).

[52] F. Gross, J. W. Van Orden and K. Holinde, Phys. Rev. C **41**, 1909 (1990).

[53] F. Gross, J. W. Van Orden and K. Holinde, Phys. Rev. C **45**, 2094 (1992).

[54] F. Gross and J. Milana, Phys. Rev. D **43**, 2401 (1991).

[55] F. Gross and J. Milana, Phys. Rev. D **45**, 969 (1992).

[56] F. Gross and J. Milana, CEBAF preprint CEBAF-TH-94-01 (1994).

[57] F. Gross, Phys. Rev. C **26**, 2203 (1982).

[58] A. A. Logunov and A. N. Tavkhelidze, Nuovo Cimento **29**, 380 (1963).

[59] A. A. Logunov et al., Nuovo Cimento **30**, 134 (1963).

[60] V. G. Kadyshevsky, Nucl. Phys. **B6**, 125 (1968).

[61] R. Blankenbecler and R. Sugar, Phys. Rev. **142**, 1051 (1966).

[62] S. J. Wallace and V. B. Mandelzweig, Nucl. Phys. **A503**, 673 (1989).

[63] E. D. Cooper and B. K. Jennings, Nucl. Phys. **A500**, 553 (1989).

[64] G. E. Brown and A. D. Jackson, *The Nucleon-Nucleon Interaction* (North-Holland, Amsterdam · Oxford, 1976), p. 99.

[65] W. W. Buck and F. Gross, Phys. Rev. D **20**, 2361 (1979).

[66] S. N. Mukherjee *et al.*, Phys. Rep. **231**, 201 (1993).

[67] M. G. Olsson and K. J. Miller, Phys. Rev. D **28**, 674 (1983).

[68] H. J. Schnitzer, Phys. Lett. **76B**, 461 (1978).

[69] W. H. Press, B. P. Flannery, S. A. Teukolsky and W. T. Vetterling, *Numerical Recipes, The Art of Scientific Computing* (Cambridge, New York, 1986).

[70] *see, for example*, A. R. Edmonds, *Angular Momentum In Quantum Mechanics* (Princeton University Press, Princeton, New Jersey, 1974), p. 75.

[71] E. P. Wigner, Z. Physik **43**, 624 (1927).

[72] C. Eckart, Revs. Mod. Phys. **2**, 305 (1930).

[73] A. R. Edmonds, *Angular Momentum In Quantum Mechanics* (Princeton University Press, Princeton, New Jersey, 1974), p. 63.

[74] I. S. Gradshteyn and I. M. Ryzhik, *Table of Integrals, Series, And Products*, corrected and enlarged ed. (Academic Press, San Diego, California, 1980), pp. 497, 3.954.

Biography

I was born February 3, 1961 to Zeng Dean and Liu Xiaoqin in the Guangdong province of People's Republic of China. My childhood was spent in and around Guangzhou, where I eventually entered college at the South China Normal University. After graduating in 1982 with a B.S. in physics, I began a 5 year stint as an university lecturer at South China Normal University.

In 1987, I began my graduate study at Old Dominion University in Norfolk, Virginia. I was married June 18, 1988 to Rodney P. Meyer. My Master of Science in physics was received in December of 1989, and I began my research at the Continuous Electron Beam Accelerator Facility (CEBAF) the following May. I gave birth to my son Robert W. Meyer August 15, 1992 in Norfolk, Virginia. I became a citizen of the United States July 14, 1993. I belong to both a scholastic and physics honors societies, $\Phi\kappa\Phi$ and $\Sigma\Pi\Sigma$.

PUBLISHED PAPERS:

HEAVY MESONS IN A RELATIVISTIC MODEL,
J. Zeng, J. W. Van Orden and W. Roberts, Phys. Rev. D**52**, 5229 (1995).

PAPERS PRESENTED AT PROFESSIONAL MEETINGS:

A RELATIVISTIC MODEL OF HEAVY MESONS,
J. Zeng, J. W. Van Orden and W. Roberts, Fourteenth International IUPAP Conference on Few Body Problems in Physics, Williamsburg, Virginia, 26-31 May 1994.